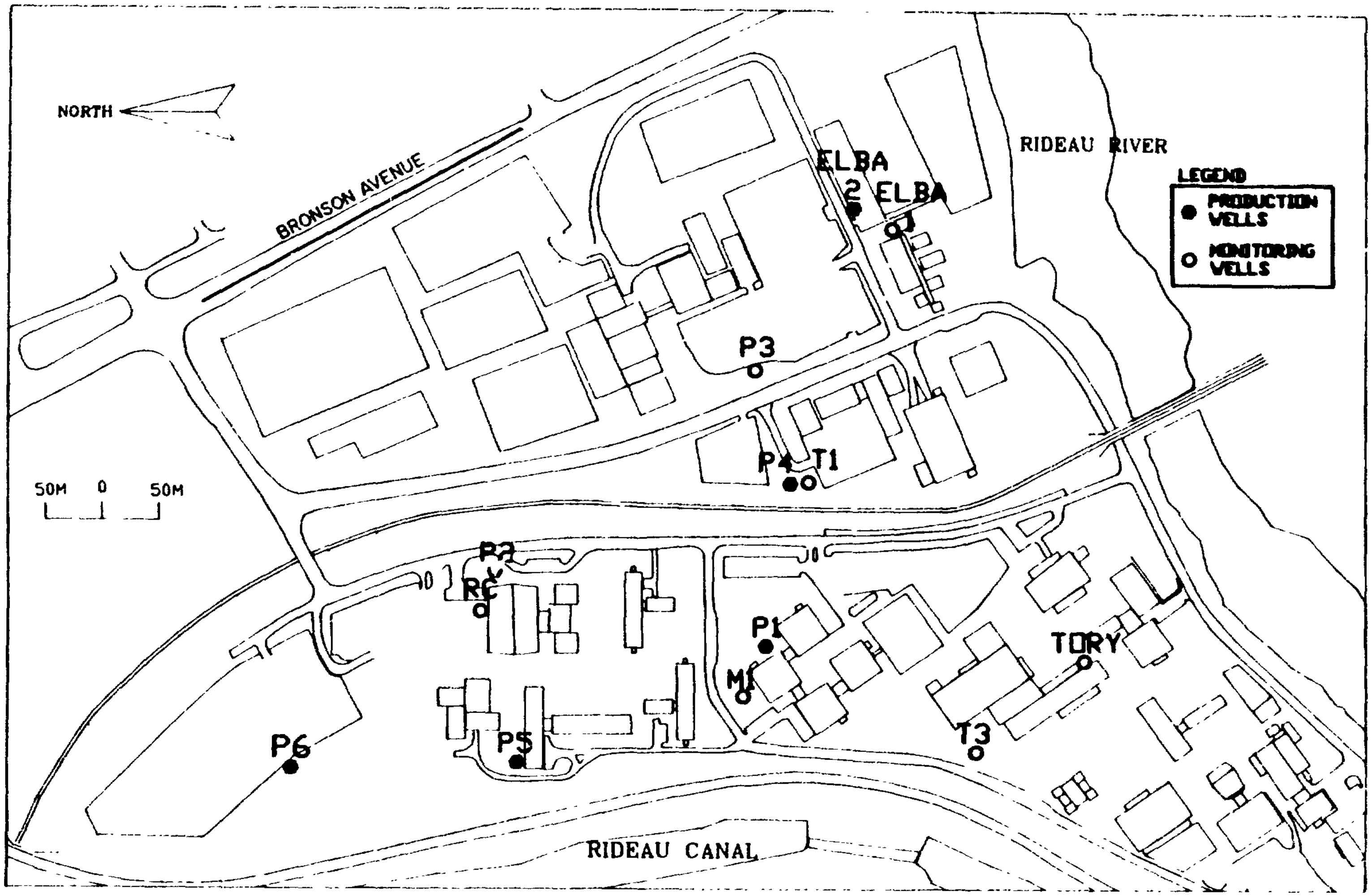

Figure 2 Location of production and monitoring wells within study area.

1

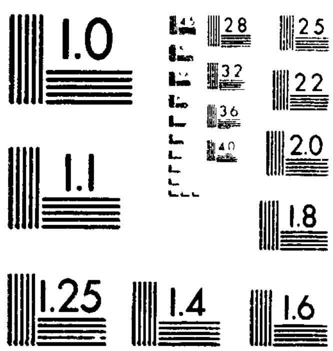

THE HYDROGEOLOGY

OF THE

CARLETON UNIVERSITY CAMPUS

OTTAWA, ONTARIO

by

Heather C. Wilson, Hon. B.Sc.

A thesis submitted to

the Faculty of Graduate Studies and Research

in partial fulfilment of

the requirements for the degree of

Master of Science

Ottawa-Carleton Geoscience Centre

and

Department of Earth Sciences

Carleton University

Ottawa, Ontario

April, 1990

ISBN 0-315-59055-6

The undersigned hereby recommend to

The Faculty of Graduate Studies and Research

acceptance of the thesis,

THE HYDROGEOLOGY OF THE CARLETON UNIVERSITY CAMPUS

OTTAWA, ONTARIO

submitted by Heather C. Wilson, Hon. B.Sc.

in partial fulfilment of the requirements

for the degree of Master of Science

....
Thesis Supervisor

....
Chairman, Department of
Earth Sciences

Carleton University

ABSTRACT

Geological, geophysical and geochemical data were used to investigate the very complex hydrogeology of the Carleton Unversity campus. Lithology logs correlated with borehole geophysical logs, including temperature, temperature gradient, density, gamma ray, resistivity and induced polarization, have been employed to locate formations and formational contacts in the subsurface. Six major fault blocks and five main faults and cross-faults have been identified. High resolution borehole temperature and temperature gradient logs were used in combination with the stratigraphic data to determine the existence of three main water-bearing fracture zones or aquifers: the Hull Formation fracture zones; the porous and fractured zones of the Pamelia and St. Martin Formations and top of the Rockcliffe Formation; and the fractured and potentially weathered zone of the Rockcliffe-Oxford Formation contact. Chemical data in combination with ^{3}H, $\delta^{2}H$ and $\delta^{18}O$ values indicate that the fractured aquifers form or are part of different groundwater flow systems. Hydraulic head monitoring over an 11 month period confirmed the existence of at least two flow regimes and characterized the deep fractured bedrock aquifers as confined and overpressured.

ACKNOWLEDGEMENTS

While involvement in the Carleton University Groundwater Project has been a very interesting research experience, it also has been a pleasure due to the cooperation and consideration shown me by many individuals and organizations.

I would like to express my appreciation to Carleton University and the Faculty of Graduate Studies and Research for the opportunity and the financial support to conduct research concurrent with the development of the Groundwater Project. I also benefited from the personal efforts of numerous Carleton University faculty and staff. I would especially like to acknowledge the work of the Buildings and Grounds, G. Belair and M. Cummings, as well all the staff who gave invaluable assistance in accessing the wells on so many occasions. Construction Services personnel provided various bits and pieces of information. I would like to particularly thank T. Novosedlik of Construction Services for the donation of his time, patience and expertise in Autocad drafting.

I would also like to extend a sincere thank you to the people of Water and Earth Science Associates Ltd., particularly to hydrogeologists N. vanWalsum and R. Woeller for their assistance in the field and discussions afterwards. Their generosity in the provision of field equipment is also appreciated.

Olympic Drilling Company Ltd., who undertook all the well drilling for the Carleton Groundwater Project, were a pleasure to work with during all those pump tests during the summer of 1988.

The borehole geophysical work, which made much of the hydrogeological interpretation possible, was conducted by the Borehole Geophysics Section, Mineral Resources Division of the Geological Survey of Canada under the supervision of P. Killeen and J. Mwenifumbo. I am indebted to them for all their support, generous discussion and encouragement. B. Elliott and A. Tchen, also of the Borehole Geophysics Section, were involved in the production of the logs and pleasantly provided advice and assistance. I would like to thank Bill Hyatt for all his work in logging the on-campus wells and for his excellent appreciation of the sport of hockey.

I would also like to thank A. Taylor (Geological Survey of Canada) who first introduced me to the fundamentals of temperature logging and spent some uncomfortable hours in the cold instructing me in logging procedures. The GSC core library also provided useful information from Ottawa area core.

Skilled drafting done by C. Ulmann and capable field assistance provided by D. Good made the more trying times easier to bear.

Within the Department of Earth Sciences, I thank S. Hill, E.Lambton and S.Thayer for their assistance from the front office. In addition to all the camaraderie I would like to ackowledge the timely and generous assistance of A. Blais, J. Smith, S. McEachern, S. Hamilton and M. Coleman. I am especially grateful for the help received from, and given so graciously by C. Carr. I would also like to note the kindness and assistance received from fellow students A. Plouffe, H. Falck, D. Marshall, D. Thorkelson, F. Ford, S. Carr, V. Bowman and C. Dumaresq.

My thesis supervisor, F.A. Michel, has been encouraging and enthusiastic throughout. I am grateful for his support.

I would like to make a special acknowledgement of the generosity, support and help of F.J. McFarland and the hospitality of K. Clark and R. Clark who provided me with a home away from home.

Part of the financial support for the Groundwater Project was provided by federal Department of Energy, Mines and Resource and the Ontario Ministry of Energy. Further research support was provided by an NSERC operating grant to F. Michel.

TABLE OF CONTENTS

LIST OF TABLES

LIST OF FIGURES

FIGURE	DESCRIPTION	PAGE
32	Hydrograph for multilevel well	97
33	Barogram, thermogram, precipitation record and hydrographs for multilevel well, November, 1988	98
34	Cross section of multilevel well showing vertical hydraulic gradients	99

LIST OF APPENDICES

Chapter 1

INTRODUCTION

1.1 BACKGROUND

This thesis forms part of a larger project undertaken by Carleton University to develop a groundwater heat pump system for the heating and cooling of campus buildings. The use of groundwater heat pump technology for this purpose was first considered by the University in 1985. The intention at that time was to develop a groundwater supply for the cooling of the computing facilities in the Administration building. However, high water yields from the first drilled well prompted the University to expand the proposed project to provide for the heating and cooling of all the major buildings on the campus. The project was then designed for implementation in four phases.

Between 1985 and 1988 a series of production and monitoring wells were drilled on the campus. Following the assessment of the pump and injection test results, the University decided to proceed with the first phase of the project. This involved the extraction of groundwater at a rate of 120 litres per second (L/s) from two production wells, the pumping of the water via a closed pipe loop, through a series of heat exchangers and finally the reinjection of the water back into the subsurface. A portion of the University's heating and cooling plant was converted to accommodate this new system.

Phase I of the project was officially opened in February, 1990. When all phases of the project are in operation, this installation will represent the largest application of groundwater and heat exchanger technology of its kind in North America. The drilling of the production and monitoring wells, as well as the pump and injection tests, was co-funded by Carleton University, the federal Department of Energy, Mines and Resources and the Ontario Ministry of Energy.

The hydrogeological research undertaken for this project was and will continue to be an integral part of the Carleton University Groundwater Heat Pump Project. Information on the campus geology, and in particular the geology of the bedrock aquifers from which the groundwater is being withdrawn and reinjected, is important for understanding the groundwater system and for the siting of production wells. The investigations that are documented in this thesis were initiated as part of the effort to define the very complex geology and groundwater systems of the Carleton University campus.

1.2 PURPOSE AND OBJECTIVES

The purpose of this thesis research was to investigate and describe the undisturbed hydrogeological conditions existing beneath the Carleton University campus. The location of the campus, the study area, is shown in Figure 1.

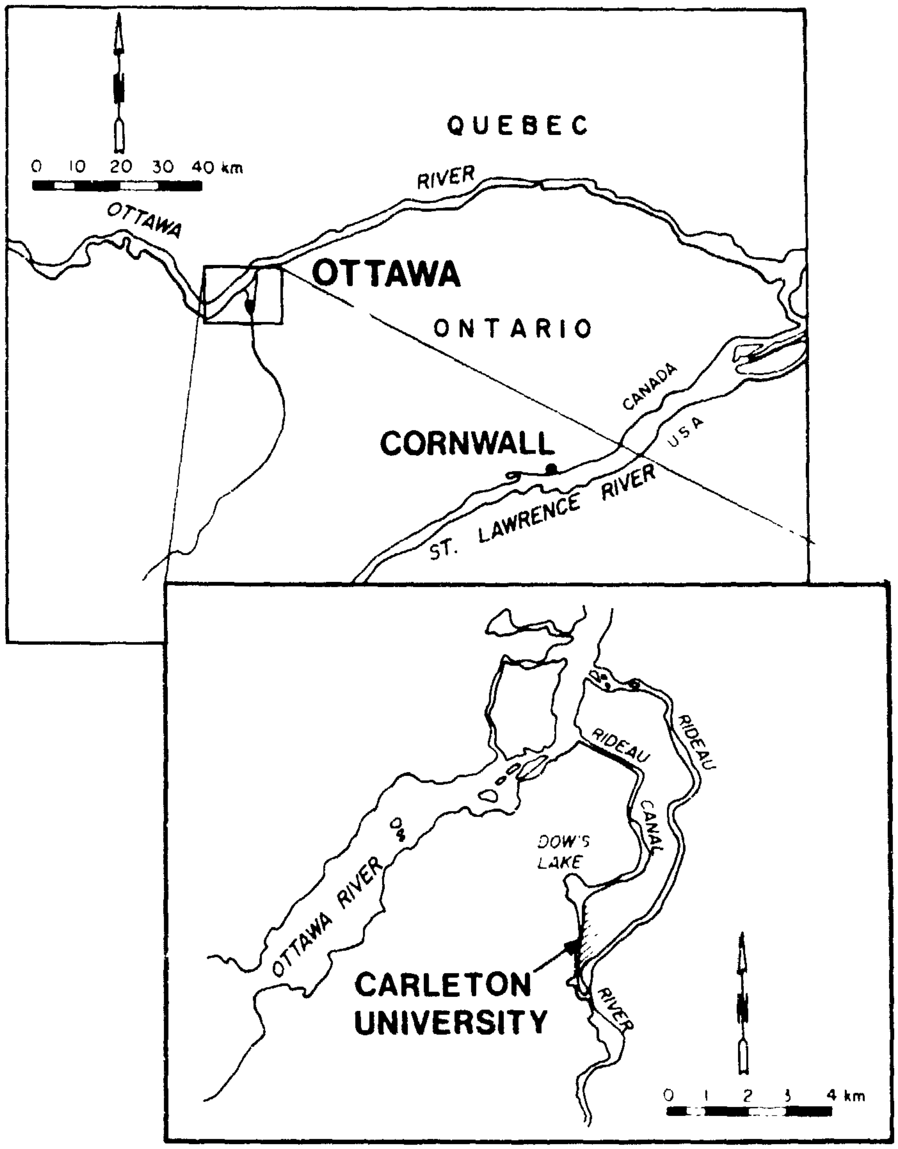

Figure 1 Location of study area.

The objectives of this research were:

1. To identify the bedrock formations accessed by Carleton's production wells and to use this information in conjunction with other bedrock data to confirm the local stratigraphy and the location of the major fault zones within the study area;

2. To correlate the results of the pump tests with the local bedrock structure and stratigraphy as determined from the analysis of the borehole geology and geophysics; and

3. To use the water chemistry and hydraulic head data to define the local groundwater flow system(s) in the unpumped state.

To accomplish these objectives a compilation and analysis of geology, geophysical and geochemical data collected during and following the Heat Pump Project field tests was undertaken.

1.3 SCOPE OF WORK

The field program included: the collection of borehole drilling chips; the monitoring of the well water levels; the borehole geophysical logging of the production wells; and the downhole water sampling of the production and monitoring wells. The wells were monitored on a regular basis from September 1988, the time of the last pump/injection test, to August 1989, when the well-heads were altered for the heat pump system. Well water levels were recorded to determine the temporal and spatial variations in the hydraulic head. The borehole geophysical logging of temperature, temperature gradient, density, gamma ray, resistivity and induced polarization, was conducted in February and March, 1989. Certain repeat logs were run as late as October, 1989. The well water geochemical sampling was conducted primarily in May and June of 1989, however, follow-up sampling was continued up to the fall of 1989. The well water was analysed for major ion chemistry and for tritium, deuterium and oxygen-18 isotopes.

The locations of monitoring and production wells used in this study are shown in Figure 2. The elevations and depths of the wells are depicted in Appendix 1.

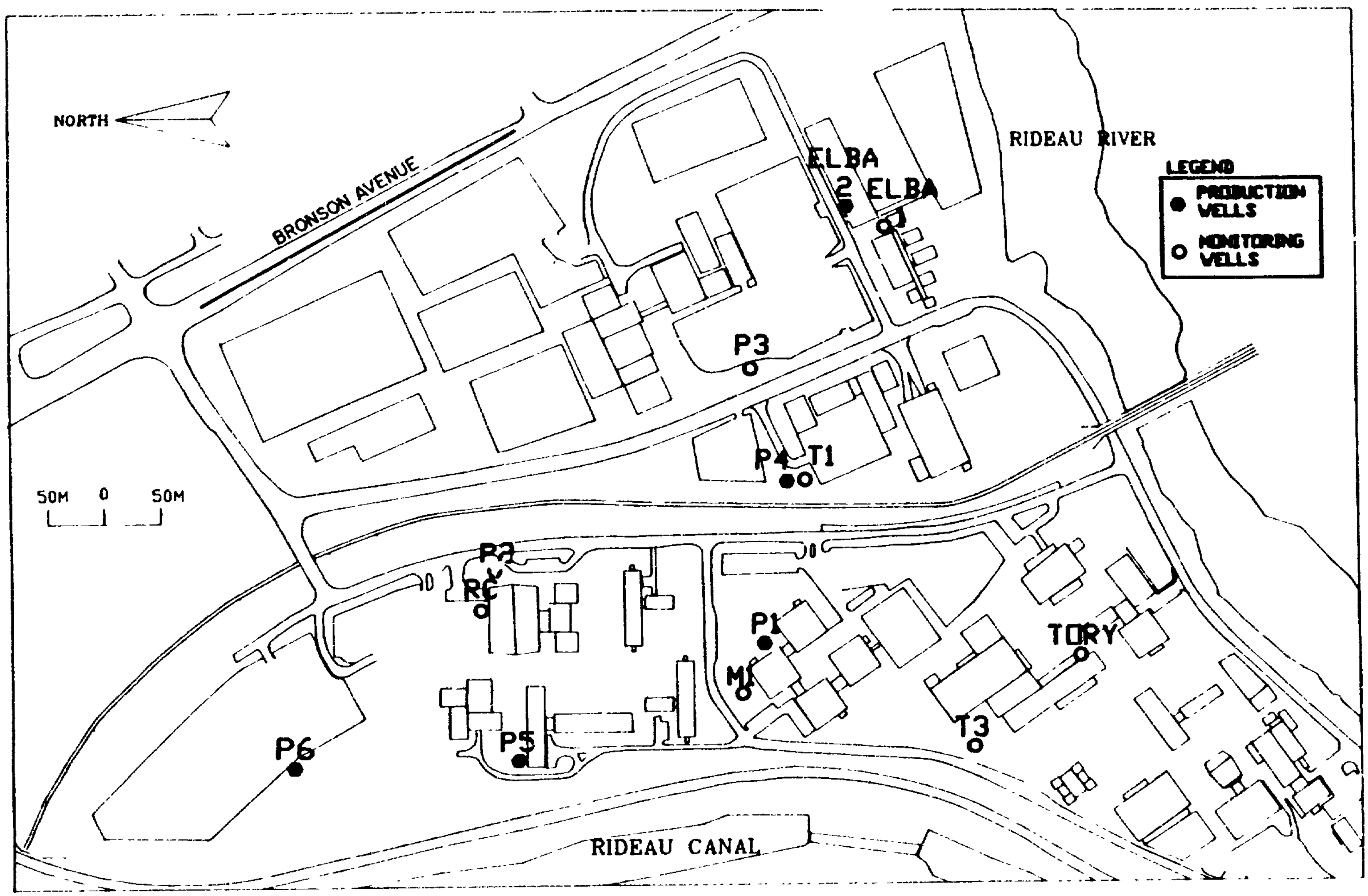

Figure 2 Location of production and monitoring wells within study area.

1.4 OUTLINE OF THESIS

The text is divided into six chapters. Chapters Two and Three provide a description of the general geological and hydrological setting of the site. Chapter Four describes thc methodology used during the study. Chapter Five presents and discusses the results from the borehole geological, geophysical and geochemical data, as well as the hydraulic head monitoring. The discussion and synthesis of the study's overall findings are presented in Chapter Six and the conclusions are presented in Chapter Seven.

Chapter 2

GEOLOGICAL SETTING

2.1 REGIONAL GEOLOGY AND STRATIGRAPHY

Carleton University is located in the Ottawa-St. Lawrence Lowland, a structurally controlled basin underlain by Palaeozoic sedimentary strata unconformably overlying Precambrian basement rocks (Wilson, 1956). This basin of Palaeozoic sediments is well defined by Precambrian highlands which flank its northern, western and southern sides (Figure 3). The lateral contacts between the Palaeozoic sedimentary strata and the Precambrian rocks are often marked by fault controlled escarpments which form some of the most prominent physiographic features in the region.

The sedimentary strata are relatively flat-lying or gently dipping throughout most of the basin, except along the northern margin, where the bedrock is deformed by extensive faulting. This faulting has dislocated the sedimentary strata, including the bedrock in the study area, into tilted and down dropped fault blocks (Wilson, 1946).

The faulted Palaeozoic rocks are overlain by Quaternary deposits. These unconsolidated sediments mask the unevenness of the bedrock surface, covering

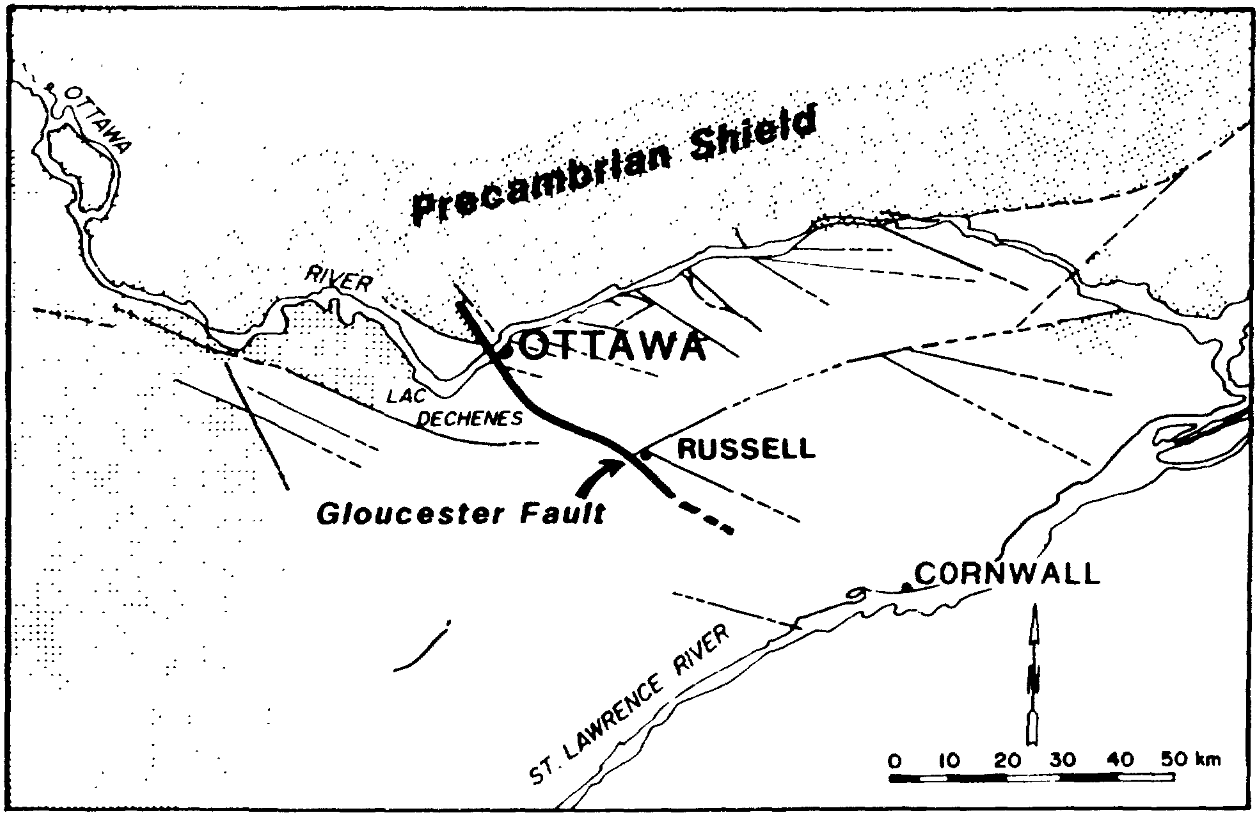

Figure 3 Location of the Palaeozoic sediments and the major faults in the Ottawa - St. Lawrence Lowlands (after Wilson, 1946).

the tilted fault blocks and pre-glacial erosional features. The result is a gently undulating surface topography.

At the Carleton University site there is less than 15 m of topographic relief across the campus, with altitudes ranging from 59 to 73 metres above sea level (masl). The Quaternary sediments range in thickness from less than a metre to over 50 metres. They consist of glacial till and discontinuous layers of marine or lacustrine clay and sand (Michel, 1985). Landfill, including construction and metal debris, is buried in various parts of the campus, particularly in the northern part. Gravel-rich deposits have been located in several drill holes and may be fluvial deposits marking the location of old river channels eroded into the bedrock surface. In most cases these channels or valleys lie along fault lines in the Palaeozoic rocks. These structurally controlled depressions may be linked to a regional bedrock valley which extends north of the study area from Dow's Lake (Figure 1) along the line of a major regional fault, known as the Gloucester Fault (Figure 3) (Brandon, 1960).

Table 1, compiled from Wilson (1923), Kay (1942), Wilson (1946), Vollrath (1962), McFall and Davidson (1979), Williams and Telford (1986) and Steele-Petrovich (1986; 1989), summarizes the Palaeozoic stratigraphy of the Carleton University area. The lithostratigraphic nomenclature used is from Wilson (1946).

Table 1 The Palaeozoic Stratigraphy Underlying Carleton University Campus

Age	Group	Formation	Description	Lower Contact	Thickness
Upper Ordo-vician		Billings	Dark grey to black, non-calcareous to slightly calcareous fossiliferous shale	Transitional conformable; upper limit of lst beds > 2cm thick	Up to 30m
		Eastview	Dark to medium grey limestone interbedded with dark grey, calcareous shales	Disconformable; defined by lower limit of shale interbeds >5cm thick	Up to 7m
		Cobourg	Light to dark grey sublithographic to coarsely crystalline limestone with calcareous shaly partings	Transitional conformable; locally marked by top of thin shale unit overlying calcarenite beds	Up to 37m
Middle Ordo-vician	Ottawa Super-group: Trenton	Sherman Fall	Light to dark grey sublithographic to crystalline limestone, shaly limestone interbedded with calcarenite	Sharp conformable; marked by top of pure calcarenite unit	Up to 30m
		Hull	Light to medium grey calcarenite interbedded with shaly fossil-iferous calcilutite, 12m interval of coarse calcarenite at top of formation	Transitional conformable; placed at top of dark grey sublithic beds and in middle of gradual increase in shale units	Up to 37m
		Rockland	Medium to dark grey sublitho-graphic limestone with abundant shaly partings particularly in upper part	Transitional conformable; placed at top of generally massive limestone	Up to 13m
		Leray	Brownish to dark grey, massive calcarenite with beds of calcilutite and shaly calcilutite, fine textured dark limestone at the base	Conformable; placed at base of massive limestone unit or fine textured dark limestone	Up to 9m

Age	Group	Formation	Description	Lower Contact	Thickness
Middle Ordo-vician	Black River	Lowville	Light to dark grey, sublithographic argillaceous limestone with shale, fossiliferous and calcarenite intervals; increasingly dolomitic towards the base; "birdseye" effect in fine-grained limestone characteristic of formation, stromatolitic and oolitic limestone, and medium to dark concretions characteristic of lower member	Conformable; arbitrarily placed below first bed of fine-grained "birdseye" limestone; also defined as lower limit of occurrence of limestone with CaO/MgO >15	Up to 67m
		Pamelia	Silty to sandy dolostone with shaly partings and thin interbeds of quartz sandstone	Disconformable; placed at the base of sandy beds	Up to 9m
		St. Martin	Impure limey dolomite	Conformable; placed at the top of the green and grey shale, green siltstone and shale interbeds >10cm thick	Up to 3m
		Rockcliffe	Impure, shaly fine-grained greenish grey to grey sandstone with upper 12m interval of dark grey to dark green siltstone	Disconformable; sharply defined by difference in lithology at base of quartz sandstone	Up to 51m
Lower Ordo-vician		Oxford	Light to medium brownish to greenish grey dolostone with lesser shaly and sandy interbeds	Conformable; placed at top of the highest occurrence of sand in any quantity	Up to 65m
		March	Interbedded light grey to brown quartz sandstone, dolomitic quartz sandstone, sandy dolostone and dolostone	Conformable; arbitrarily placed at the lowest dolomitic layer	Up to 6m
Cambro-Ordo-vician		Nepean	Medium to course-grained cream coloured quartz sandstone with occasional conglomerate interbeds	Disconformable; contact with the Precambrian basement rocks	Up to 80m

These Palaeozoic strata formed from sediments deposited by successive marine invasions during the Cambro-Ordovician and Ordovician. Most of the formations, described in the forward of Appendix 2, are thought to have been deposited in an intracontinental shelf environment (Williams and Telford, 1986).

2.2 STRUCTURAL GEOLOGY

The structural features of the Ottawa-St Lawrence Lowland are the result of successive periods of tectonic activity. The Ottawa valley lies within a large complex structure, the Ottawa-Bonnechere Graben. The Graben is characterized by prominent fault systems on the north and a prominent zone of normal faulting and a small subsidiary graben on the south (Lumbers, 1982). Figure 3 shows the extent of this displacement.

The Ottawa-Bonnechere Graben is thought to be part of a much larger St. Lawrence rift system (Kumarapeli and Saull, 1966). The St. Lawrence rift system may be genetically related to the development of the mid-Atlantic rift and the opening of the Atlantic basin. The main phase of tectonic activity within this rift valley system is thought to have taken place in the Mesozoic (Kumarapeli and Saull, 1966), when the region was under extension (Williams and Telford, 1987). However, the normal faulting within the Palaeozoic strata has not been precisely dated. Some of the faults have been traced from Palaeozoic rocks into the

Precambrian basement. Michel (1985) suggests that at least some of the major faults in the Ottawa area initially formed during the time of Palaeozoic sedimentation and have subsequently been reactivated. At present the region is undergoing compression. The maximum contemporary compressive stress is regionally oriented northeast as determined from local pop-ups (Williams and Telford, 1986).

One of the normal faults on the southern margin of the Ottawa-Bonnechere Graben is the Gloucester Fault or Fault Zone, a major structural feature in the Ottawa area of the Palaeozoic basin. The Zone consists of a series of steeply dipping individual faults and is characterised by the branching of faults from fault junctions (Williams and Telford, 1987). This fault zone forms the west and southwest margin of a large, down-dropped block that extends eastward from the city of Ottawa. The largest known displacement along the Gloucester Fault, approximately 550 m, occurs near Russell, Ontario (Figure 3).

2.3 STUDY AREA

The Gloucester Fault is the major structural feature within the study area, as illustrated in Figure 4. It is thought that the fault zone is marked by a series of sub-parallel breaks which strike northwest across the campus. Total vertical displacement on campus is estimated to be 180 to 200 metres (Michel, 1985).

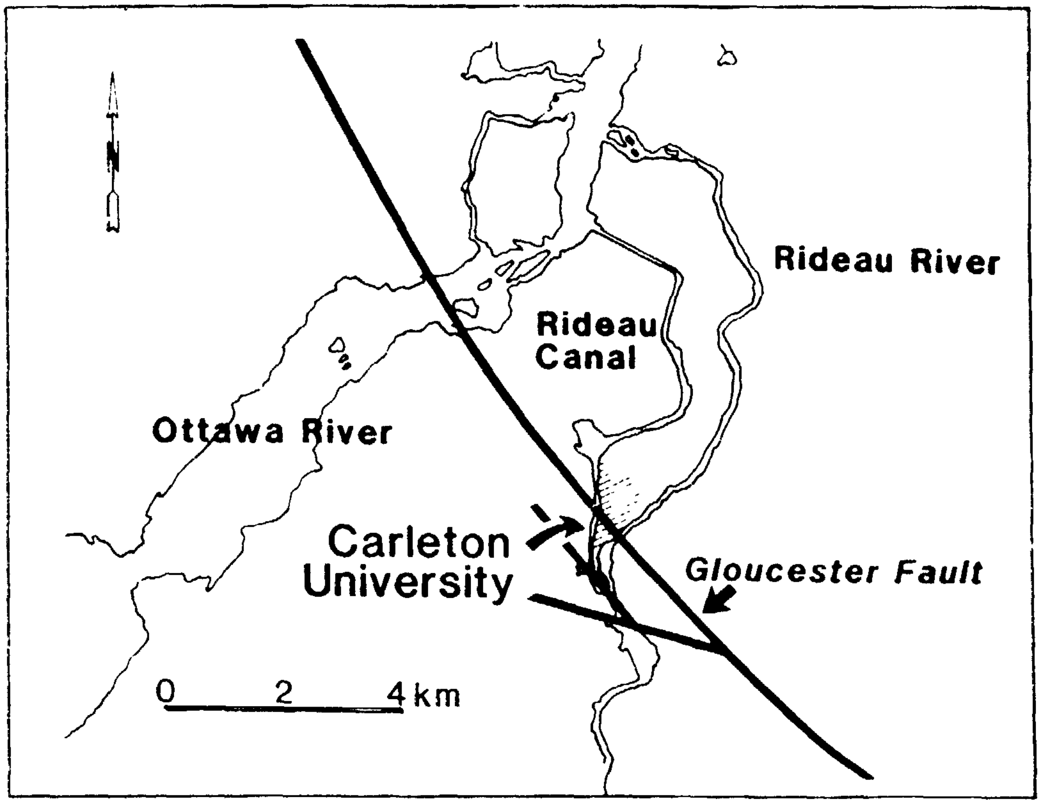

Figure 4 Location of the Carleton University cam,.us relative to the Gloucester Faults (after Simpson, 1978).

The surmised locations of these faults and related cross faults are shown in Figure 5.

As in many fault zones within the region, the initially horizontal bedding is tilted toward the downthrown block. The easterly dip of some of these rocks is visible in an outcrop along the Rideau River adjacent to the campus. Dips measured across the outcrop varied between 10° and 60° (Michel, 1985).

As can be expected within a fault zone, the vertical to subvertical fractures are numerous. Examination of fracture spacing at bedrock exposures south of the study area shows fractures to be relatively closely spaced and frequently only centimetres apart. Many are filled by secondary minerals, particularly calcite. Joint and fracture measurements taken at outcrops along the Rideau River south of the University campus indicate that the dominant trend for the joints and vertical to subvertical fractures corresponds with the northwest-southeast orientation of the major faults of the area (Vollrath, 1962; Simpson, 1978; Williams and Telford, 1986). Figure 6 shows the fracture orientations obtained, by Simpson (1978), from bedrock exposures within the Gloucester fault zone south of the study area. The majority of the fractures observed at these outcrops are extensional, reflecting the nature of the paleo-stress fields (Simpson,1978).

The density of bedding plane fractures, as determined from drill core taken north of the Carleton campus (GSC LeBreton Street and Observatory Crescent wells)

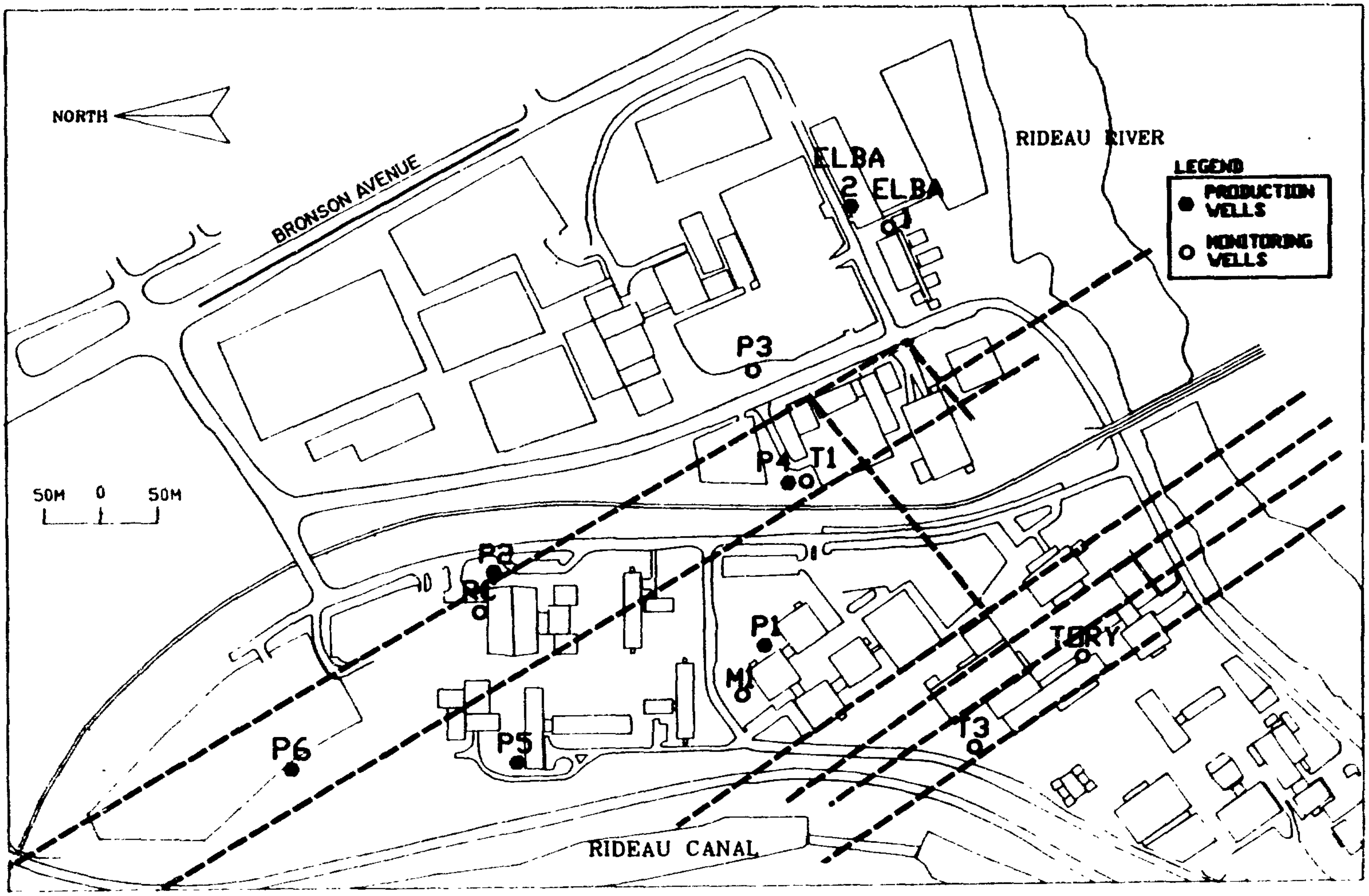

Figure 5 Approximate location of major faults, cross faults and production wells within the Gloucester Fault Zone underlying the Carleton University campus (after Michel, 1985).

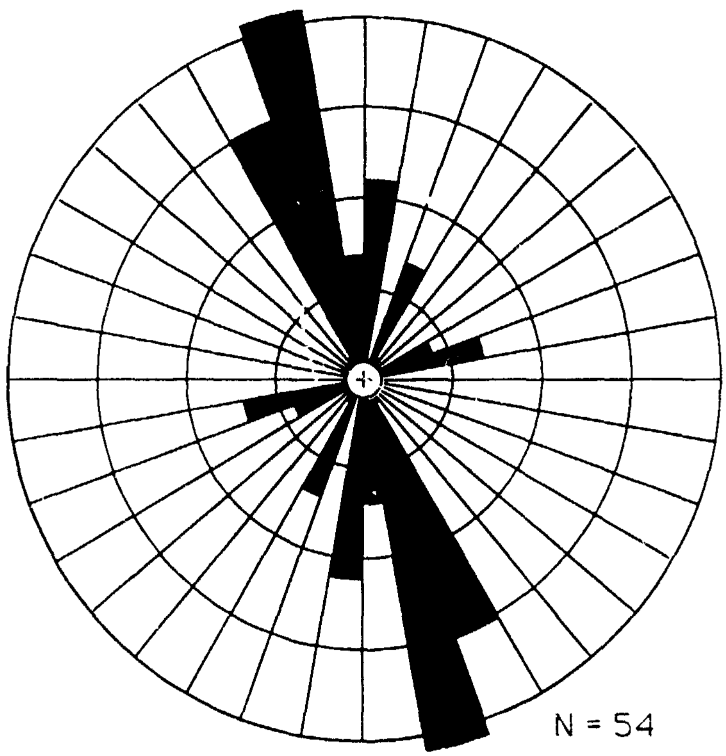

Figure 6 Fracture orientations determined from Ottawa Supergroup bedrock in the main Gloucester Fault Zone south of the study area. Data from Simpson (1978).

varies significantly between formations (Michel, 1985). The formations identified as having the highest density of open bedding plane fractures are the St. Martin and the formations which overlie and underlie the St. Martin, namely the Lower Lowville, Pamelia and Rockcliffe Formations. The Sherman Fall and Rockland Formations are also classified as potential aquifers based on their fracture densities. Two formations, the Leray and Hull, have been assessed as potential aquitards in the system, due to the presence of massive calcarenites in these formations.

If open and interconnected, bedding plane and vertical fractures could have a significant impact on the hydraulic conductivity found in the study area.

Chapter 3

HYDROLOGICAL SETTING

3.1 REGIONAL HYDROSTRATIGRAPHY

The Gloucester fault zone and associated fracture networks are the major geological features controlling groundwater flow in the study area. The capacity of the fracture flow within the fault zone at the Carleton University site provides a different groundwater supply scenario than that predicted for local fault zones by regional groundwater studies.

Brandon (1960), Scott (1967) and Charron (1978) undertook regional groundwater studies of the Ottawa area and parts of the Ottawa-St.Lawrence Lowlands. Brandon (1960) and Scott (1967) assessed the region's various rock formations in terms of their groundwater potential and well yields. Charron (1978) made a hydrochemical study of groundwater flow in the region between the Ottawa and St. Lawrence Rivers east of Ottawa. The following description is a brief compilation of the hydrostratigraphic information from those reports.

The Nepean sandstone aquifers, particularly the upper and lower units, will supply substantial well water yields, between 2.6 and 10.5 L/s. The Rockcliffe, St. Martin, Oxford and March Formations, all hydrologically similar, provide sufficient well yields for domestic supply (2.6 to 7.9 L/s). The Rockcliffe, Pamelia and St. Martin Formations have average well yields of 5.1 L/s. In most cases the jointing or fracturing of the rock is of importance since the more productive parts of the formations are associated with well developed jointed and fractured zones. The Ottawa Supergroup formations, plus the Eastview Formation, are productive in areas where horizontal and vertical joints are well developed. Movement of groundwater within these formations is often restricted to those well developed joints and seams that are usually in the calcareous shale layers. The massive beds within the Ottawa Supergroup formations have not yielded water. The zone, within these formations, most noted for its water bearing fractures is the weathered bedrock surface. This productive layer ranges from 0.3 to 1.8 m in thickness. Deep drilling into the Ottawa Supergroup formations often produces sulphurous and brackish waters and is not recommended. The presence of adequate aquifers in the surficial deposits overlying the Ottawa Supergroup reduces the utilization of the bedrock aquifers. The Billings Formation is known for its usually turbid and brackish water but is tapped for domestic use. All of the groundwater in the aforementioned bedrock aquifers is under artesian pressure. The general chemical character of the groundwater from the various formations is shown in Figure 7.

It is clear from the regional studies that the fracturing of bedrock locally increases its ability to transmit water. However, it is also reported that the fracturing within fault zones is sealed by secondary mineralization, namely calcification (Wilson, 1946; Brandon, 1960; Scott, 1967; and Charron, 1978). As a

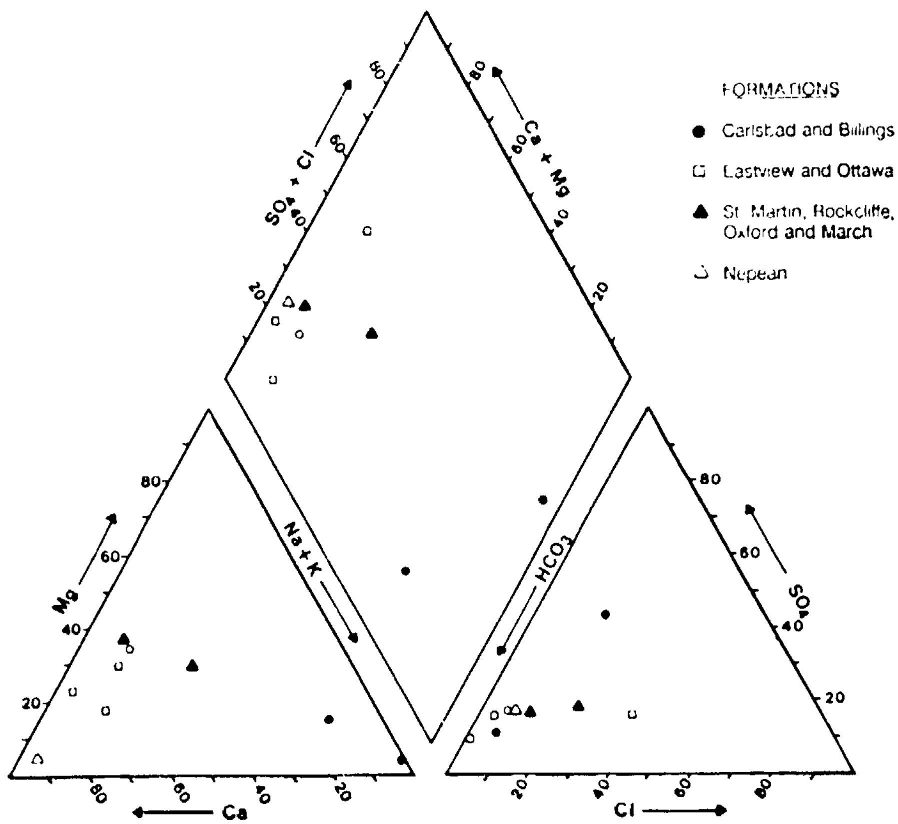

Figure 7 Trilinear diagram showing the major ion composition of groundwater samples obtained from various bedrock aquifers within the Ottawa region. Chemical analysis data from Brandon (1960).

result, deep drilling is not normally considered as a viable option in the immediate Ottawa-Hull area because of the numerous faults present. It is considered particularly ill-advised to drill for groundwater in lowered and tilted fault blocks, especially in areas where the thick sections of massive limestone and shale predominate. The reason given for the poor yield from wells completed in these settings is that those formations which are considered as the better aquifers (the sandstones and shaly dolostones of the Nepean Formation through to the St. Martin Formation) are sealed off from their areas of outcrop or recharge zones (Brandon, 1960).

In general, the bedrock aquifers in the region are considered to have relatively low transmissivities. Results from pump tests cited in the regional surveys show that bedrock wells rarely have a specific capacity of more than 1 L/s/m of drawdown after 10 hours of pumping.

The possibility that the fault zones within the region may be, given the right conditions, zones of improved water yield was alluded to by Charron (1978). Four distinct areas of higher specific capacity wells, defined as greater than 2 L/s/m of drawdown, were located more or less along the trend of the east-west leg of the Gloucester Fault east of Russell (Figure 3). Charron (1978) suggested that these higher capacities may be indicative of permeable zones associated with the fault. The bedrock wells in those areas were of medium depth, but all were less than 61 m deep.

3.2 REGIONAL GROUNDWATER FLOW SYSTEMS

The extent of aquifer recharge varies significantly across the region due to differences in depth to bedrock, overburden type, and the nature of the bedrock and surface conditions.

The Ottawa climate is described as continental, with large temperature variations throughout the year. Normal mean temperature extremes are as low as -15°C during January and as high as 26°C in July. The average annual temperature is 6°C, the mean winter temperature -9°C and the mean summer temperature 19°C. The average dates for the last spring frost and the first fall frost are May 11 and October 1, respectively. The mean annual precipitation is spread fairly evenly throughout the year, averaging about 879 mm, with a mean annual snowfall of 227 cm (Environment Canada, 1988).

Based on historical records, mostly from shallow wells, maximum recharge occurs during the latter part of March and the early part of April. Well levels fall during the course of the summer, except after a period of heavy rain, and reach a minimum level at the end of August. This is in response to increases in evapotranspiration from the end of March through to August. Recharge of the groundwater is minimal during the summer months as most of the precipitation is either absorbed by vegetation and then transpired back to the atmosphere, returned directly to the atmosphere by evaporation, or is lost through runoff.

Some recharge occurs during the autumn after evapotranspiration rates decrease and before infiltration is deterred by frozen ground (Brandon, 1960; Scott, 1966; Charron, 1978). While the magnitude of the seasonal groundwater level fluctuations can vary 1 to 2 metres from year to year, the general trend of the hydrograph remains the same.

Groundwater drainage basins and the recharge and discharge zones have not been determined for the immediate Ottawa area. They have, however, been determined for some of the adjacent areas. Brandon (1960) concluded that the regional groundwater flow from the area west of the Gloucester Fault is northward toward the Lac Deschenes basin of the Ottawa River (Figure 3). A regional northward flow was also determined by Charron (1978) for the area east of Ottawa. Charron (1978) used hydrogeochemical models to determine the regional groundwater flow system and defined the area along the southern shores of the Ottawa River as a discharge zone for groundwater flowing northward from the central part of the St. Lawrence Lowland. Groundwater flow directions assessed for a groundwater basin immediately to the east of the study area also trend north/northwest (Geo-Analysis, 1986). Extrapolation of these flow regimes into the Ottawa area places the study area in a transient flow zone or along the southern margin of a regional discharge zone. It is uncertain whether these groundwater flow regimes can be applied to the groundwater flow regime under investigation within the study area. The Carleton University Groundwater Project wells are considerably deeper (122 m) than most of the wells used to establish the regional groundwater flow patterns. For example, the 400 wells used in the Charron (1978) study had a mean depth of 36 m, some as shallow as 9 m. However, the water chemistry from all but one of the deeper wells (75 m) was in agreement with the hydrogeochemical trends used in Charron's flow model.

3.3 STUDY AREA

A preliminary review of the groundwater potential of the Carleton University campus was undertaken by Michel (1985). The underlying bedrock was assessed in terms of its porosity, water-bearing zones, and the occurrence of bedding plane fractures as noted in Section 2.2. The units with the highest average porosities are dolostone units in the St. Martin Formation and shaly sandstone of the Rockcliffe Formation. The porosities of the remaining formations are generally low. The eastern and western sections of the campus were considered to have the best possibility for water supply based on the depths to potential water-bearing formations.

All of the on-campus wells, ranging from 30 to 160 m deep, are artesian indicating that the bedrock aquifers penetrated are not hydraulically connected to the adjacent surface water bodies, Dow's Lake and the Rideau River. Michel (1985) concluded from the results of pump tests carried out in 1985 that some of the study area faults do not form impermeable barriers to groundwater flow while others form partial boundaries. Yields up to 9.5 L/s were obtained during those 1985 pump tests (WESA, 1986).

Water and Earth Science Associates Ltd. (WESA) was retained by the University to supervise the drilling of production and monitoring wells (Figure 2) and to perform a series of pump and injection tests as part of the assessment of the groundwater supply for the heat pump project. This phase of the groundwater project provided an opportunity to acquire stratigraphic as well as hydrological information about the site's subsurface. Research for this thesis was initiated at this time as an integrated part of the groundwater project field investigations involving WESA, Dr.F.A. Michel and the author.

The fractured nature of the site's hydrogeologic regime and the preferential connection between certain wells became evident during reconnaissance testing. It was evident from the Elba 2 pump test results that the central and eastern fault blocks were only poorly hydraulically connected (WESA, 1986). This was determined on the basis of the different response times for the monitoring wells and was attributed to the hydraulic effects of a major fault. Further pump test data confirmed this pattern. The pump test data were used to calculate aquifer parameters for computer model calibrations and to make a quantitative assessment of the hydraulic connection between all of the production wells (WESA, 1988). The nature of the well interconnections is partially illustrated by the drawdown curves shown in Figure 8.

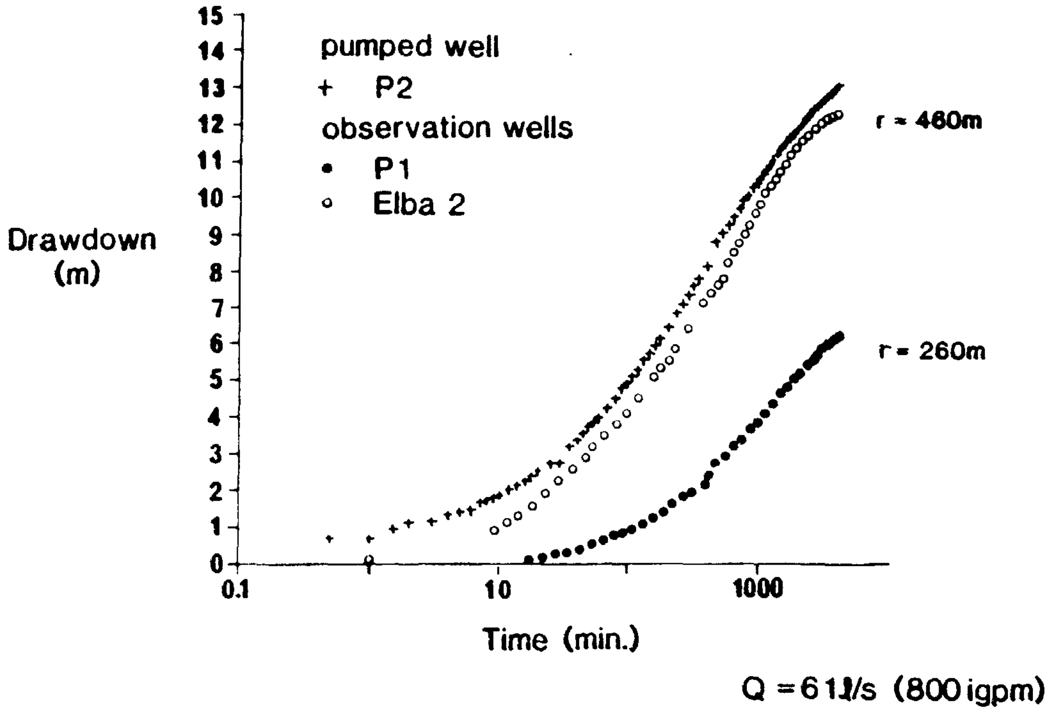

Figure 8 Pump test results for three on-campus wells.

It was found that certain faults acted as negative (impermeable) boundaries while others formed zones of preferential permeability. An example of the latter condition is illustrated by the response of the Elba 2 well to the pumping of well P2 (Figure 8). The almost instantaneous and similar response of relatively widely separated wells, such as P2 and Elba 2 is a characteristic response to pumping for a fractured aquifer. In addition, many of the pump test drawdown versus time curves, WESA (1988) exhibited features, such as asymptotic drawdown lines and changes in slope, which are also characteristic of fractured aquifer responses to pumping (Streltsova-Adams, 1978; Raven, 1986).

The relationship between the bedrock structure, well yields, and well interconnections is complex. The juxtaposition of low and high capacity wells, as shown in Figure 9, suggests that yield is very much a function of the bedrock structure and an apparently heterogenous fracture network. The heterogeneity of this fracture network is reflected in the wide range of values determined for the transmissivity and storativity of the fractured aquifers exploited by the wells. The transmissivities calculated from the production well drawdown data ranged from 60 to 470 m^2/day. The range in the transmissivity values calculated for the multilevel monitoring well was even greater; 62 to 4631 m^2/day. Storativity values had a wide range as well, from 0.00002 to 0.0036 in the production wells and from 0.00003 to 0.037 in the multi-level monitoring well.

Based on the well interconnections, the wells were divided into two groups: P2,

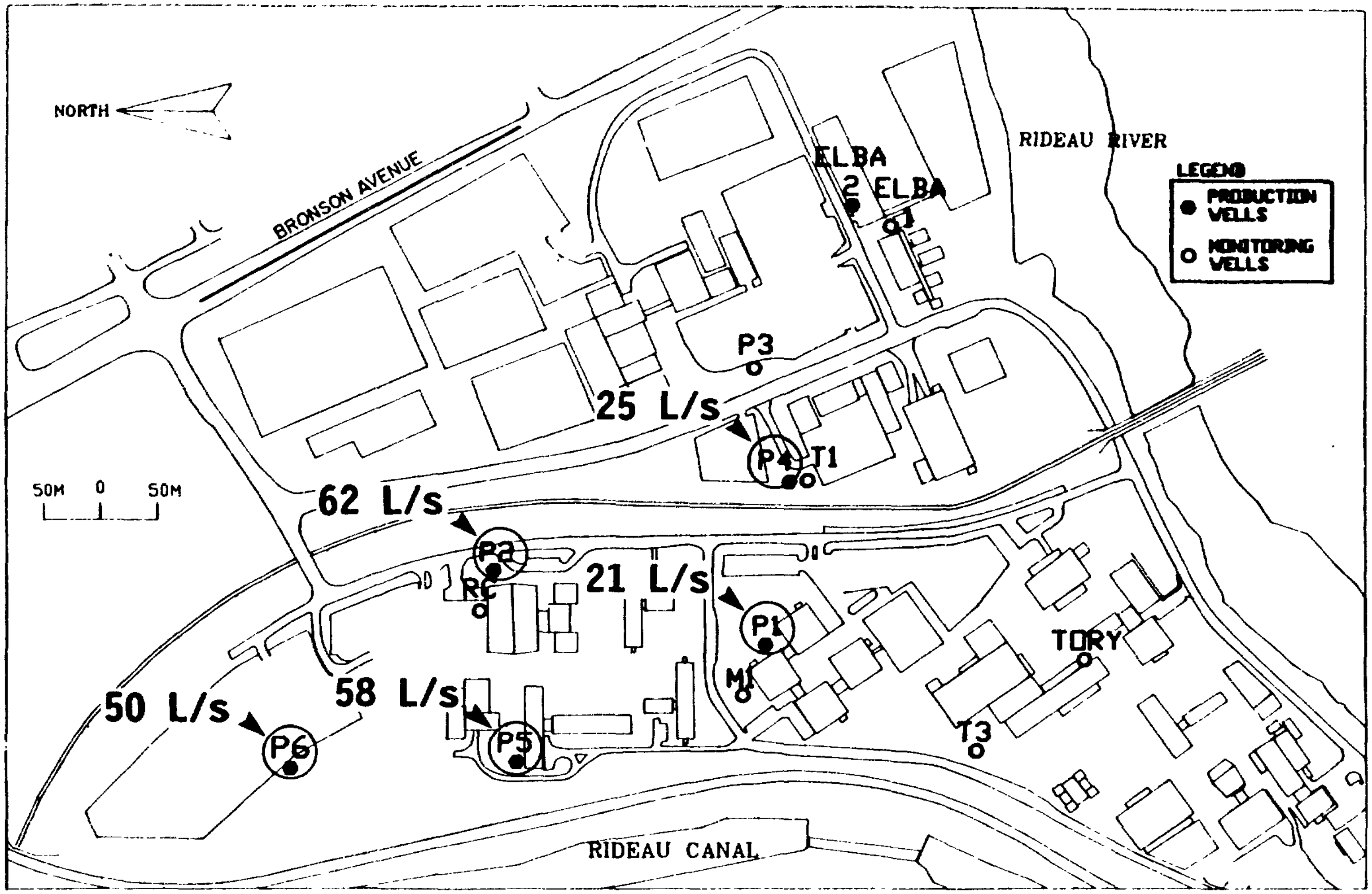

Figure 9 Well yields of on-campus production wells (after WESA, 1988).

P3, P5, P6 and Elba 2 in Group I; and P1 and P4 in Group II. This division was also supported by the chemical analysis of well samples taken during the pump tests (Figure 10). Group II wells had total dissolved solids (TDS) values greater than 1000 milligrams/Litre (mg/L), while the Group I wells, P2 et al., had TDS values of less than 700 mg/L. Both the pump test results and the hydrogeochemistry suggest that there are two imperfectly linked groundwater "aquifer" flow systems on the site (WESA,1988). Results from the pump tests clearly demonstrate that the fractures, presumably at depth are partially open, interconnected and able to act as major conduits for groundwater flow.

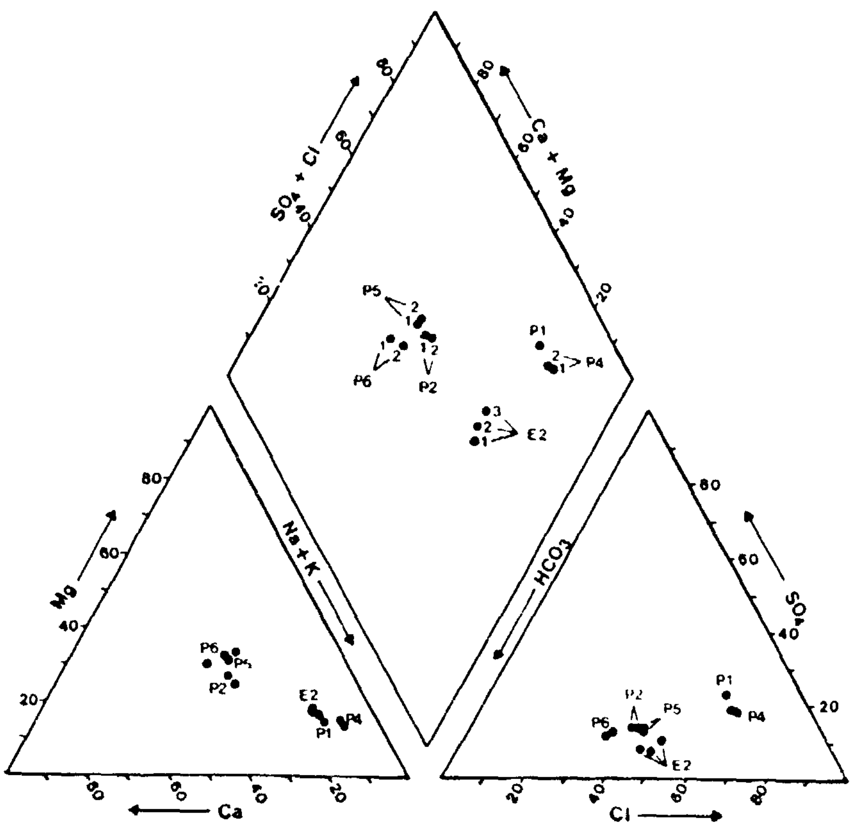

Figure 10 Trilinear diagram showing the major ion composition of pump test samples. Chemical analysis data from WESA (1988).

Chapter 4

METHODS

4.1 DRILLING AND GEOLOGIC LOGS

The six production wells (P1, P2, P4, P5, P6 and Elba 2) and four monitoring wells (M1, P3, T1 and T3) shown in Figure 2, were drilled between 1985 and 1988, using a reverse rotary rig with a tricone bit. Three additional monitoring wells, RC, Elba 1 and Tory, which were drilled prior to the Groundwater Project, are also shown in Figure 2. The production wells are 30.5 cm in diameter to a minimum depth of 61 m and 25.4 cm in diameter for the remaining depth. All of the production wells are at least 122 m deep. The wells were steel cased from the surface through the unconsolidated overburden into the top 6 to 7 m of bedrock. The casings were grouted into the bedrock.

The M1 monitoring well is a bundle-type multilevel installation (Cherry et al., 1983). The M1 borehole is 15.2 cm in diameter through its entire depth of 160 m and was completed and cased in the same manner as the production wells. A nest of 7 individual, 12 mm diameter tubes and 1 PVC tube were installed within the casing and the open borehole. The sampling intervals were separated by 1 to 1.5 m plugs of cement and infilled with coarse gravel. The seal between the lower two tubes failed during installation; consequently those two intervals, M1-B and M1-1 may be interconnected. The monitoring wells, T1 and T3, were drilled as test wells to depths of 95 m and 98 m, respectively. Both are 15.2 cm in diameter for their entire length. The monitoring well P3/M2 was drilled to 150 m and completed as a production well, however, due to a low yield, P3 was recategorised as monitoring well (M2). An illustrated inventory of the wells is provided in Appendix 1. All of the boreholes are vertical.

Bedrock cuttings were collected at 1.5 m (5 ft.) intervals during the drilling of all 10 wells. These cuttings were used to compile percentage lithology logs for each of the boreholes. Other information such as evidence of secondary mineralization, including the occurrence of pyrite and secondary calcite, was also noted on the logs.

Drilling of the production and monitoring wells provided information on the depth to bedrock. These bedrock elevations were plotted on a campus map along with depth to bedrock information from geotechnical drilling, building excavation data and surface geophysics (Epp, 1989; Michel, 1985). The data made available from all of these sources is variable across the campus, which has resulted in an uneven distribution of data points across the campus. The bedrock elevations were used to construct a bedrock topography map for the campus and to assist in the location of fault traces.

4.2 BOREHOLE GEOPHYSICS

Each of the production wells, plus P3/M2, was logged with the Geological Survey of Canada (GSC) Research and Development borehole logging system (Bristow and Conaway, 1984; Bristow, 1979). Full gamma ray spectra, induced polarization (IP), resistivity, density and temperature measurements were digitally recorded on 9 track magnetic tapes and simultaneously displayed on a multi-pen chart recorder as described by Urbancic and Mwenifumbo (1986).

The boreholes were initially logged with the temperature probe at a logging speed of 6.0 m/minute with a sample interval of 200 milliseconds (equivalent to a length of 2 cm). Temperature logging was carried out using an active probe containing a voltage to frequency convertor and 15 cm long tip of thermistor beads. The system has a noise equivalent of less than 0.0001°C. The system design includes an approximate inverse factor which is designed to remove the smearing effect of the thermal time constant (Bristow and Conaway, 1984).

Gamma ray logging was conducted at 3.0 m/minute with a sampling interval of 1 second (5 cm depth interval). The scintillation detector used was a 32 mm x 127 mm sodium iodide (thallium activated) crystal. The electrical logging, including apparent resistivity and IP, were carried out with 0.4 m normal and 0.1 m MN symmetrical lateral arrays, at a logging speed of 3.0 m/minute and a 1 second period. The gamma-gamma probe was not calibrated for the site and the density measurements presented are on an arbitrary range from low to high.

Magnetic susceptibility was also included in the first suite of logging, but was discontinued because of the lack of discernable results, as the noise limit exceeded any measurable quantities present. Spontaneous potential (SP), initially part of the suite of logs, was also discontinued because of the interference from underground installations.

The borehole logging began in February 1989; each borehole was logged with the suite of sondes. Repeat runs were done with several of the probes in order to verify the results. With the exception of the temperature logs, all of the borehole logging was completed by the end of April 1989. A series of temperature logs was run in each borehole from February to May 1989 in order to record any temporal variations. Additional runs of the temperature log were made in well P6 in October, 1989.

The borehole geophysics data were used in conjunction with the geological logs to identify formations and formation boundaries, to locate fractures and to locate the groundwater entry and exit points.

4.3 GROUNDWATER CHEMISTRY

Groundwater samples were collected from the production wells in May and June 1989, eight months after the last pump and injection test. Downhole samples were collected using a sampler lowered on the same cable, pulley and depth meter system used for the geophysical logging. The downhole sampling points, up to 6 per well, were selected to correspond to the main groundwater entry and exit points identified by the temperature logs. Other sampling intervals were added to ensure sampling coverage of the upper and lower parts of each borehole.

Samples were collected with a PVC grab sampler with ball and socket seals. The ball and socket fittings are at each end of the sampler. As the sampler is lowered down the well the balls are kept floating free of the socket by the water flowing through the body of the sampler. When the sampler is brought to a halt and then moved upwards, the balls are pressed into the sockets, thereby capturing water at the desired depth. Consequently, care was taken to lower and raise the sampler in a continuous and steady manner and to come to a complete stop at the sampling point. The sample volume required for chemical analysis necessitated two runs to each sampling interval. Sampling was started at the uppermost point and continued sequentially down the borehole.

Groundwater samples were also collected from levels in the multi-level well (M1) to correspond to well P1 sampling levels. Groundwater from two of the levels were collected by taking advantage of the artesian flow. Samples from one other level were collected using a peristaltic pump. At least two internal volumes (the volume of the water in the entire length of the tube and in the sample interval) were purged before the samples were collected. This step eliminated one of the selected intervals since the recovery rate was too slow to allow for minimal purging as well as the collection of an adequate volume of sample.

Field measurements were made for: Eh (Pt electrode), pH, temperature, electrical conductivity (EC), alkalinity, and sulphide. The pH was determined using a Corning (pH) 106 electrode and a temperature compensating meter. The pH electrode was calibrated, before the sampling of each well, in two buffer solutions which bracketed the range of values encountered in the groundwater. The Orion platinum redox electrode, used for Eh measurements, was calibrated against a ferrous-ferric solution. The Pt electrode was used in combination with a Corning portable meter. Alkalinity and sulphide measurements were performed using Hach kits; alkalinity by acid titration and sulphide by colorimetry.

One litre of groundwater was collected, at each sampling point, for laboratory analysis of major ions. Another 250 ml of filtered, acidified sample was collected for Fe and Mn analysis. Two additional 125 ml samples were collected for isotope analysis. Another 250 ml sample was collected at one interval per well and pretreated with zinc acetate for a sulphide analysis. The sample depth for the sulphide sample was selected on the basis of the maximum sulphide concentration determined in the field measurements. A duplicate set of samples were collected from Well P6. (The first set was collected with a stainless steel thief sampler. The stainless steel sampler was replaced because of its size, an overly sensitive trip switch and poor cable connections.)

All the laboratory analyses, with the exception of the isotope measurements, were carried out by Bondar-Clegg laboratories of Ottawa. Analyses of major cations as well as strontium, iron and manganese were carried out by atomic absorption spectrophotometry. Alkalinity and bicarbonate were determined by acid titration.

All stable isotope analyses, namely deuterium, oxygen-18 and carbon-13, were performed by gas mass spectrometry and the results expressed as delta-permil (δ-^{o}/oo) differences from known standards. Analytical precisions are listed with the results. All tritium measurements were made by liquid scintillation counting. Results are expressed in tritium units (T.U.); one T.U. is defined as 1 atom of ^{3}H per 10^{8} atoms of ^{1}H. Analytical precision is generally +/- 8 T.U.. The carbon-14 result is given as a percent of modern carbon (pmC). Analytical precision is +\- 2. Table 2 summarises the geochemical analyses undertaken and lists the laboratories that were involved.

The downhole samples that were collected with the grab sampler are referred to in the following text as the "well samples". The pump test discharge samples are referred to as "pump test samples".

Table 2

Table 2 Summary of Geochemical Analyses

Analysis	Sample	Laboratory
Inorganic Chemical Analysis	Well samples (P1, P2, P4, P5, P6, Elba 2 and M1)	Bondar-Clegg Co. Ltd. Ottawa, Ontario
Oxygen-18	Well samples (P1, P2, P5, P6 and M1)	University of Ottawa, Ontario
Deuterium and Tritium	Well samples (P1, P2, P5, P6 and M1)	University of Waterloo, Ontario
	Rideau Canal sample (07/89)	University of Waterloo, Ontario
Oxygen-18 and Deuterium	Pump test samples (P1, P2, P3, P4, P5, Elba 2, T1, T3, T4)	University of Waterloo, Ontario
	Rideau Canal sample (07/89)	University of Waterloo, Ontario
Carbon-14 (with Carbon-13)	Pump/Injection test sample (P2 to P4)	University of Waterloo, Ontario
Carbon-13	Drill cuttings (P2)	University of Ottawa, Ontario
	Secondary calcite in drill cuttings (P2)	University of Ottawa, Ontario

4.4 HYDRAULIC HEAD MONITORING

Hydraulic head measurements were made on all of the production and monitoring wells from September 1988 to August 1989.

The well monitoring program began just before the last pump and injection test and continued until construction for the groundwater project prevented access to the wells. Water levels were measured using an electric-contact, water-level tape. Water levels at the multilevel well were measured with a calibrated wire attached to the water-level tape circuit. A tube extension and measuring tape had to be used to measure the hydraulic head in tubes experiencing flowing artesian conditions. All well heads were surveyed to the nearest 0.001 masl.

Measurements were made on a daily, biweekly and then monthly basis. Measurements were made for most of October and November 1988 to record daily fluctuations, as well as any response to the draining of the Rideau Canal. These readings were taken at the same time of day; early evening. Head responses to precipitation events were monitored during the summer of 1989. Diurnal variations were monitored in late July and early August 1989.

The data were used to determine the hydraulic gradient across the campus, to record the temporal and spatial trends in the hydraulic head and to observe the groundwater system's response to climatic conditions. This information was used in conjunction with the pump test data in the characterization of the aquifers.

The corresponding climatic data for precipitation, temperature and atmospheric pressure were obtained from the Atmospheric Environment Service, Department of the Environment. The climatic data were recorded at the Ottawa International Airport weather observation station which is located 7.5 km south of the Carleton University campus.

Chapter 5

RESULTS

5.1 LITHOLOGY AND BOREHOLE GEOPHYSICS

5.1.1 Bedrock Topography

The bedrock topography, as derived from previous and recent drilling and building excavation records, is shown in Figures 11 and 12. As indicated by Michel (1985), in his preliminary estimate of the bedrock surface, there are three major steep sided valleys or lineaments that strike northwesterly across the study area. These depressions are not evident today at the study area (Figure 12) because of infilling by glacial sediments. The sharp, scarp-like sides of these valleys delineate the positions of the major faults within the study area. The cross faults were located using the results of the borehole stratigraphy.

5.1.2 Borehole Stratigraphy

The stratigraphic sequence encountered in each borehole was identified on the basis of drill cutting lithologies and borehole geophysical logs. An example of the percentage lithology logs, compiled from drill cuttings, is shown for well P5 in Figure 13. The complete set of lithology logs with interpretive notes can be

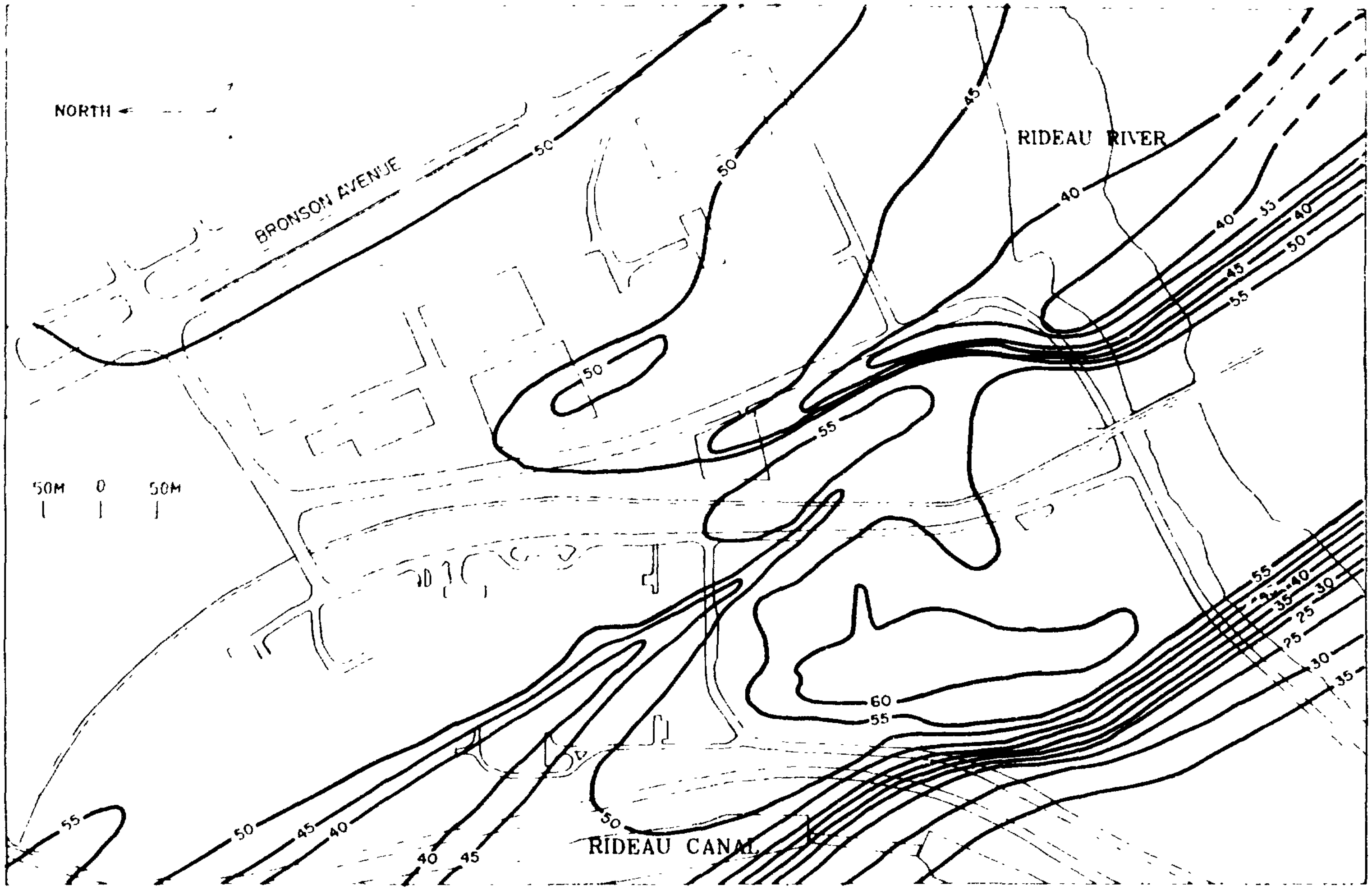

Figure 11 Bedrock surface contours in metres above sea level. Contour interval 5 m.

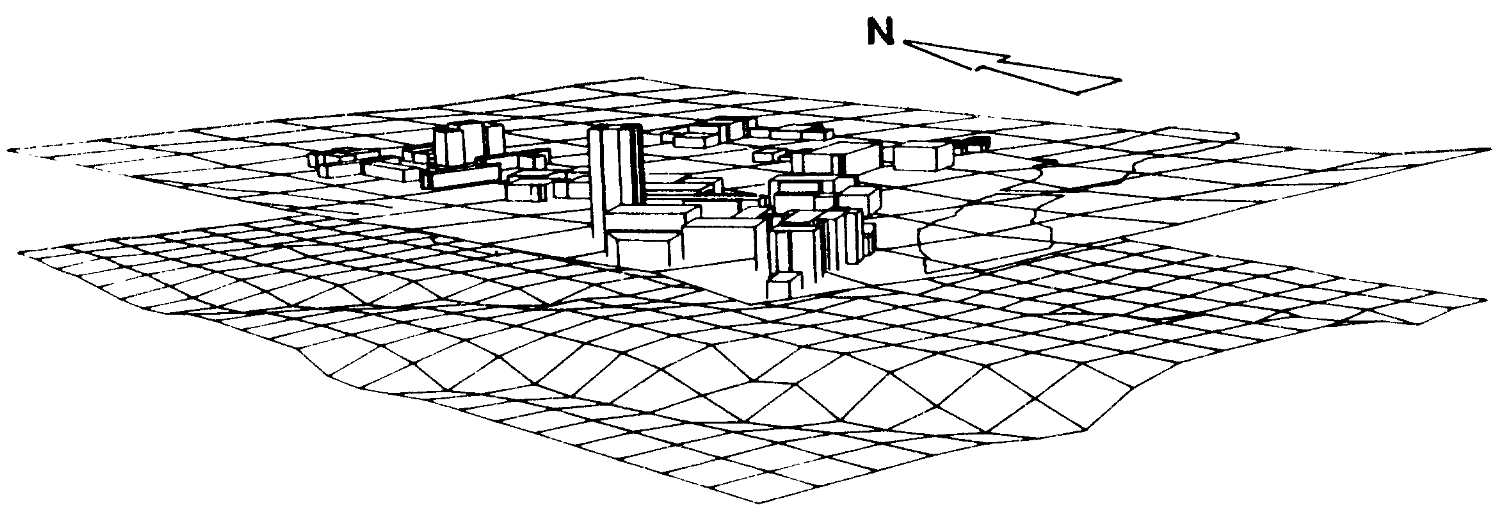

Figure 12 Three dimensional view of bedrock topography in campus subsurface. Vertical separation between bedrock surface and ground surface exaggerated.

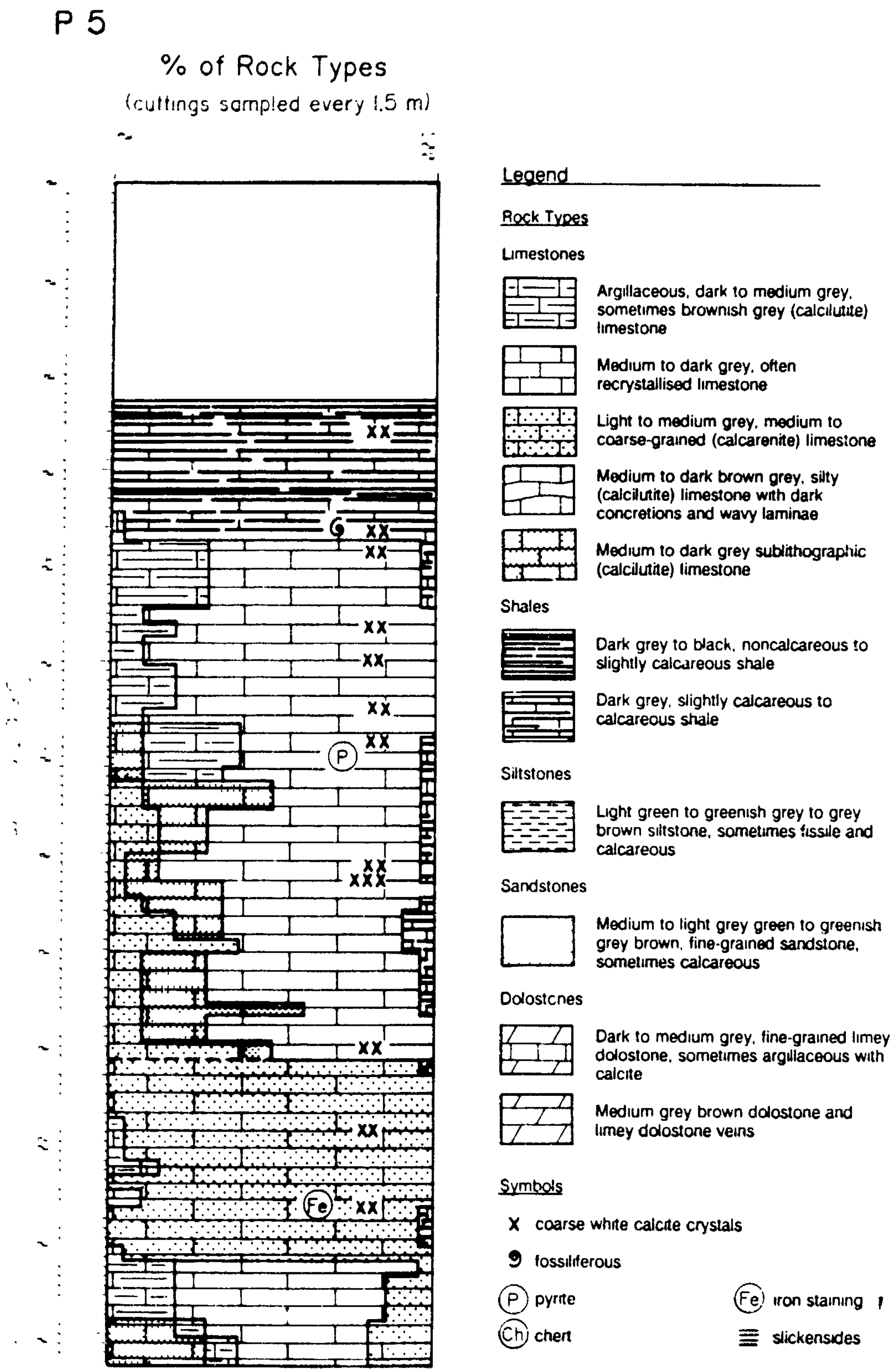

Figure 13 **Percentage lithology log for well P5.**

found in Appendix 2. The lithologies identified follow the descriptions of formations and formational contacts summarized in Table 1. Of the geophysical logs conducted, gamma ray and resistivity were found to be the most useful for verifying lithologies and for defining formational contacts.

Stratigraphic positions solely based on the lithology logs are questionable. This is due to the increased likelihood of significant mixing of cuttings from various depths during drilling as a result of the wide borehole, the rock types and the volume of water encountered. Examination of the gamma ray and apparent resistivity logs provided a means to verify the depth to certain shale-rich and pure carbonate beds, thereby confirming the stratigraphic positions of the boreholes. The shaly strata were identified by an increase in the gamma ray count rate and a decrease in resistivity values. The purer carbonate units are characterized by a marked decrease in the gamma ray count rate and an increase in the apparent resistivity (Keys and MacCary, 1971; Dyck et al., 1984). The lithology log along with the gamma ray and apparent resistivity logs for well P5 are shown in Figure 14 to illustrate the correlation between the logs. The suite of geophysical logs for each well can be found in Appendix 3.

Placement of the formational contacts was somewhat problematic because of the transitional nature of many of the contacts. The definition of the contacts is more suited to core or outcrop situations, such as the lower limit of shale interbeds greater than 5 cm thick (Eastview-Cobourg contact), or the lower limit

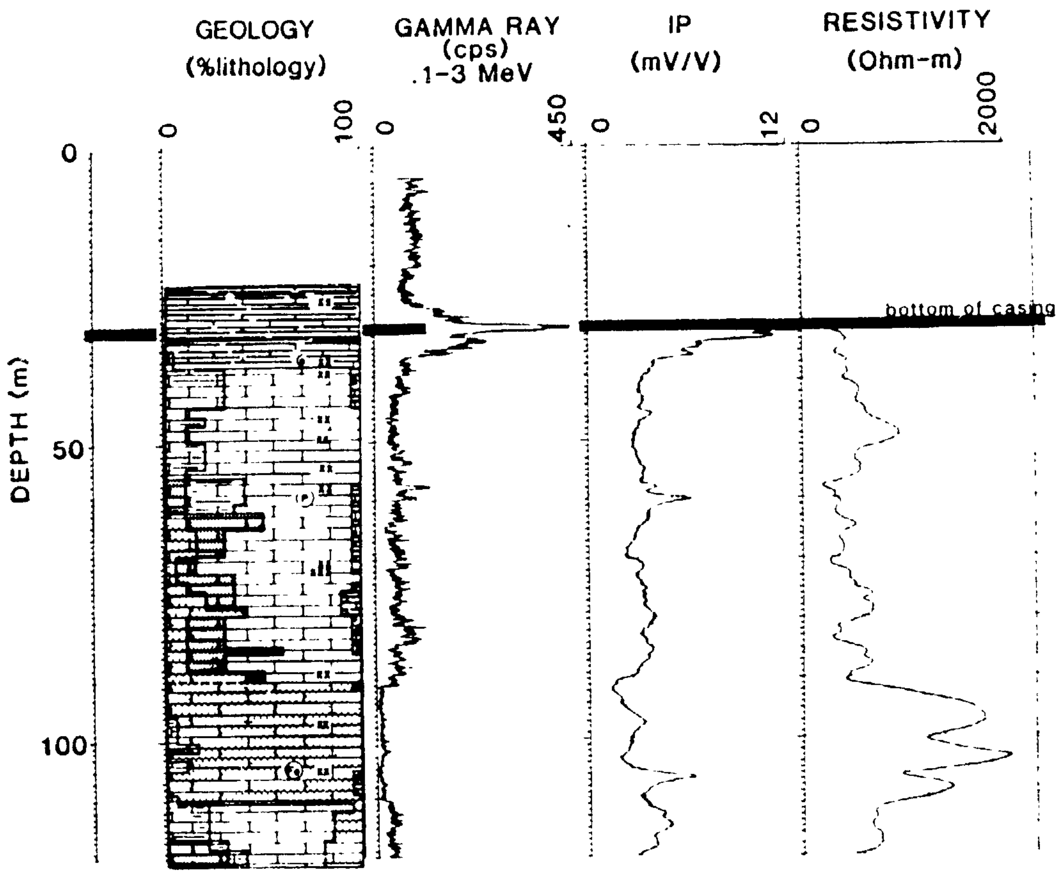

Figure 14 Correlation between the gamma ray spectra and electrical logs and the geological percentage log for well P5. Refer to Figure 13 for lithology log legend.

of the occurrence of limestone with a CaO/MgO ratio greater than 15 (Lowville-Pamelia). For such transitional contacts, the boundaries were placed in the middle of the transitional zone while keeping in mind the thicknesses reported for the various formations (Chapter 2, Table 1). An account of the placement of each formational contact, and the correlations made between lithologic and geophysical logs, can be found with the geological and geophysical logs in Appendix 3.

Figure 15 shows the relative stratigraphic position as determined for each of the logged boreholes. Information provided by the geophysical logs was also used to help define the stratigraphic position of wells that could not be accessed for geophysical logging (wells M1, T1, and T3). This stratigraphic information included the site specific range of thickness for the various formations, the presence of shale-rich and pure carbonate marker beds, and the verification of the presence of certain formations such as the St. Martin. The stratigraphic positions of the monitoring wells, M1, T1 and T3 are shown in Figure 15.

As illustrated in the generalised section, wells P2, P3, P5, P6 and Elba 2 intersect shales, shaly limestone and fine to coarse-grained carbonates. Wells P1, P4, T1, T3 and M1 intersect shaly limestones, siltstones, sandstones and dolostone.

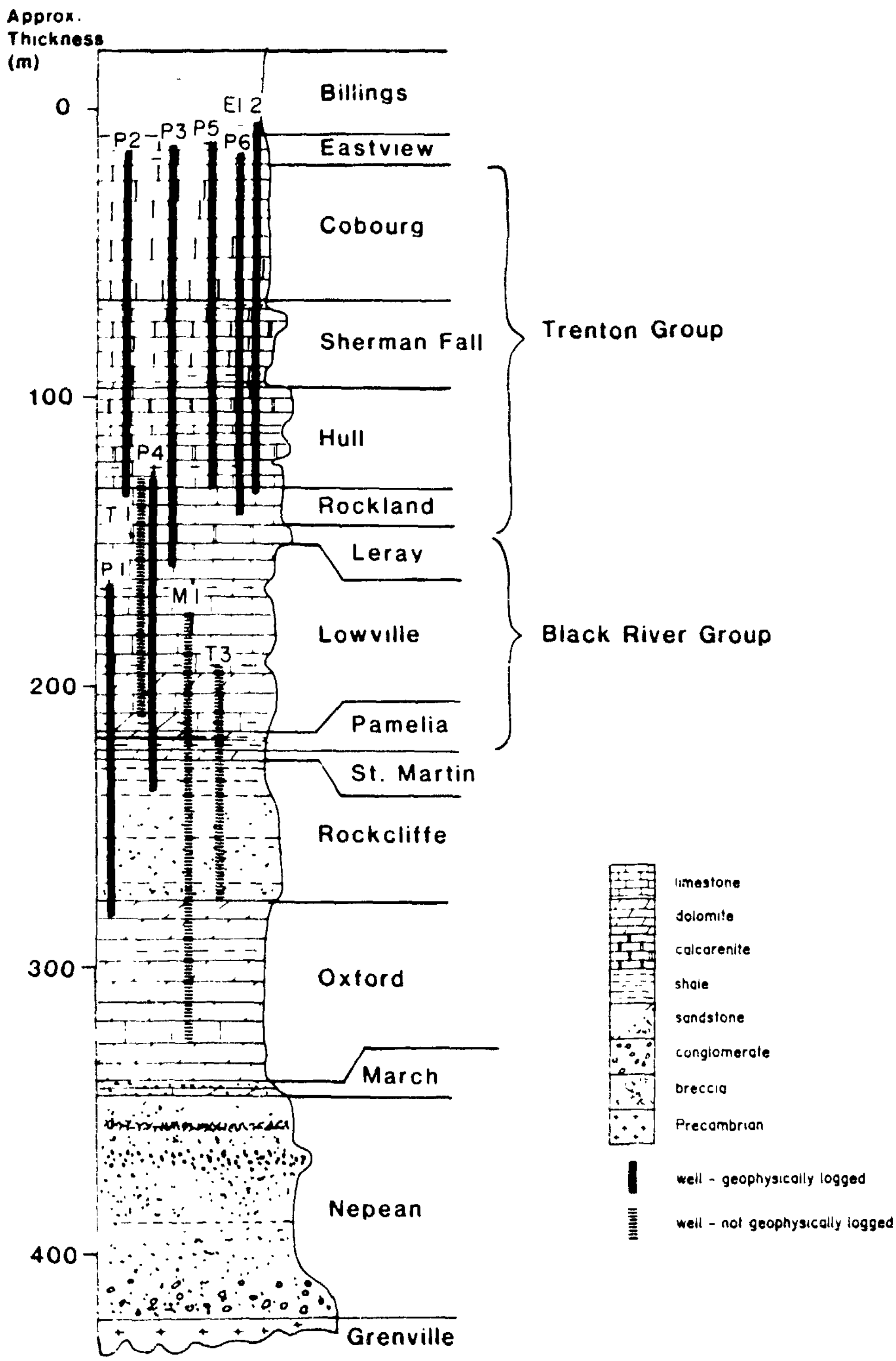

Figure 15 Generalized stratigraphic section with borehole positions.

5.1.3 Fractures

The location of fracture zones were identified in the boreholes from the induced polarization (IP), density and apparent resistivity logs. This interpretation is illustrated in Figure 16 for well P5. Fractures were identified by relative decreases in density and apparent resistivity values. In Figure 16, significant fracturing appears to occur in the shaly units at about 58 and 70 m and in a carbonate unit at 106 m.

In some boreholes, high IP values and low apparent resistivity values indicated the presence of pyrite and iron staining, which was later verified by examining the borehole cuttings under a binocular microscope. The presence of iron staining is a potential indicator of fractures or joints which have been or are open to the seepage and storage of groundwater (Lewis and Burgy, 1964).

5.1.4 Groundwater Movement

The parameters used to identify groundwater movement in each borehole were temperature and temperature gradient. The density log was also examined to see if there was any correlation between groundwater movement and identified fractures.

Temperature logs taken in thermally stable boreholes through a uniform geologic formation normally display nearly straight lines with a relatively constant slope.

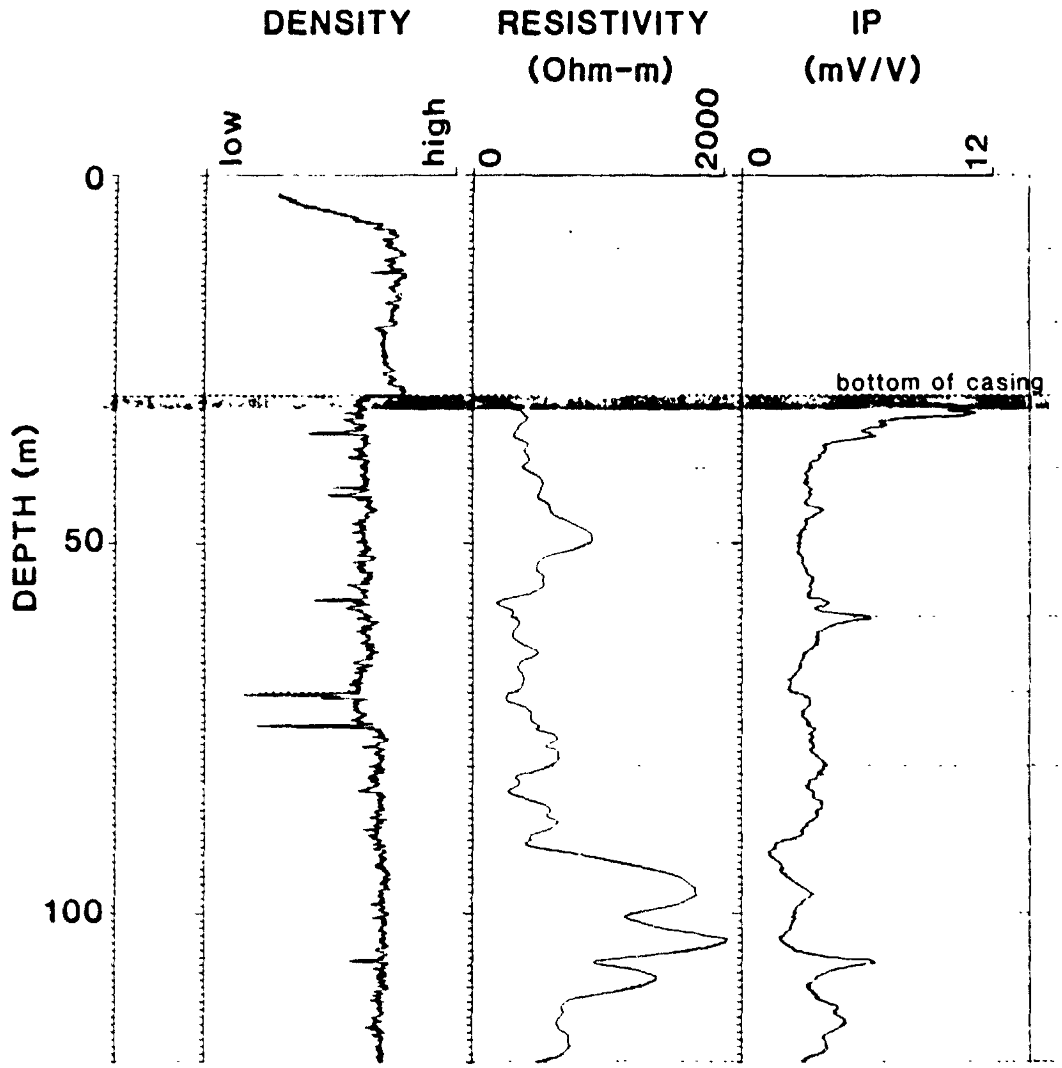

Figure 16 Comparison of density, apparent resistivity and IP logs for well P5. Relative decreases in density and resistivity, at 106 m for example, correlate with the increases in IP and the presence of iron compounds at the same depth.

The temperature increases slowly with depth at a rate corresponding to the local geothermal gradient. This gradient is a function of the thermal conductivity of the rock adjacent to the borehole and heat flow from below (Keys and Brown, 1978). Conaway (1987) suggested that changes in the slope of the temperature log can occur due to several factors, including:

1) variations in thermal resistivity of the rock with depth along the borehole;
2) surface climatic changes;
3) thermal effects of drilling and other procedures in the borehole;
4) local heat sources at depth, or heat sinks, such as groundwater movement outside the borehole;
5) disturbances of the borehole fluid such as free convection or fluid flow in the borehole; and
6) distortion of heat flow by complicated geological structure.

Factor 5 created the signals most useful in determining groundwater entry and exit points in groundwater filled boreholes. Flowing groundwater entering or leaving the borehole often results in an offset in the temperature log and a prominent spike in the temperature gradient profile (Conaway, 1987). The offset is caused by the differences in temperature between the water in the borehole and the water entering the borehole or a change in temperature in the borehole due to the exit of water (Conaway, 1987; Drury et al., 1984; Boldizar, 1958). Inflowing water may also be detected by irregular temperature changes. These changes are due to water movement during the mixing of inflowing water with water already in the borehole (Conaway, 1987).

Water movement within the borehole may also be due to convection, which results in the oscillation or "noise" in the temperature and temperature gradient readings. The probability that the groundwater in a borehole will be disturbed by convectional currents increases with both temperature and borehole diameter (Drury et al., 1984; Sammel, 1968).

The effects of factors 2 and 4, climatic changes and local heat sources, were also taken into account in the interpretation of the Carleton borehole temperature logs.

Surface climatic changes, such as seasonal air temperature fluctuations, are reported to produce thermal gradients large enough to cause significant convection in water filled wells. These are transient variations in borehole temperatures that have been observed to extend 10 to 30 m down a well (Sorey, 1971). Climatic changes associated with the last glaciation affect borehole temperature measurements down 400 m or more (Beck, 1977; Jessop and Judge, 1971). Therefore, the impact of those climatic changes would affect the entire profile of the Carleton University wells and would not account for discrete temperature variations in the logs. There is a temperature gradient reversal that is commonly observed in the top 100 m or less of deep wells in central and eastern Canada. This reversal and temperature minimum is thought to be the result of a gradual increase in the surface temperatures over the last 100 years (Drury et al., 1984; Lewis, 1975).

The impact of local heat sources, such as campus buildings and the tunnel system, on the temperature profiles of Carleton University wells was noted by Michel (1985). These heat sources are expected to affect the borehole temperatures to depths of several tens of metres.

Temperature disturbances caused by groundwater flow in the Carleton boreholes varied from slight to large enough to dominate the temperature field within the borehole. The entry and exit of groundwater, indicated by an offset in the temperature log and a prominent spike in the temperature gradient, are illustrated for well P5 in Figure 17. The temperature and temperature gradient logs and interpretive notes for all of the logged wells can be found in Appendix 4.

The movement of water along the borehole, between entry and exit points, is determined by the relative hydraulic heads; the water moves down gradient (Drury et al., 1984). If the velocity of the flow in the borehole is high relative to the distance travelled, the temperature log will approach a straight vertical line. This indicates isothermal conditions in the fluid along that part of the well. In such situations, the groundwater movement is substantial enough to dominate the temperature field within the borehole.

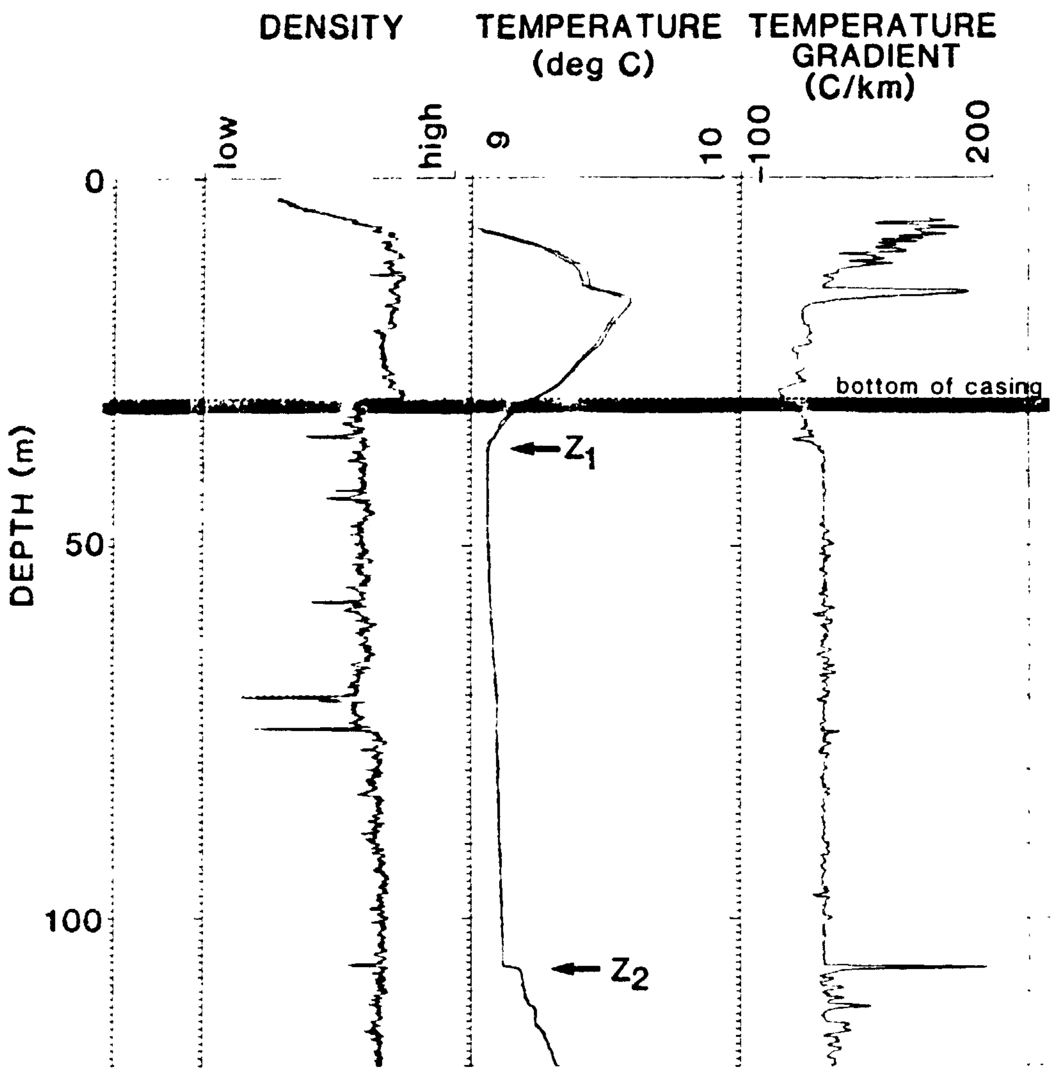

Figure 17 Correlation between the density, temperature and temperature gradient logs for well P5. Point Z_2 corresponds to a major groundwater entry point. The temperature profile between points Z_2 and Z_1 shows the effect of the upward movement of the groundwater from point Z_2.

This was the case within wells Elba 2, P2 and P5. In each well, the groundwater enters in discrete narrow zones or fractures at depth and flows upward. In the case of well P5, shown in Figure 17, some of the upward flowing groundwater exits in the upper part of the borehole. Isothermal conditions exist between the major entry and exit points, e.g., between points Z_1 and Z_2 (Figure 17). The irregular and transient variations in temperature readings in the upper part of the borehole are the result of surface temperature effects, and thermal effects from the surrounding buildings (Michel, 1985).

Groundwater entry and exit points were also identified in the logs for wells P1, P3 and P4. The vertical flow in these boreholes does not dominate the temperature field as in the other wells. Due to the absence of strong flow within the borehole, the temperature gradient reversal and temperature minimum are evident in the logs in these three wells (Appendix 4).

Temperature logs in P6 exhibit significant temperature fluctuations, including seasonal reversals in flow, throughout the entire depth of the borehole. These fluctuations are thought to be due to the inflow of shallow groundwater. It appears that there is significant downward flow within the borehole. Since the flow direction is determined by the vertical hydraulic gradient within the borehole, one must conclude that the shallow aquifer at the P6 site has at times a higher hydraulic head than most of the deeper aquifers. The vertical gradient changes over time as the various hydraulic heads change in response to seasonal climatic conditions. These fluctuations complicate the interpretation of the temperature logs, particularly the upper half.

The major groundwater entry points in wells P2, P3, P5, P6 and Elba 2 were all observed at a variety of depths within the Hull Formation. The major exit points, with the possible exception of P6, are all within the upper part of the Cobourg Formation, just below the borehole casing and grouting.

In the case of wells P1 and P4, the major entry points are near the top of the Rockcliffe Formation and in the St. Martin and Pamelia Formations. Well P1 also has a groundwater entry in the upper part of the Oxford Formation encountered at the bottom of the borehole. There are fluctuations from approximately 43 to 53 m in the P4 temperature log, which may be due to the diffuse groundwater inflow. This interval is located in the upper half of the Lowville Formation. The major exit point in P4 is located at the top of the Lowville Formation near the contact with the Leray Formation and a few metres below the borehole casing and grouting. In well P1, the major exit points appear to be in the lower half of the Lowville Formation.

The groundwater exit and entry points located in the wells by temperature logging correspond to some of the fractures identified by the density, resistivity and IP logs. The relative intensity of the density log peaks does not reflect the relative significance of those particular fracture zones for groundwater flow.

5.1.5 Discussion of Lithology and Borehole Geophysics Results

A summary of all the geological information derived from the borehole analysis is presented in Figure 18. The fault locations are adopted from the bedrock surface map (Figure 11). Based on the stratigraphic information compiled to date, the campus can be divided into six fault blocks which are identified in Figure 19 by the numbers Ia, Ib, Ic, IIa, IIb and III.

The fault blocks in which wells P2, P3, P5, P6 and Elba 2 are located (Ia, Ib, Ic) are downfaulted relative to the central and western blocks (IIa, IIb and III) (Figure 19). Wells in these eastern and northern blocks are constructed in shales, shaly limestones and fine to coarse-grained carbonates. The formations intersected range from the Billings (Elba 2) and Eastview Formations down to Hull and Rockland Formations. Minor vertical displacement between those wells, namely between Elba 2 and P3 and between P5 and P2, substantiate the existence of faults and cross faults within these eastern and northern sectors of the campus (Figures 15 and 19).

Most of the approximately 200 m vertical displacement which exists across the campus has occurred on the north-south fault and the cross fault between the central and eastern blocks (Figure 19). The cross fault is located between wells P1 and P2. The resulting juxtaposition of bedrock types is shown in Figure 18.

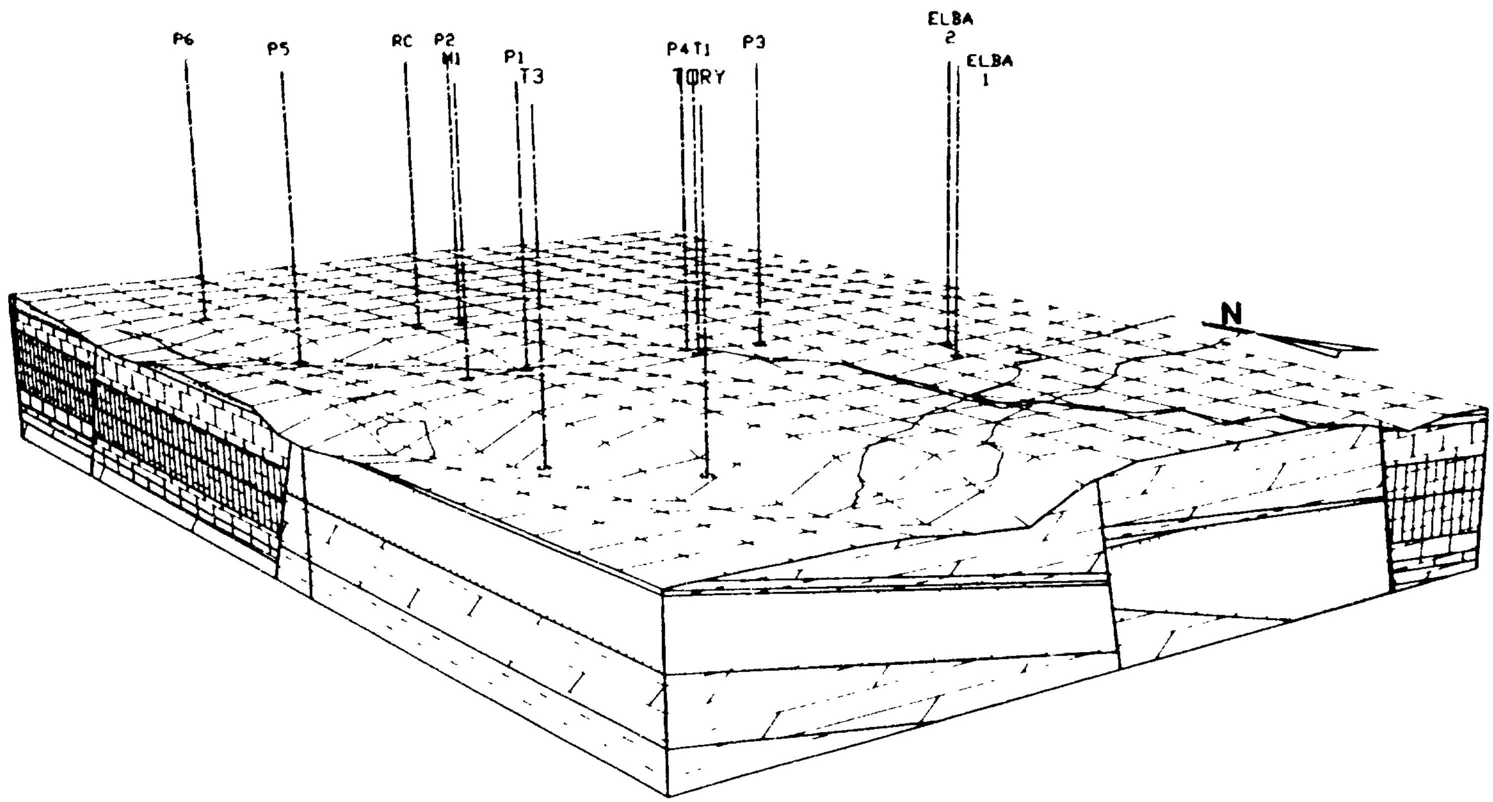

Figure 18   Block diagram of study area stratigraphy and faults.

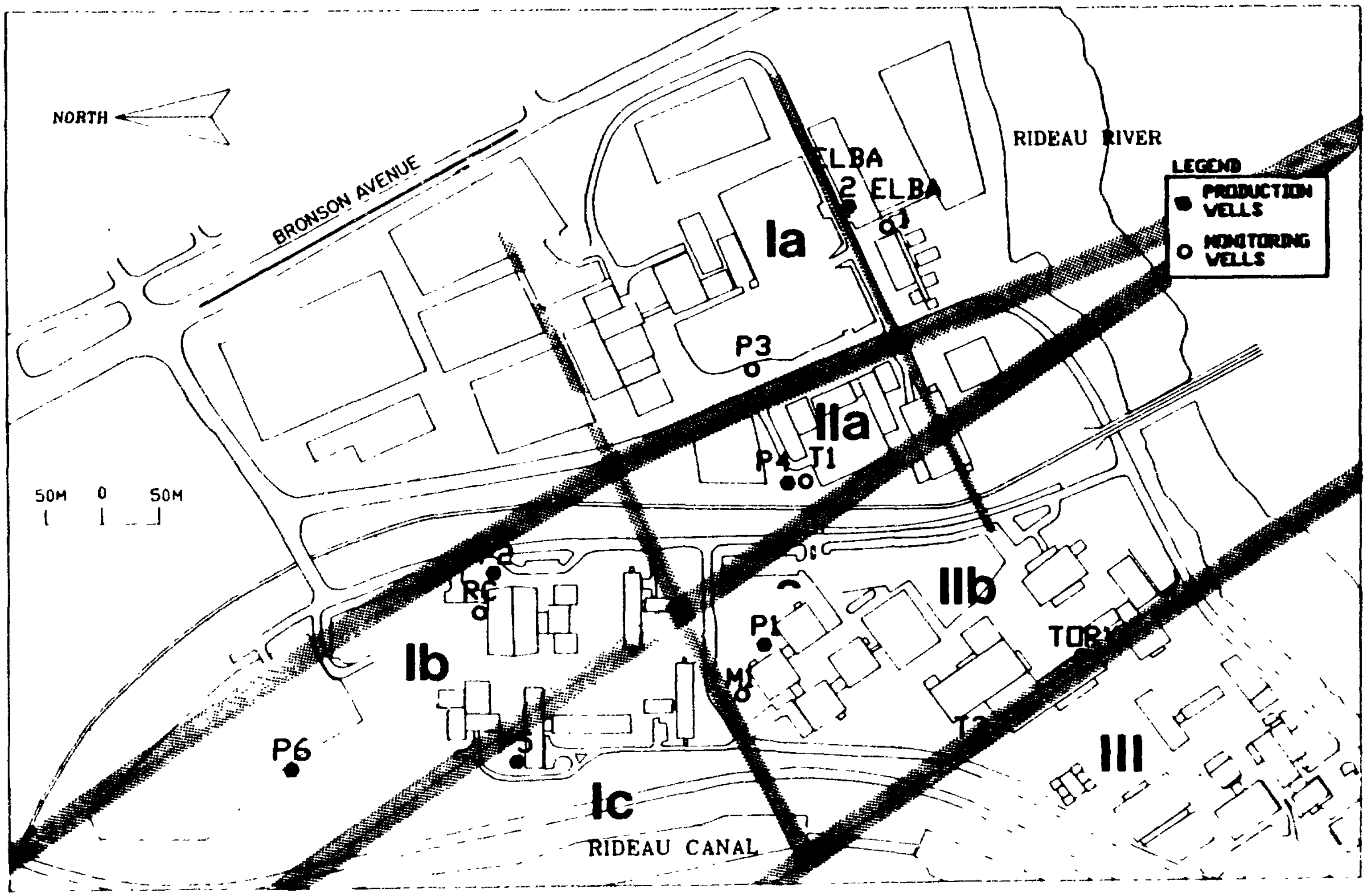

Figure 19 Location of major faults, cross faults and fault blocks within study area.

Wells located in the central blocks (IIa and IIb, Figure 19), namely wells P4, P1 and M1, intersect shaly limestones, shales, sandstones and dolostones. The formations intersected include the Rockland, Leray, Lowville, Pamelia, St. Martin, Rockcliffe and Oxford Formations.

The western fault block (III, Figure 19) starts stratigraphically lower than the central fault block. Well T3 is located on the eastern edge of this block and is constructed in carbonates, siltstones, shales and sandstones. The formations intersected range from the Lowville Formation down to the Rockcliffe Formation.

The other major section of information derived from the borehole analysis is groundwater flow in the boreholes. The locations of the groundwater entry and exit points identified in each logged well are shown in their geological context in Appendix 4.

It is assumed that the groundwater entry points located in the various wells coincide with the locations of the major water-bearing fracture (high permeability) zones. This assumption is based on the fact that the depths of most of the groundwater entry points agree with the depths of increased discharges which were noted during the well drilling. It is recognized that there was a 5 to 10 m margin of error in the drilling record.

The water-bearing fractures in fault blocks Ia, Ib and Ic are all located in the Hull Formation. One set of water-bearing fractures is situated in the upper third of this formation, within the massive calcarenite beds. Another major water-bearing zone is located at the base of the Hull Formation, near the contact with the Rockland Formation. The location of these water-bearing fractures within the fault blocks appears to be consistent stratigraphically from borehole to borehole.

There appear to be two major water-bearing fracture intervals in the IIa and IIb fault blocks. Water-bearing zones occur in the section from the Pamelia to the upper Rockcliffe Formations, and a fractured and potentially weathered zone at the Rockcliffe-Oxford Formational contact. The location of these high permeability zones remains relatively constant with respect to the stratigraphy within the individual (IIa and IIb) fault blocks.

The major groundwater exit points identified in the geophysical logs are also depicted in Appendix 4. Exit points in the boreholes of the Ia, Ib and Ic fault blocks are predominantly within the upper part of the Cobourg Formation, usually just below the grouted borehole casing. The exit points in the wells located in fault blocks IIa (P4) and IIb (P1) are within the top and lower half of the Lowville Formation, respectively. The exit of groundwater in these intervals may represent a significant loss of water from the wells due to seepage from the open boreholes.

The borehole logging also revealed the nature of the flow within the boreholes. With the exception of well P6, the predominant flow was upward, which suggests that the higher water pressures (higher hydraulic heads) are located at depth. This conclusion coincides with observations made at the time of well drilling. For well P6 there is a significant inflow from shallow aquifers and a downward flow from those shallow entry points. The fact that this well is hydraulically connected to shallow groundwater aquifers has significance for its use in the groundwater heat pump project, particularly for reinjection purposes.

No logged wells exist in fault block III.

5.2 GROUNDWATER GEOCHEMISTRY

There are two main purposes of the geochemical component of this study. One is to describe the basic geochemistry of the groundwater supply at the site, and second, if possible is to use the geochemistry to identify and interpret the effects of the various geologic controls on the groundwater flow pattern. The geochemical characteristics of the groundwater were determined by analyzing samples from the production and monitoring wells. Results from the laboratory analyses and field measurements are listed in Appendix 5. The charge balance error for each major ion analysed is also listed with these results. Some of the analysed samples have a significant positive charge excess; possible reasons for this are discussed in Subsection 5.2.3. The samples were collected down the boreholes at various levels in order to detect potential differences in water chemistry with depth. Some minor variations were detected and are noted in the following subsections. As discussed in Chapter 4.0, Methods, one well (P6) was sampled twice; two sets of results are listed for this well in Appendix 5. Due to a possible malfunction of the sampler, the first P6 sample set may not have been from the depths specified.

5.2.1 Major Ion Chemistry

Major ion chemistry for each well is plotted on trilinear diagrams in Appendix 6. A composite trilinear diagram of all well data is in Figure 20.

The study area waters fall into two categories based on differences in pH, major ion chemistry and total dissolved solids (TDS) values. One group of well samples, which are referenced as Type I groundwaters, has no dominant cation, while the anion composition is dominated by approximately equal concentrations of bicarbonate and chloride ions. The groundwaters of Type I chemistry, plot in the vicinity of P5, as shown in Figure 20. The chemical composition of the second group of samples, labelled Type II, is dominated by sodium and chloride ions, with minor concentrations of calcium, magnesium, sulphate and bicarbonate ions. In Figure 20, the Type II groundwaters plot in the vicinity of samples M1.

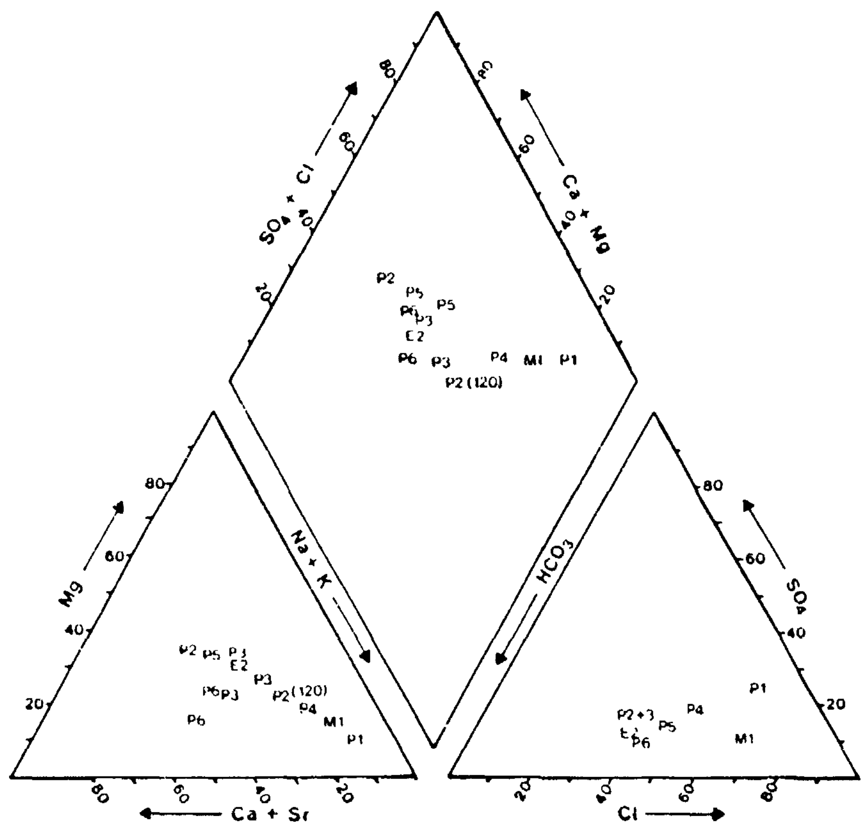

Figure 20 Trilinear diagram showing the major ion composition of wells in study area.

The electrical conductivity and pH values of samples from wells P2, P3, P5, P6 and Elba 2 (Type I) average 1100 μS/cm and 7.8, respectively. The TDS values of these samples range from 500 to 924 mg/L. The conductivity and pH values of samples from wells P1, P4 and M1 (Type II) average 2268 μS/cm and 8.2, respectively. The TDS content of the Type II waters range from 612 to 1852 mg/L.

Characterisation of Type I (Low Conductivity) Samples

The trilinear plots of all the samples from each Type I well are shown in Appendix 6.

The samples with low conductivity are from wells located in the eastern and northern fault blocks. Shale, argillaceous limestones and fine to coarse-grained crystalline limestone are the bedrock types intersected by this group of wells. To determine the possible relationship between this groundwater type and the surrounding lithologies, an attempt was made to identify the sources of the ionic constituents found in the groundwater. These sources may be determined by an examination of the ionic relationships plotted in Figures 21 to 23.

The first ionic relationship considered is between sodium and chloride ion concentrations (Figure 21). A line representing halite as the sole source of the sodium and chloride ions in the groundwater is marked on the graph. The linear concentrations of iron, manganese, calcium, sodium, bicarbonate, chloride and dissolved carbon dioxide, as well as lower pH, and lower potassium and strontium concentrations than the other Type I samples. The Fe and Mn concentrations are at least one order of magnitude greater than those found in any of the other wells, including Type II wells. These differences may be due to the inflow of shallow groundwater identified by the temperature logs (Section 4.3). The iron and manganese concentrations may result from the interaction of the shallow groundwater with metal debris buried within the landfill overlying the bedrock. Pieces of this metallic debris were encountered during drilling of the P6 well.

The low magnesium and strontium concentrations may also be the result of inflowing shallow groundwater which has less Mg^{2+} due to the lack of contact with magnesium and strontium enriched limestones and shales. The saturation indices listed in Appendix 5 show that the P6 waters are supersaturated with respect to calcite, but just saturated to undersaturated with respect to dolomite. Higher Ca^{2+} and HCO_3^- concentrations and lower pH values indicate that the P6 well waters are in equilibrium with surrounding carbonates at (high) P_{CO_2} levels typical of open system dissolution (Drever, 1982; Holland et al., 1964). As expected, the waters of well P6 have the highest Eh readings. The field Eh measurements of the Type I wells range from -189 to -69 mV (-440 to -320 mV by Pt electrode), indicating a pervasively reducing environment. The readings from well P6 average greater than -49 mV (-300 mV by Pt electrode).

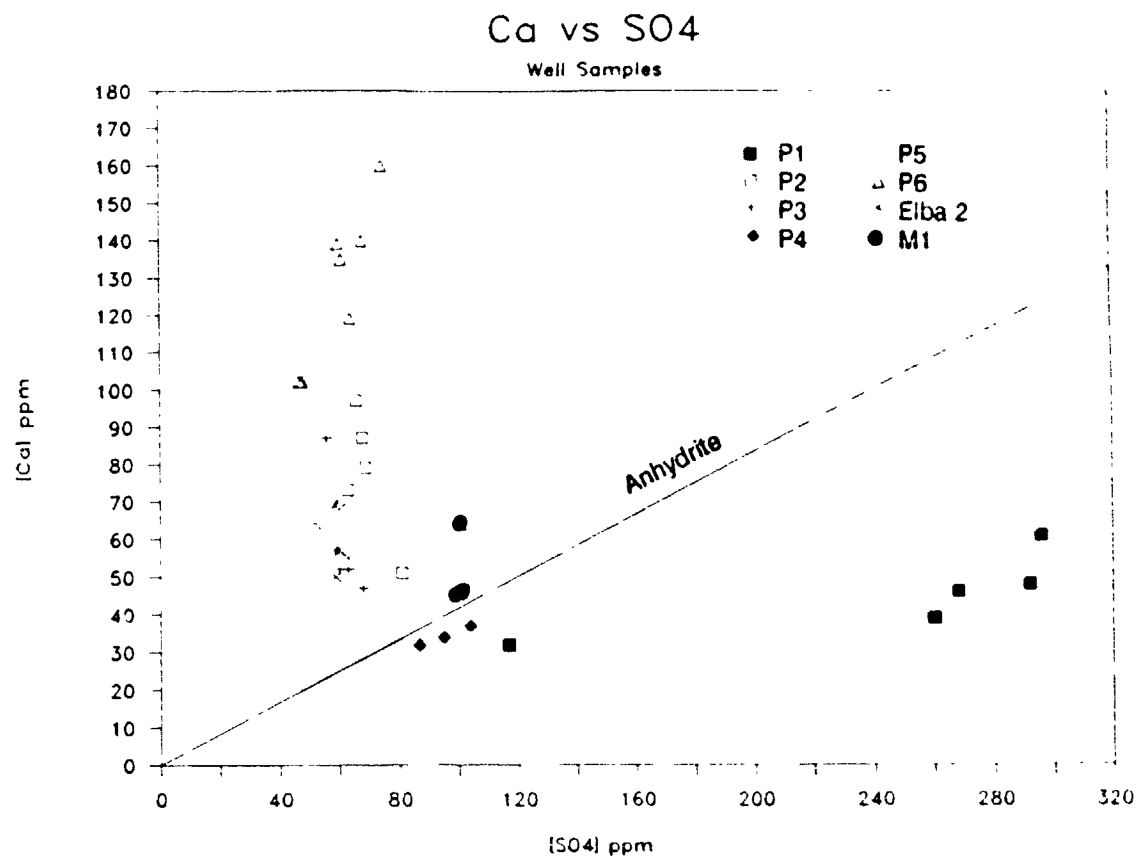

Figure 22 [Ca^{2+}] versus [SO_4^{2-}] plot of well water samples.

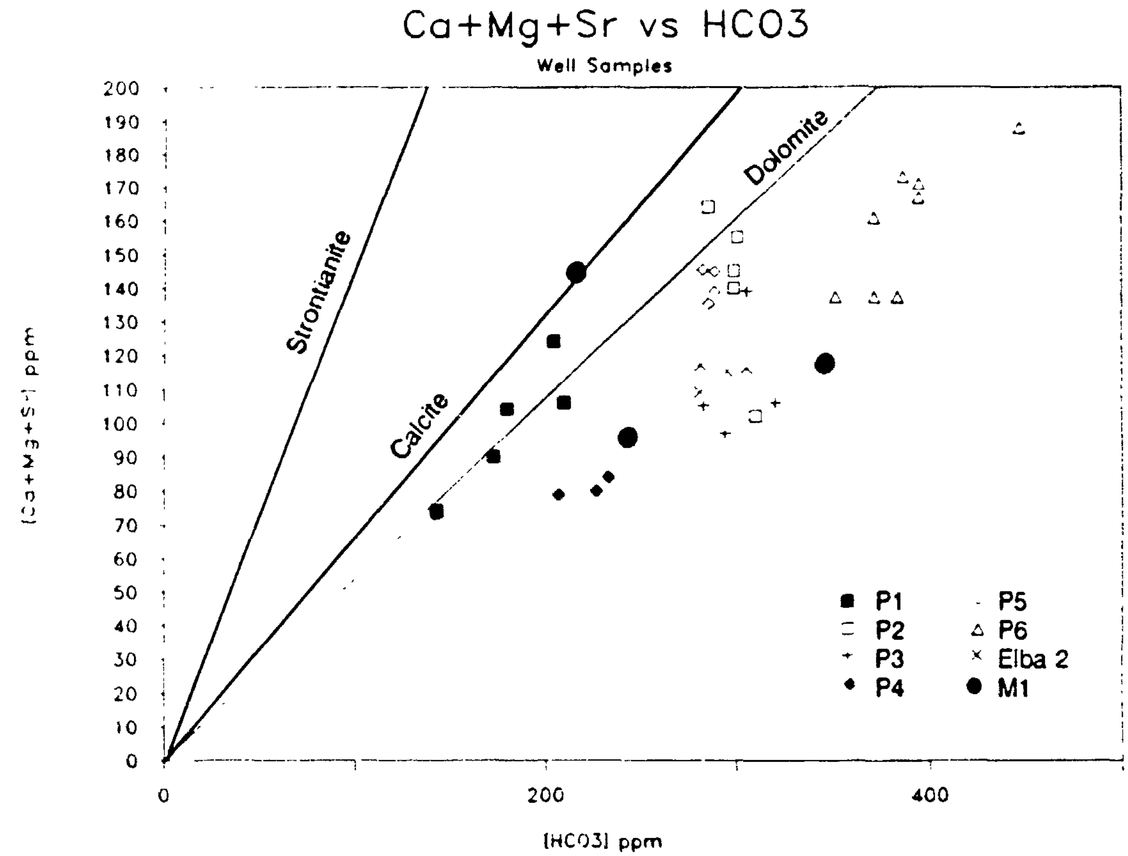

Figure 23 $[Ca^{2+}, Sr^{2+}, Mg^{2+}]$ and $[HCO_3^-]$ plot of well water samples.

relationship between the sodium and chloride ions of Type I samples is evident from the plot. Most of the data points from wells P2, P3, P5, P6 and Elba 2 lie on or are very close to the halite line, which indicates that dissolution of halite is the primary source of Na^+ and Cl^- in Type I groundwaters. Those samples which plot just below the line reflect a slight excess in Cl^- which may be due to the dissolution of very minor amounts of sylvite (KCl). The deep sample from well P2, P2-122 m, contains excess sodium that was probably acquired through cation exchange, where calcium, magnesium, and potentially strontium ions have been preferentially adsorbed onto clay surfaces in shale units, while sodium has been released into the groundwater.

Calcium and sulphate ion concentrations are plotted along with the anhydrite ($CaSO_4$) dissolution line in Figure 22. Type I samples, all of which have lower sulphate concentrations than the Type II water samples, plot above the line to such an extent that the calcium concentration increases significantly with no increase in the sulphate concentration. This suggests that the chemistry of Type I waters is dominated by carbonate dissolution with a minimal amount of gypsum dissolution.

The other major ionic relationship considered, is the calcium and magnesium ion concentrations versus the bicarbonate ion concentration. Since strontium is present in significant quantities, and since it parallels calcium in chemical behaviour, the strontium ionic concentration is included in the ionic relationship plotted in Figure 23. The dissolution lines for calcite, dolomite and strontianite ($SrCO_3$) are also included on the graph.

The sample points that plot on or close to the lines represent those groundwaters which have compositions dominated by carbonate dissolution. Type I groundwater samples plot below the calcite, dolomite and strontianite dissolution lines suggesting a significant loss of Ca^{2+}. This calcium ion loss may be due to $CaCO_3$ precipitation. The saturation indices listed in Appendix 5, show that there is widespread saturation with respect to calcite, strontianite and dolomite in these groundwaters. The Ca^{2+} loss is particularly evident for wells Elba 2, P6 and P3.

The [Ca]+[Sr]/[Mg] ratios of the samples, listed as averages in Table 3, also suggest a deficiency in calcium and/or an excess of magnesium in the groundwater ([Ca]+[Sr]/[Mg]$<$1.5) (Freeze and Cherry, 1979; Langmuir, 1971). The higher magnesium concentrations may be in part due to the dissolution of magnesium enriched limestones. Limestones of the Black River Group of Eastern Ontario (Table 1) are reported to contain higher than average percentages of magnesium carbonate (Goudge, 1938). The CaO/MgO ratio of local samples from the Cobourg Formation, a formation that is intersected by the Type I wells, is as low as 15/1.

Four samples in the Type I group, all from well P6, have relatively high [Ca]+[Sr]/[Mg] ratios (2.2 to 4.1). The P6 groundwater also has higher

Table 3 Average Ca/Mg and (Ca+Sr)/Mg ratios

Well	$[Ca^{2+}]/[Mg^{2+}]$	$([Ca^{2+}]+[Sr^{2+}])/[Mg^{2+}]$
P1	0.95	1.20
P2	1.12	1.27
P3	1.10	1.26
P4	0.70	0.86
P5	0.85	1.01
P6	2.25	2.33
P6(2)	3.46	3.52
Elba 2	0.85	0.99
M1	0.81	1.01

concentrations of iron, manganese, calcium, sodium, bicarbonate, chloride and dissolved carbon dioxide, as well as lower pH, and lower potassium and strontium concentrations than the other Type I samples. The Fe and Mn concentrations are at least one order of magnitude greater than those found in any of the other wells, including Type II wells. These differences may be due to the inflow of shallow groundwater identified by the temperature logs (Section 4.3). The iron and manganese concentrations may result from the interaction of the shallow groundwater with metal debris buried within the landfill overlying the bedrock. Pieces of this metallic debris were encountered during drilling of the P6 well.

The low magnesium and strontium concentrations may also be the result of inflowing shallow groundwater which has less Mg^{2+} due to the lack of contact with magnesium and strontium enriched limestones and shales. The saturation indices listed in Appendix 5 show that the P6 waters are supersaturated with respect to calcite, but just saturated to undersaturated with respect to dolomite. Higher Ca^{2+} and HCO_3^- concentrations and lower pH values indicate that the P6 well waters are in equilibrium with surrounding carbonates at (high) P_{CO_2} levels typical of open system dissolution (Drever, 1982; Holland et al., 1964). As expected, the waters of well P6 have the highest Eh readings. The field Eh measurements of the Type I wells range from -189 to -69 mV (-440 to -320 mV by Pt electrode), indicating a pervasively reducing environment. The readings from well P6 average greater than -49 mV (-300 mV by Pt electrode).

Elevated sodium and chloride concentrations in the P6 waters may be caused by the migration of road salt runoff from an adjacent parking lot. This is a form of contamination which has been shown to affect shallow groundwaters (Langmuir, 1971). There are no corresponding increases in potassium concentration that would suggest that cation exchange has played a significant role in the accumulation of the Na^+ ions.

Characterisation of Type II (High Conductivity) Samples

These samples were collected from wells P1, P4 and M1, which are located in the central fault block and therefore intersect shaly and dolomitic limestone, siltstone, sandstone and dolostone formations. Type II samples are also included on the ionic relationship plots (Figure 21 to 23). On the sodium versus chloride graph, Type II samples generally plot above the halite dissolution line. This suggests that Type II groundwaters contain a considerable amount of excess sodium, probably acquired through cation exchange where calcium, magnesium, and potentially strontium ions have been preferentially adsorbed onto the clay surfaces while sodium has been released into the groundwater. The P1 samples have undergone the most extensive amount of cation exchange, possibly due to a longer flow path and/or the abundance of shale in the formations within which the aquifer(s) are found. Sample M1-122 m is the one exception, since it falls just below the NaCl line, indicating a slight excess of Cl^-. This may, as in the case of the Type I samples, be due to the dissolution of very minor amounts of sylvite (KCl).

Calcium and sulphate ion concentrations are plotted along with the anhydrite ($CaSO_4$) dissolution line in Figure 22. All of the Type II samples have high sulphate concentrations and, with the exception of the M1 samples, plot just below, to substantially below the gypsum line. This could be due to Ca^{2+} loss through precipitation and/or cation exchange. Based on the observations made regarding the NaCl plot, the loss of calcium ions from the P1 samples, and possibly the P4 samples, is probably attributable to cation exchange. Samples can also plot below the gypsum dissolution line due to the addition of sulphate from a source other than gypsum, such as the oxidation of sulphide minerals. The latter process is unlikely to have occurred in the subsurface of the study area because of the reduced nature of the groundwaters. The field Eh measurements of the P1 and P4 samples range from -9 to -180 mV (-430 to -260 mV by Pt electrode). Oxidation of sulphide in the samples potentially could have occurred at the time of sampling and/or in the laboratory. Field measurements of H_2S are all higher than the lab values for the same samples.

The M1 samples, particularly M1-122 m, plot above the gypsum dissolution line. This suggests that the M1-122 m waters may be more dominated by carbonate dissolution than the other Type II samples and/or the waters in M1-122m sampling interval have undergone sulphate loss by sulphate reduction to hydrogen sulphide.

The calcium, strontium and magnesium concentrations versus the bicarbonate concentrations for the Type II waters are also plotted on Figure 23. The P1 samples of this group straddle the dolomite line, suggesting that dolomite dissolution is a major factor in the chemistry of these waters. The M1-122 m sample plots on the calcite line. This suggests, as noted above, that the plotting of the M1-122 m sample above the gypsum line in Figure 22, is due to the dominance of carbonate dissolution and not to sulphate loss. The P4 samples and the remaining M1 samples fall below the dolomite line. These groundwaters may have undergone loss of Ca^{2+}, and Sr^{2+}, due to calcite precipitation. The P4 and M1-82 m samples both contain excess Mg ($[Ca]+[Sr]/[Mg]<1$) and are saturated to supersaturated with respect to calcite, dolomite and strontianite (Appendix 5). In light of the results of the sodium versus chloride plot, some of the Ca^{2+} loss observed in the P4 and M1-82m samples is probably also due to cation exchange.

The samples from well P4, have noticeably lower TDS values than the other Type II samples. This difference in TDS values was not evident in the pump test samples (Section 3.2). In comparison to the other Type II well waters, the P4 well samples also have lower concentrations of all the major cations, except magnesium, and lower chloride concentrations. In the trilinear plot, Figure 20, the P4 samples fall on a straight line between Type II and Type I.

5.2.2 Isotopic Analysis

Groundwater from all of the production and monitoring wells was analysed for its oxygen-18 and deuterium (^2H) contents. Measured $\delta^{18}O$ and δ^2H values for each sample, including well and pump test samples, are listed in Appendix 7 and plotted in Figure 24. The Ottawa area Meteoric Water Line (MWL), as well as the isotope values of a surface water sample (from the Rideau Canal), are plotted with the groundwater samples.

The measured $\delta^{18}O$ values for the study area groundwaters range from -12.7 $^{\circ}$/oo to -9.2 $^{\circ}$/oo . This range of values is within the range exhibited by local modern precipitation (Figure 25), which suggests that all of the groundwater tapped by the wells was recharged from local precipitation during climatic conditions similar to the present.

In Figure 24, groundwater from wells P2, P3, P5, P6, and Elba 2 (Type I waters) plot below the MWL and on the lower margin of the precipitation scatter envelope of Figure 25. The P6 samples, plot a bit lower than the other Type I samples.

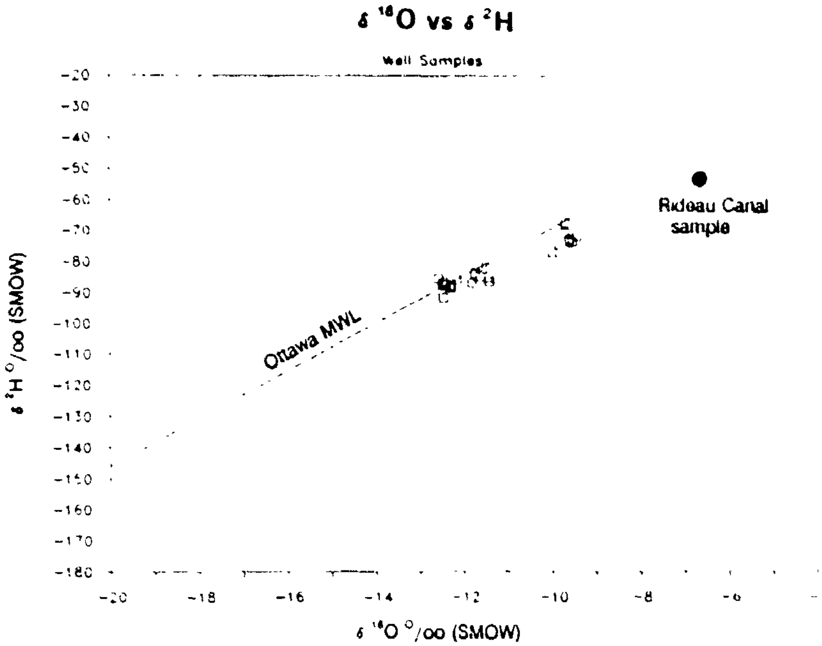

Figure 24a Plot of $\delta^{18}O$ and $\delta^{2}H$ values for well and pump test samples plotted with Ottawa area Meteoric Water Line (MWL) (Fritz et al, 1987) and Rideau Canal surface water sample.

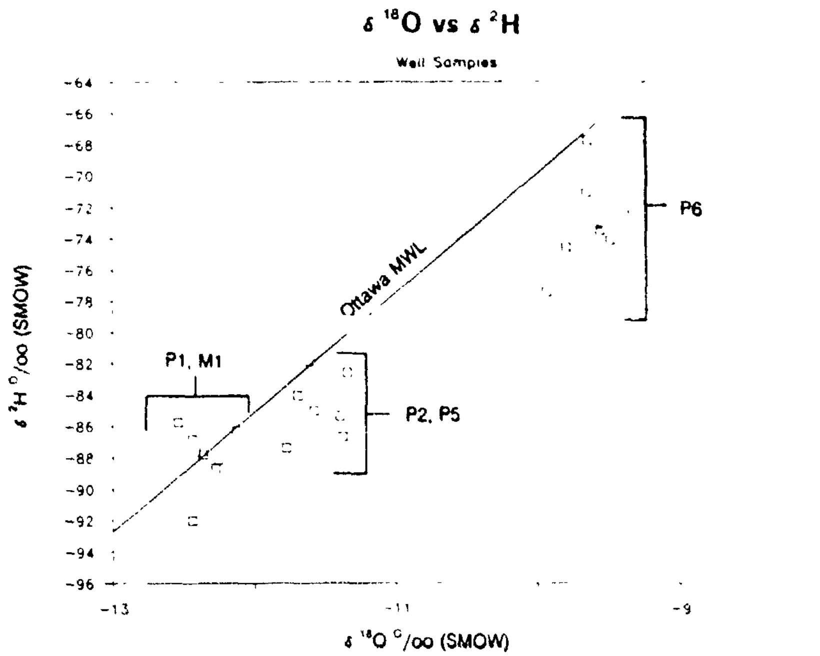

Figure 24b Detail of Figure 24a.

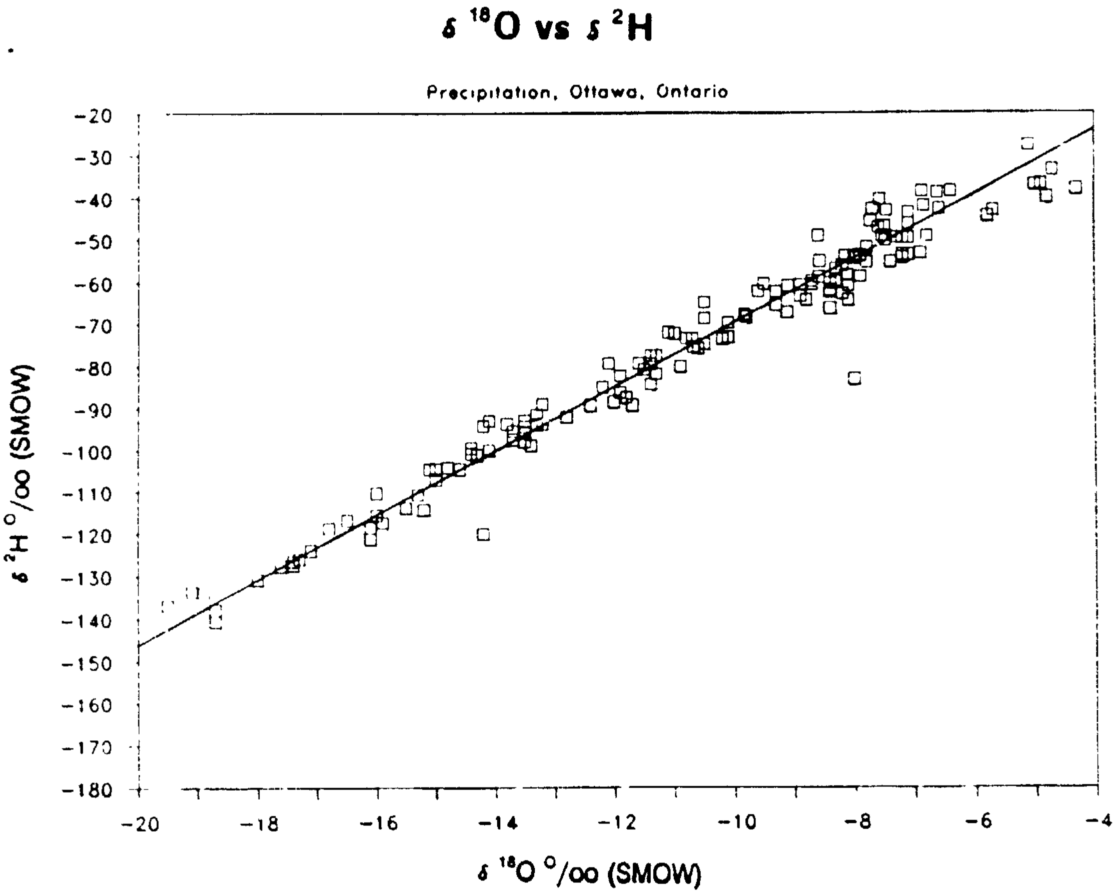

Figure 25 Plot of $\delta^{18}O$ and $\delta^{2}H$ values for Ottawa area precipitation (1975 to 1989). Data for individual samples from R. Drimmie, University of Waterloo (pers. comm.). Ottawa MWL from Fritz et al. (1987).

Type II groundwater samples, from wells P1, P4, T1 (the monitoring well of P4) and M1, all plot on or very close to the MWL and within the precipitation envelope.

The local surface water sample from the Rideau Canal plots below the MWL, and just on the outside edge of the precipitation envelope. The plotting of this sample illustrates the isotope effects associated with evaporation of surface waters. The P6 well samples may also exhibit, but to a lesser degree, the effects of evaporation (Figure 24). This indicates that there could be an influx of shallow (unsaturated) groundwater into the well. Figure 24 also shows that there are consistent differences in the oxygen-18 and deuterium values of the Type I versus Type II waters. The Type I samples plot in a less negative range than the Type II waters. These dissimilar values may be due to differences in temperature effects at the time of recharge, the Type I waters being recharged at times of warmer temperatures. This indication of possible differences in recharge conditions, between the two types of groundwater, supports the assumption that the groundwater types are associated with two different flow systems.

Determination of the mean residence time of the groundwaters was attempted using both tritium and carbon-14 dating. The data from these analyses are listed in Appendix 7. For the Type II samples, from wells P1 and M1, no measurable tritium was detected. This suggests that the mean residence time for the Type II groundwater is at least 35 years. The tritium levels in samples from the Type I

2

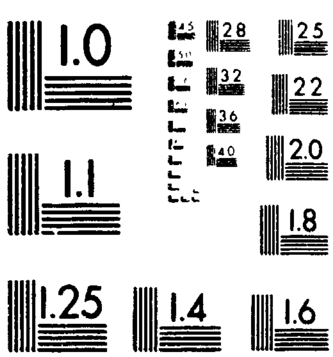

MICROCOPY RESOLUTION TEST CHART
NATIONAL BUREAU OF STANDARDS
STANDARD REFERENCE MATERIAL 1010a
(ANSI and ISO TEST CHART No 2)

wells, P2, P3, P5 and P6, ranged from 15 +/- 8 to 41 +/- 8 T.U. and yielded mean residence times that correspond to recharge in the pre-1957 or post-1971 periods (Michel et al., 1984).

The carbon-14 activity for P2 pump test sample was 48 +/- 2 pmC. This activity represents a radiocarbon mean residence time of 3400 to 4000 years as determined with use of the Pearson mixing model (Clark, 1984) and a carbon-13 dilution factor of 0.75. The data used in this calculation are included in Appendix 7.

The apparent discrepancy between the tritium and radiocarbon mean residence times for the Type I sample could be due to subsurface mixing of groundwaters of different mean residence times and/or to carbonate dissolution and precipitation processes. Calcite saturation and precipitation are widespread in the groundwaters of the study area and would result in the addition of a component of radiogenically dead carbon to the dissolved carbonate content. Thus, the maximum age of the groundwater sampled is 4,000 years, but it could be much less.

5.2.3 Discussion of Groundwater Geochemistry

From the relationships of the major ionic constituents discussed in Section 5.3.1, it is apparent that the general character of the two groundwater types are substantially controlled by two processes: carbonate dissolution, and cation exchange. These two processes have affected the two groundwater types to different degrees. In both cases, the major constituents of the study area groundwater can be directly related to the bedrock units in which the respective wells are located.

The chemical character of the Type I well waters is dominated by the dissolution of limestones, potentially Mg enriched limestones. The effects of cation exchange, such as the replacement of calcium, magnesium and strontium ions in solution by sodium ions, is evident, but the process plays a minor role in the chemistry of these samples. The exchange is facilitated by the abundance of shale units and interbeds in the surrounding bedrock. The presence of chloride, and additional sodium, can be attributed to the dissolution of very minor amounts of halite within the shale and carbonate beds.

The chemical character of the Type II well waters is the result of the dissolution of carbonates, limestones and dolostones, and cation exchange. Cation exchange appears to play a much more dominant role in the chemistry of the Type II samples, and is probably the major source of sodium ions in these groundwaters. The comparatively greater influence of cation exchange on the Type II waters, than on the Type I waters, may be due to a combination of the lithology of the wells and a longer mean residence time of the waters. In the formations within the central fault blocks, where these wells are located there is an abundance of shale. Dissolution of minor amounts of NaCl is the probable source of the chloride ions.

Saturation index data (Appendix 5), verify that all groundwaters sampled are saturated, or at least near saturation with respect to calcite and dolomite. Such saturated, and even supersaturated conditions, are not uncommon in carbonate aquifers (Freeze and Cherry, 1979; Back and Hanshaw, 1970; Holland et al., 1964). The maintenance of supersaturation conditions, within the Carleton aquifers, may be due to the combined influence of cation exchange, the ionic strength of the groundwater solution and common ion effects.

The fact that the groundwaters are supersaturated may provide an explanation for the positive charge balance error in the chemical analysis. The suspended $CaCO_3$ in the samples, which could have formed as a result of temperature changes during sampling or the inclusion of minute suspended carbonate particles, may have caused an overestimation of Ca, Sr, and Mg concentrations. Given the level of supersaturation in these groundwaters, all future chemical samples should be filtered when sampled and kept refrigerated until analysed.

Although it is not uncommon for groundwater in carbonate terrains to be saturated with respect to calcite and dolomite, it is not as common for groundwater to be saturated with respect to strontianite (Hem, 1985). All of the well samples, with the exception of the P6 samples, have notably high strontium concentrations. The usual source of strontium in groundwater is mainly from trace amounts found in all limestones. Other potential sources include strontianite ($SrCO_3$) and celestite ($SrSO_4$), both of which usually occur as beds or lenses disseminated in the limestone (Skougstad and Horr, 1963). However, Figures 26 and 27 show that there is little if any correlation between the dissolution lines of these two minerals and the ionic concentrations within the groundwater samples. Strontium can also be adsorbed by clay minerals in shales through ion exchange. The fact that the strontium values, of the P6 well samples are an order of magnitude lower than those from the other wells suggests that the Sr source is from deeper formations. As noted previously, the geochemistry of the P6 well samples is affected by the influx of shallow groundwater.

It should be noted that in the case of wells, P4 and P6, there are significant differences in the chemical composition of the pump test samples compared to the well samples. In well P4, the TDS values from the downhole samples average 660 mg/L while the pump test samples average about 1400 mg/L. The pump test samples of well P6 have TDS values of approximately 550 mg/L, while the well samples average 720 mg/L TDS. The difference between the static well and pumped well samples for P6 may be attributed to the impact of the inflowing shallow aquifer water. It appears that when the well is pumped, the water from the deeper aquifers supply the major component, if not all, of the discharge water. In the case of well P4, the pumped samples are closer in chemical composition to the other Type II samples than the static well P4 samples. The

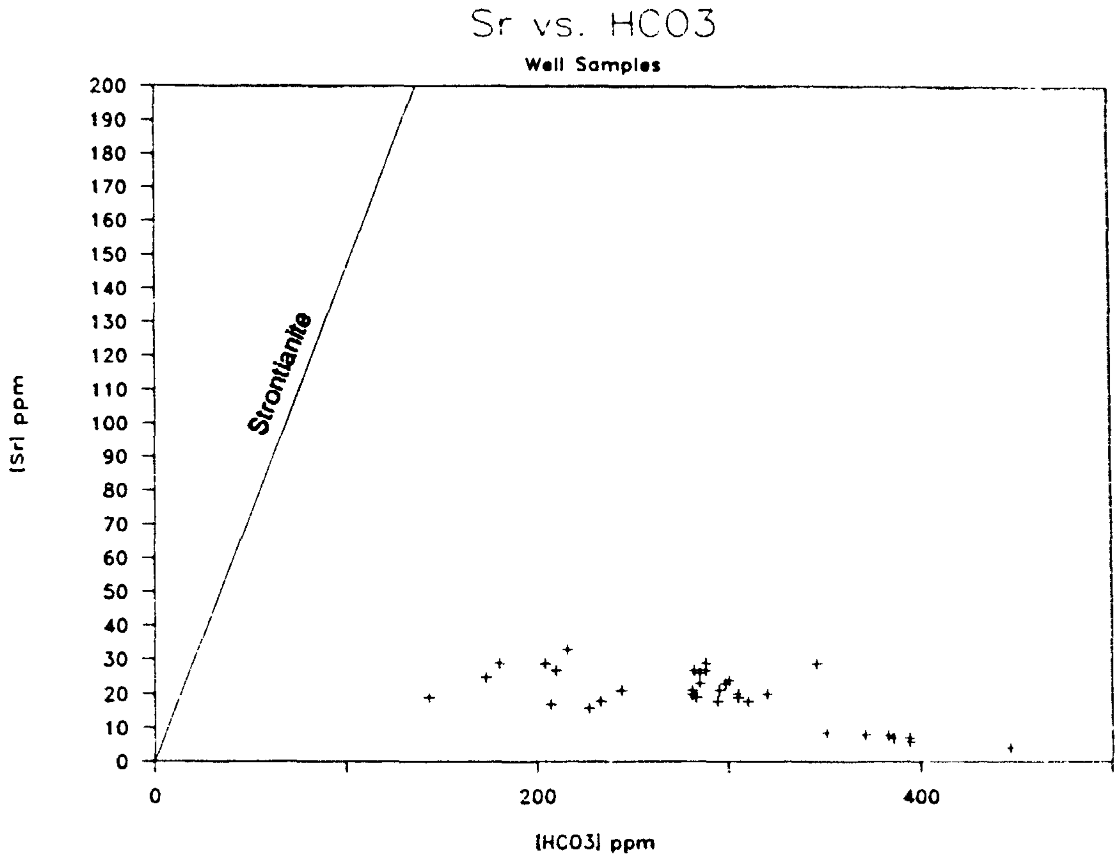

Figure 26 [Sr^{2+}] versus [HCO_3^-] plot of well water samples.

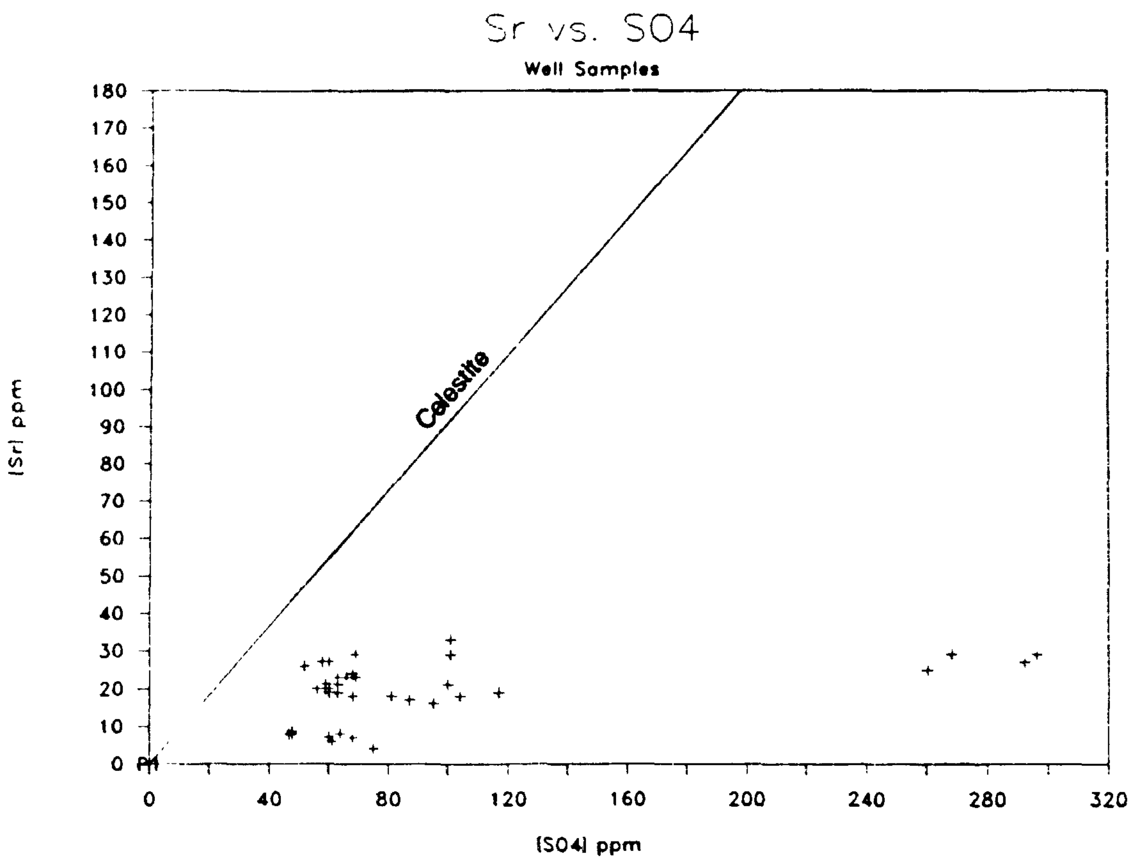

Figure 27 $[Sr^{2+}]$ versus $[SO_4^{2-}]$ plot of well water samples.

fact that the samples from a static P4 well plot on a straight line between the Type I and Type II samples suggests that mixing of the two water types is occurring at the P4 location. The shift in chemical composition, during pumping, indicates that P4 is better connected to the Type II waters, and that the Type I waters supply only a small component of the total yield during pumping.

It is evident from the differences in chemical composition of the groundwater samples, that there are at least two geochemical regimes in the Carleton University groundwater environment. The geochemical regimes appear to be bounded by the study area's major faults. The two regimes are also identified by their isotope values both in terms of their mean residence times and recharge conditions.

5.3 HYDRAULIC HEAD MONITORING

Measurement of the spatial and temporal variations in hydraulic head are fundamental to the study of groundwater regimes. Temporal fluctuations in hydraulic head, in response to precipitation and changes in temperature and pressure, can provide information on the different hydrogeologic regimes within a groundwater system. Recording the spatial variations in hydraulic head can reveal the natural pattern of groundwater movement. The hydraulic heads of the Carleton University wells were monitored on a regular basis for eleven months.

The following is a summary and analysis of that water level data. The water level records are found in Appendix 8.

5.3.1 Production and Single Level Monitoring Wells

The production wells and all but one of the monitoring wells are uncased for most of their depth. Consequently, the water level measured is a composite of the hydraulic heads for the various aquifers intersected by each well. The one exception to this is the multilevel well (M1) which has separate sampling intervals; results for the multilevel are summarised in Section 5.3.2.

Hydrographs for the production and monitoring wells are shown in Figures 28 and 29. These water level records, (October 1988 to August 1989) follow the seasonal recharge and head decline pattern described for Ottawa area wells by Brandon (1960). The greatest recharge period is in the early spring, March to early April, during spring snow melt. Hydraulic heads decline continually through the summer months. This is followed by a minor rise in levels during the fall, due to a reduction in evapotranspiration, and a steady decline through the winter and surface freeze-up period. The maximum seasonal fluctuation during 1988/89 ranged from 0.5 m (well P4) to 0.8 m (well P6). All of the wells are artesian and most are flowing artesian for at least part of the year.

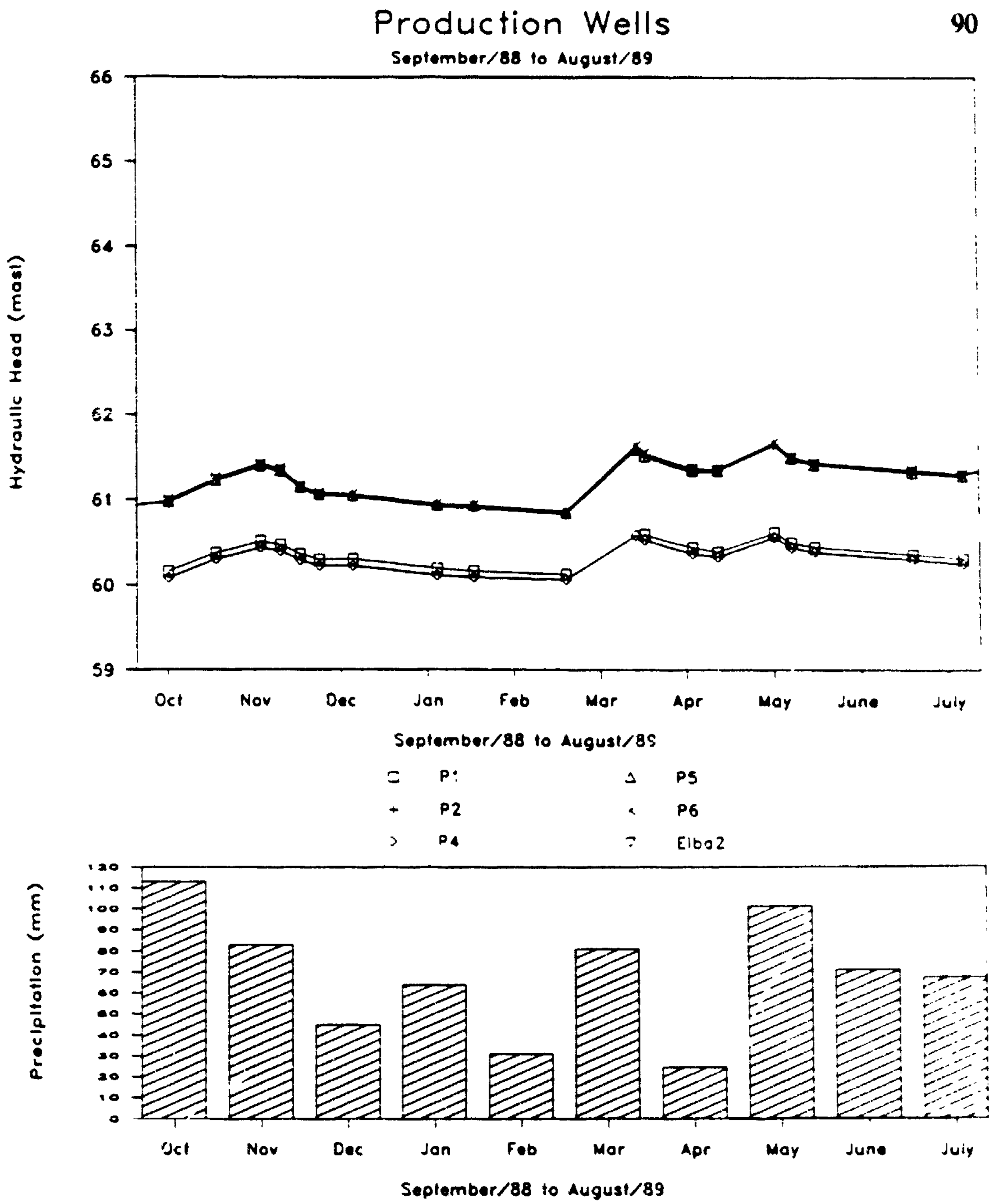

Figure 28 **Hydrograph for production wells.**

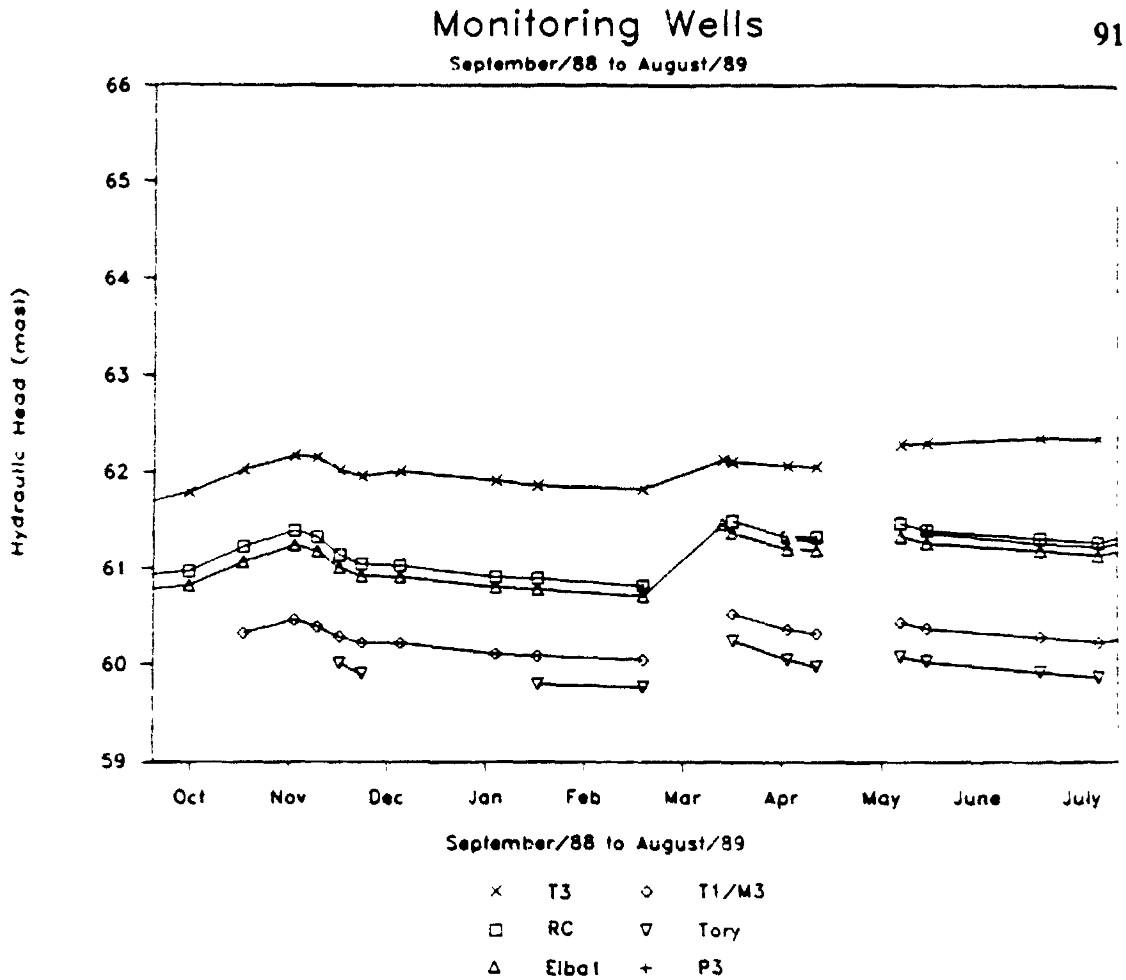

Figure 29 Hydrograph for monitoring wells.

Diurnal fluctuations in hydraulic head were observed in all of the wells. The maximum daily fluctuation measured was 6 cm (in well P6 during the latter part of July, 1988). Typically, the highest hydraulic head occurred during the late afternoon and evening and the lowest in the early morning hours after sunrise. However, this trend varied depending on changes in temperature, pressure and precipitation. Data from one set of diurnal shift observations are recorded in Appendix 8.

The diurnal shift in hydraulic head complicated the monitoring of potential responses to individual precipitation events since it was impossible to separate the effects of temperature, atmospheric pressure and precipitation. Variation of well water level due to the combined effects of temperature, pressure and precipitation is illustrated by the October hydrographs for wells P2 and P4 and the corresponding barogram, thermogram and precipitation records (Figure 30).

The well monitoring also revealed a distinct spatial variation of hydraulic head across the study area (Figures 28 and 29). The hydraulic heads measured in wells P2, P3, P5, P6, Elba 2, and in associated monitoring wells Elba 1 and RC, were consistently at least 0.7 m greater than the heads measured in wells P1, P4 and T1. The heads in P1 and P4 were, in turn, at least 0.4 m greater than the heads in the Tory well. Levels in the remaining monitoring well, T3, were higher than in all of the other wells, however, the water levels measured in T3 are probably more representative of shallow aquifer (overburden) hydraulic heads. (Well T3

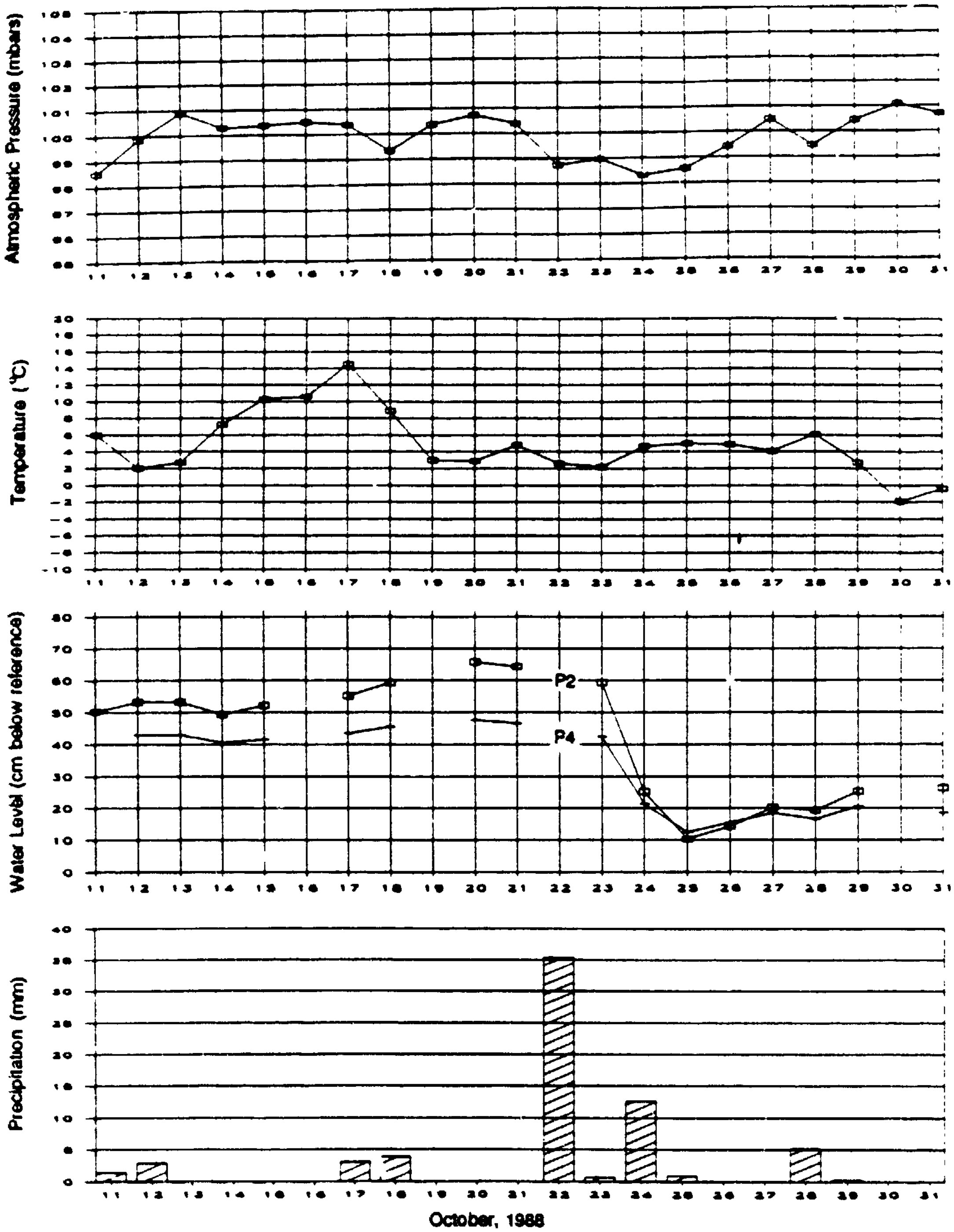

Figure 30 Barogram, thermogram, precipitation record and hydrographs for P2 and P4, October, 1988.

was originally drilled to a depth of 97.5 m, but suffered a borehole collapse that reduced its depth to the top of the bedrock at between 40 and 45 m.)

The grouping of wells based on hydraulic head levels corresponds to their respective locations within the fault blocks. Wells P2, P3, P5, P6 and Elba 2 are all located in fault blocks Ia, Ib and Ic (Section 5.1.5, Figure 19). The second group, P1 and P4, with the lower hydraulic heads, is located within fault blocks IIa and IIb. The Tory well, which has the lowest observed hydraulic head within the study area, is located within the fault zone separating blocks IIb and III.

While there are notable differences in head separating these groups of wells, the difference in head within each group is relatively minor. The horizontal hydraulic gradients within the various fault blocks, as determined from the hydraulic heads plotted in Figure 31, range from 0.0001 to 0.0005. These are very low gradients. The difference in hydraulic head between P4 (121 m depth) and T1 (95 m depth), shown in Figure 31, suggests that there may be an upward vertical gradient within that section of the campus. This is supported by the observed predominance of upward flow and, therefore, upward hydraulic gradient, recorded in the temperature logs of most of the wells.

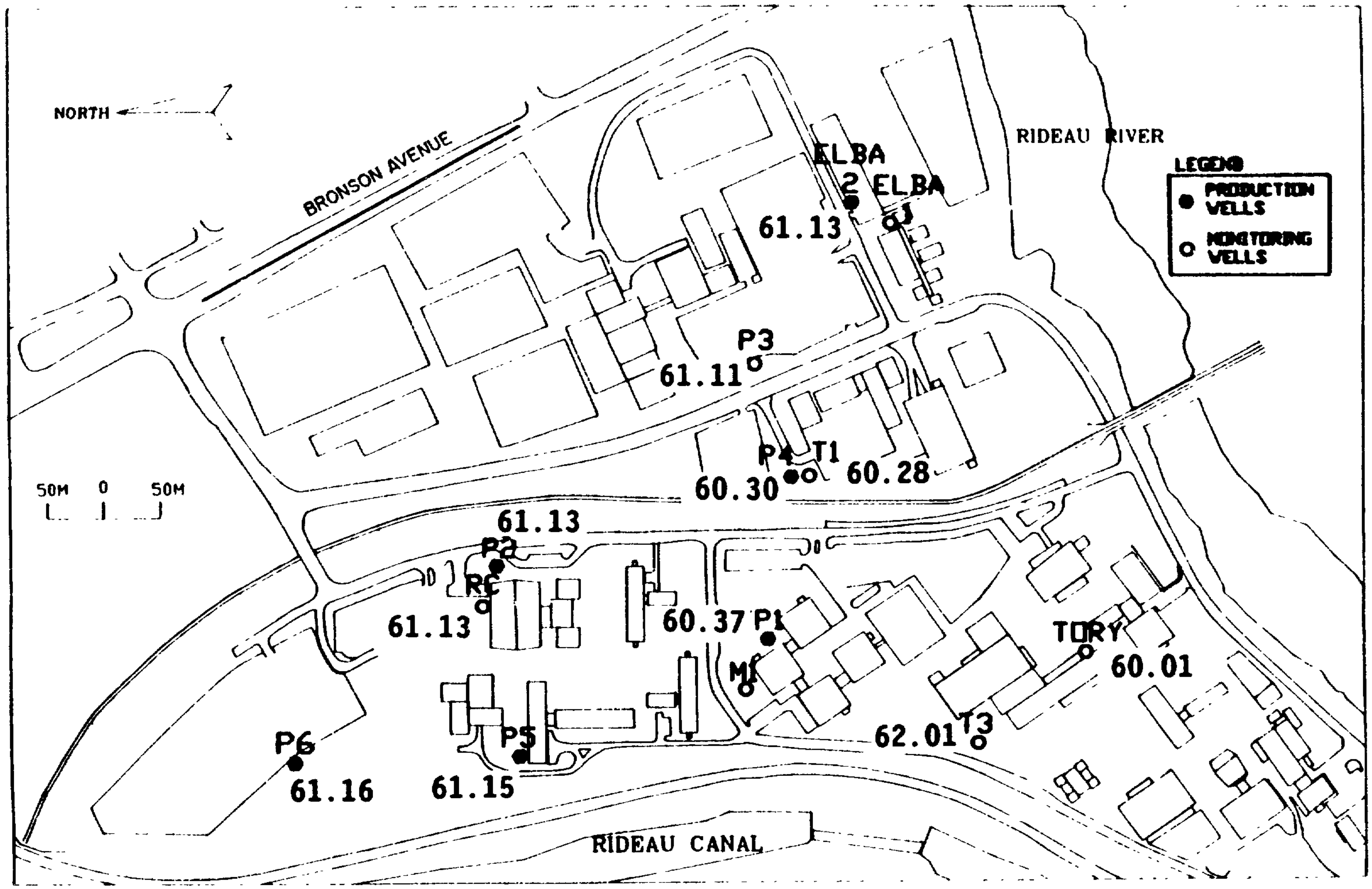

Figure 31 Map of hydraulic heads in wells of study area (hydraulic head in masl). Data from December 1, 1988.

5.3.2 Multilevel Installation

The multilevel installation is located in the central fault block and, therefore, is associated with the P1 and P4 group of wells. Hydrographs for the individual multilevel intervals, Figure 32, show the temporal variation in hydraulic head at various depths. The pattern of decline during the winter months, recharge in the spring and fall with a gradual decline over the summer months is observed at all depths. The hydrographs of the shallow intervals, M1-6 (15 m) down to M1-4 (61 m), fluctuate more over time than those of the deep sampling intervals, M1-B (137 m) and M1-1 (122 m).

Diurnal fluctuations in hydraulic head were also observed in the multilevel data (Appendix 8). These shifts may be due to the combined effects of changing temperature, pressure and recharge. The multilevel hydrographs correlate well with changes in temperature and pressure as illustrated in the plots displayed in Figure 33. The response of the deepest sample interval to pressure changes is particularly consistent.

The vertical variation in hydraulic head with depth and the resulting hydraulic gradients are shown in Figure 34. There is a marked upward vertical gradient from the high pressure zones at the bottom of the well. At times, the gradient is consistently upward throughout the entire profile of the well. At other times, depending on the head observed at the M1-2 (110 m) interval, there appears to

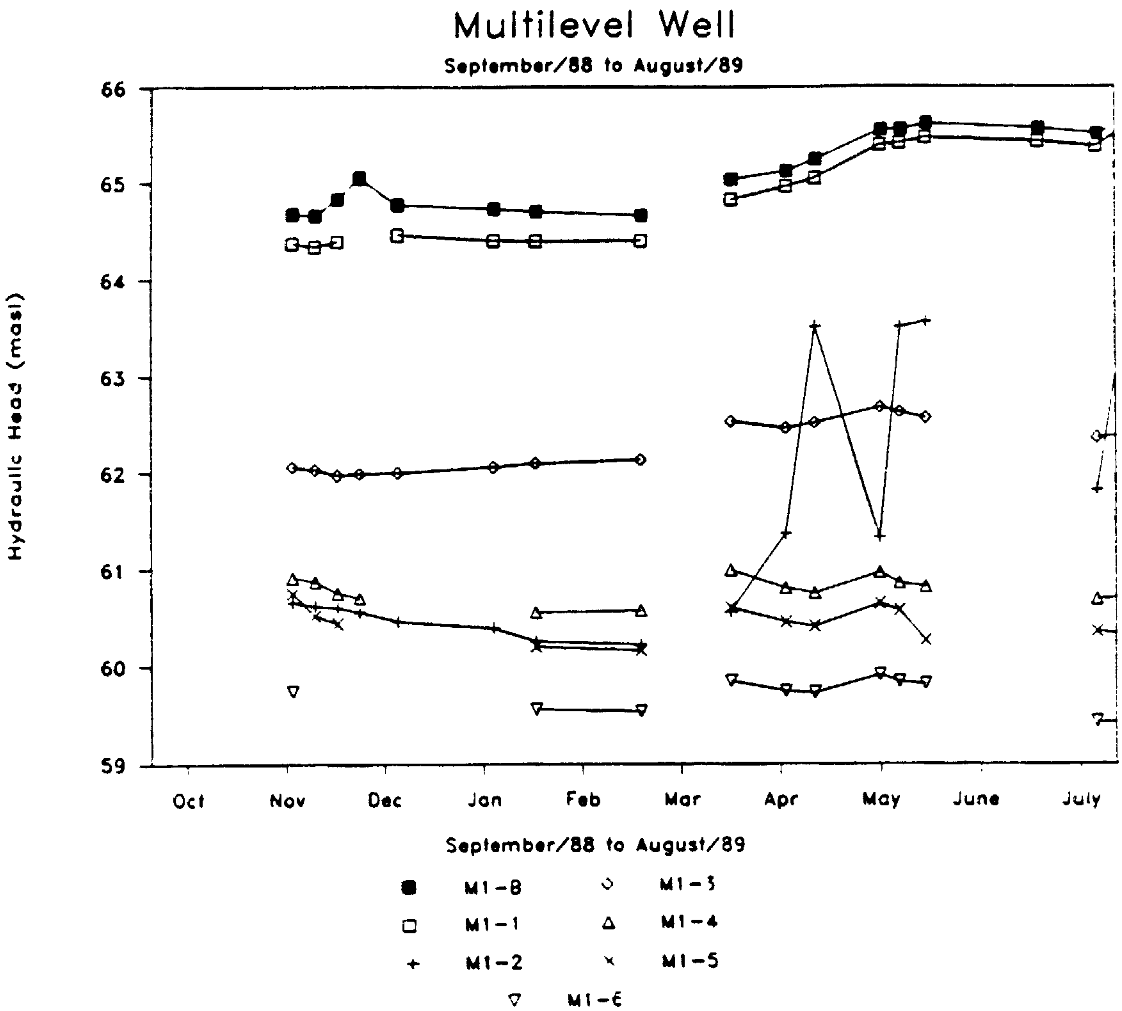

Figure 32 Hydrograph for multilevel well.

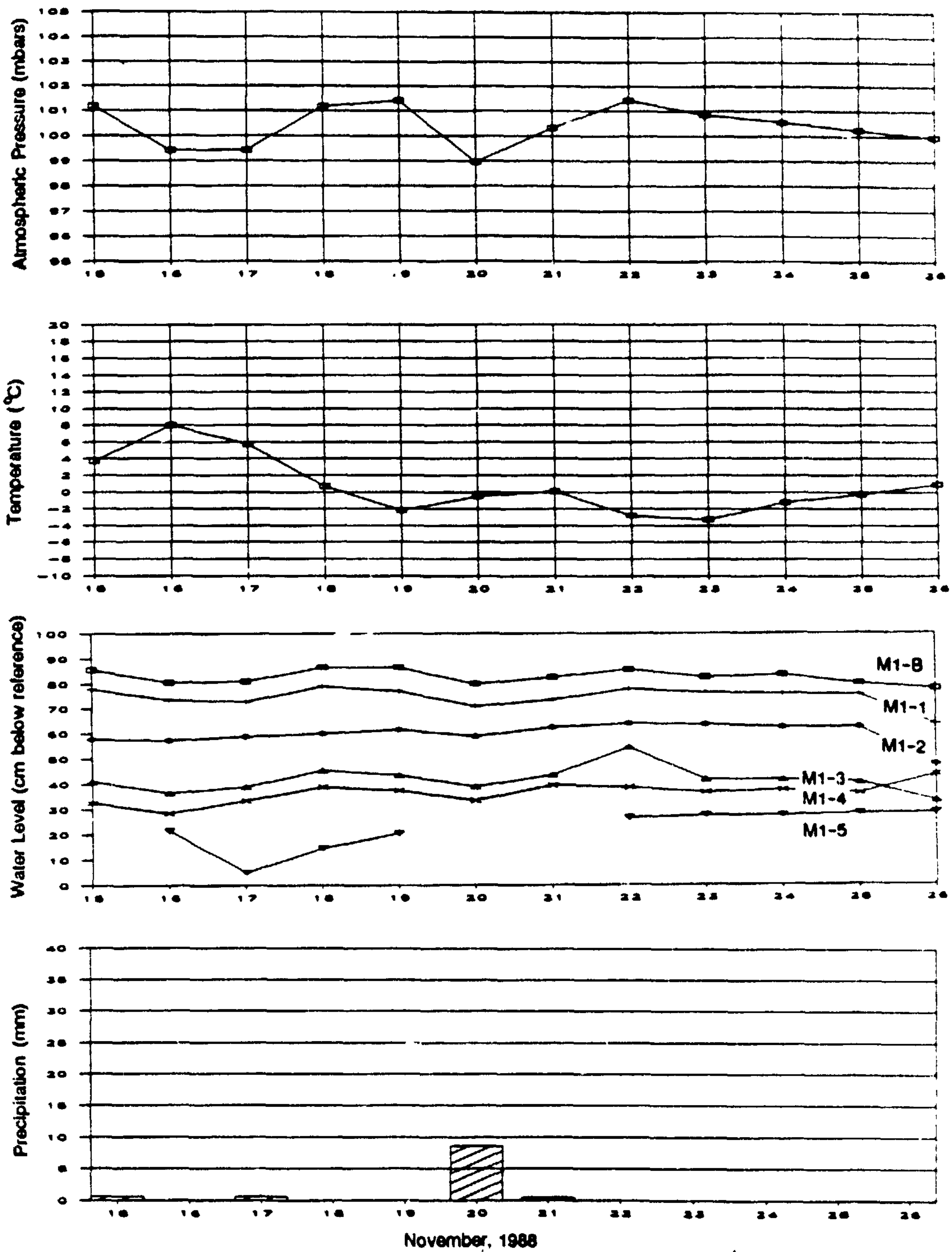

Figure 33 Barogram, thermogram, precipitation record and hydrographs for multilevel well, November, 1988.

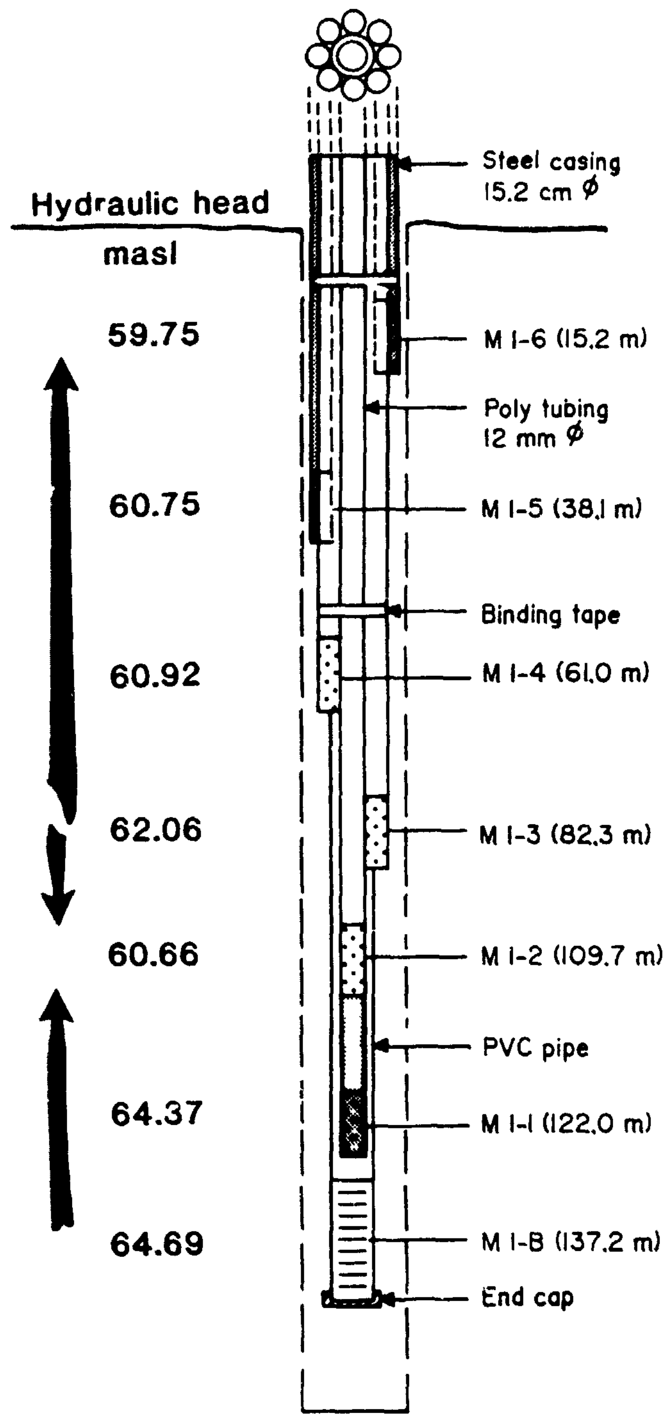

Figure 34 Cross section of multilevel well showing vertical hydraulic gradients (arrows indicate vertical hydraulic gradient).

be a low pressure zone at 110 m and a downward gradient established between 80 and 110 m. During the drilling of well M1, significant open and water-bearing fracture zones were identified at approximately 107 and 113 m. Typically the study area drilling records have over or underestimated depths by 5 to 10 m. If this margin of error is taken into account then the fracture zones are located somewhere between 97 and 117 m and 107 to 123. These depths encompass the M1-2 (110 m) and M1-1 (122 m) sample intervals. The occurrence of a permeable water-bearing fracture zone corresponds well with the high hydraulic heads measured in the M1-1/M1-B sample tubes. The erratic behaviour of the M1-2 hydraulic head may also be related to an open, highly permeable fracture zone, potentially with intermittent recharge.

5.3.3 Discussion of Hydraulic Head Monitoring

The hydrographs in Figures 28 and 29 indicate that there are at least two distinct groundwater regimes within the study area. Each regime exists within a certain section of the campus. This division of the campus, according to differences in hydraulic head, appears to correspond with the boundaries determined by the bedrock stratigraphy and well hydraulics. A third flow regime may exist in the western block and may be hydraulically connected to the Tory well, which is located adjacent to the eastern limit of the western block.

The low horizontal hydraulic gradients, particularly in the eastern and northern fault blocks, are indicative of high permeability and well interconnected, highly conductive fracture zones. Transmissivity values for the wells in the eastern and northern fault blocks are also higher due to this greater permeability.

The vertical variation in hydraulic head observed in the multilevel installation suggests poor vertical communication between the horizontal high permeability zones. The abundance of shales and argillaceous units could contribute to this poor vertical conductivity, even in these fracture-type aquifers. The shale and clayey units can clog existing fractures with insoluble residue, as well as retard vertical development of solution conduits by resisting dissolution (Thrailkill, 1985).

Higher hydraulic heads are located at depth in the multilevel, just as the major water-bearing fractures of the open boreholes are located in the lower to middle portions of the wells. Comparison of the hydraulic heads in the M1 hydrograph with the hydrographs of P1 and P4 shows that the levels in the open boreholes correspond with the levels set by the more shallow intervals (M1-5). These hydraulic heads are four to five metres below the hydraulic heads measured for the deep sampling intervals. This substantial difference in head suggests that significant head loss is occurring within the open boreholes. The upper strata may be acting as efficient spillways for the upward flowing groundwater and thereby controlling the well water levels.

Given these conditions, the difference in head between the various groups of wells may be due not only to higher pressures at depth, but also to less loss of head within the borehole. Both of these conditions are determined by the differences in hydrostratigraphy and fracture networks between the various fault blocks.

All of the wells are sensitive to temperature and atmospheric pressure fluctuations. Correlation between increases in atmospheric pressure and decreases in hydraulic head is most consistent in the deeper multilevel intervals (Figure 32). This inverse relationship between the atmospheric pressure and hydraulic head is characteristic of wells tapping confined aquifers (Rojstaczer, 1981; Freeze and Cherry, 1987; deVries and Greske, 1988).

The observed spatial and temporal changes in hydraulic head at the Carleton University site confirm that the natural pattern of groundwater movement is complex and varies significantly both laterally and with depth. This complexity can be directly related to the study area's geologic structure and stratigraphy.

Chapter 6

DISCUSSION

6.1 GENERAL

Much of the hydrogeology of the Carleton University site is defined by the Gloucester Fault zone. The large faults and associated fractures of this fault zone affect both the movement and occurrence of groundwater in the study area. The dominance of fracture flow has resulted in substantial differences between the groundwater supply characteristics of the Carleton site and those identified and described in regional groundwater studies.

The well yields obtained by the Carleton University Groundwater Project were in excess of 30 L/s. The total withdrawal and reinjection rates were in the order of 120 L/s. These are far beyond the highest yields expected from the most productive regional aquifers (Section 3.2). The hydrostratigraphy of the Carleton University site also differs from the regional hydrostratigraphy, as described in Section 3.1. For example, one of the most productive aquifers of the Carleton University site is within the strata classified as a regional aquitard.

Development of the wells for the Groundwater Project demonstrated that there is considerable variation in groundwater supply potential across the site. This complex spatial variability in supply potential is considered characteristic of fractured aquifers and of certain carbonate terranes (Rojstaczer, 1987; Novakowski, 1988). Zones demonstrating preferential permeability and close hydraulic connection between wells, such as exists between wells P2 and Elba 2, are also recognized as features of fractured reservoirs (Streltsova-Adams, 1978). The orientation of the preferential permeability zones, identified during the pump tests, corresponds with the trend of the major faults crossing the site, and with the predominant orientation of vertical and subvertical fractures within the fault zone.

For the siting of production wells, it is important, therefore, to delineate the fault zones and the extent of the associated fracture networks. Lattman and Parizek (1964) encountered open fractures and solution zones in fractured carbonate strata, extending 30 metres from the centre-line of the fracture traces. They also determined that maximum well yields could be expected from wells located precisely on fracture traces, especially at the intersection of two or more fracture traces. At the Carleton University site, there appears to be a connection between fault traces and increased groundwater flow. The coincidence between high well yields and fault traces is shown in Figure 9 (Section 3.3) and Figure 19 (Section 5.1).

As noted in Section 3.3, there are at least two possible reasons why certain fault zones within the study area exist as areas of high permeability, while other fault zones impede or retard groundwater flow. One reason for this may relate to the differences in stratigraphy across the fault. The location of the highly permeable zones, identified by the groundwater flow entry points in the geophysical logs, appear to be stratigraphically consistent across the site. These zones are truncated by the faults, particularly where there is substantial vertical displacement across the fault. The hydraulic head records for the site suggest that the faults between the central and northern/eastern fault blocks form boundaries between two different flow regimes. Under an induced negative hydraulic gradient, created during the pump tests, the flow within the various fault blocks extends laterally across the faults and/or around the impermeable sections of the fault. This movement may occur through less conductive and less developed fracture networks between the different stratigraphic sections and rock types.

A second potential cause for the differences in permeability between fault zones could be related to the fact that certain faults form boundaries between two different groundwater geochemistry regimes and, therefore, between two different groundwater types. Both types of groundwaters are saturated with respect to calcite and dolomite. Mixing of these waters may lead to a state of supersaturation (Wigley and Plummer, 1976; Section 5.2) and the precipitation of secondary calcite in the interconnecting fractures. The permeability of the fracture networks would be decreased by this process. Sealing by secondary calcite is one of the reasons given by Brandon (1960) for restricted groundwater flow within the Ottawa-Hull area fault zones.

The confined and overpressured nature of the flow regime within fracture zones is reflected in the high hydraulic heads and their response to atmospheric pressure. The hydraulic head levels of the deeper multilevel intervals also reacted to regional infiltration conditions and recharge periods. This suggests that the fractured aquifers are hydraulically connected to recharge zones. Brandon (1960), using the St. Martin and Rockcliffe Formations as an example, reasoned that the limited groundwater supply potential of the fault zones of the Ottawa-Hull area is due to the isolation of the more productive strata from their recharge areas. This does not appear to be the case at the Carleton University site. Verification of this will require continued hydraulic head monitoring during the operation and further development of the Groundwater Project.

6.2 STUDY AREA GROUNDWATER FLOW SYSTEMS

Based on the geology, geochemistry and hydrostratigraphy, described in Chapter 5, the bedrock groundwater regime of the study area can be divided into three dominant flow systems: 1) the highly permeable fractured zones in the Hull Formation, intersected by the wells in fault blocks Ia,Ib and Ic; 2) the porous and fractured zones in the Pamelia and St. Martin Formations and the top of the Rockcliffe Formation, intersected by the wells in fault blocks IIa and IIb; and 3) the fractured and potentially weathered zone at the Rockcliffe-Oxford Formation contact, intersected by the deeper wells in fault block IIb.

6.2.1 Fracture Zones of the Hull Formation

The low, horizontal hydraulic gradient within the eastern and northern fault blocks (Ia, Ib, Ic) is indicative of the high permeability of these fracture zones. The dominant water-bearing fractures in this flow regime are located in the upper half of the Hull Formation, including within massive calcarenite beds, and at the base of this formation near its contact with the Rockland Formation. The Hull Formation, particularly the upper part with its massive, well indurated calcarenite, would normally be considered a poor choice for groundwater supply (Michel, 1985). However, it is most likely the competence and relative purity of this strata that has preserved the open fractures created by past tectonic activity.

The location of this high permeability zone remains relatively constant with respect to the stratigraphy of the Ia, Ib, and Ic fault blocks. This suggests that these fracture zones may be continuous across areas with similar stratigraphy, and may provide the most significant hydrologic connection to regional flow systems and recharge zones. Even in well P3, the 150 m "dry well" (3 L/s), the water-bearing fracture zones occur in the lower part of the Hull Formation. The hydraulic head of this well is similar to the hydraulic head of other wells within the Ia, Ib and Ic fault blocks, indicating that P3 is connected to the same flow system. It is possible that some of the fractures intersected by P3 are closed or sealed and the remaining openings are not adequate to transmit the volumes of water required by the Groundwater Project.

The irregular, though minor, spatial variation in the hydraulic heads within the well network of the Ia, Ib and Ic fault blocks suggests that the flow regime is complex and may be structurally controlled by numerous cross faults. Cross faults within the fault blocks may act as sinks, creating narrow, minor groundwater basins. Unfortunately, the present well network is not dense enough to verify this hypothesis.

Geochemical traits of the Type I groundwater sampled from the wells that intersect this flow system, indicate that there is a significant mixing of different groundwater types, including relatively recent (<30 years) recharge waters. To some degree this mixing, or the extent of it, may be the result of the open borehole and the interconnections it provides to previously separate aquifers. This suggests that the groundwater from the deeper confined fractured flow zones may be more isolated from the recent recharge waters than is indicated by the geochemistry. The difference in the chemical composition between the water samples obtained in this study (the Carleton Type I well samples) and those taken from aquifers in the same formations by Brandon (1960), may also be due to isolation of the deep groundwater flow within the Hull Formation fracture zones. Brandon (1960) noted that the flow in the Ottawa Supergroup Formations is typically in joints and seams in the calcareous shale. Contact with the Ottawa Supergroup Formations frequently results in brackish, sulphurous groundwater. In comparison, the Carleton Type I waters are typically fresh and contain substantially less sodium.

6.2.2 Fracture Zones of the Pamelia to Rockcliffe Formations

Two high permeability fracture zones occur in the Pamelia to Rockcliffe Formations. These zones are encountered by wells in the IIa and IIb fault blocks. As in the northern and eastern fault blocks, the location of the fracture zones is consistent stratigraphically, borehole to borehole. This may have a bearing on the recharge of these groundwaters.

The Pamelia, St. Martin and upper Rockcliffe Formations were identified as having the greatest groundwater supply potential of all the sedimentary strata within the study area (Michel, 1985). This conclusion was based on the high primary porosity of the rocks, as well as the density and open nature of bedding plane fractures as determined from bedrock core samples taken from wells adjacent to the study area. It is possible that two kinds of porosity, pore and fracture, exist and contribute to the high permeability within this Pamelia to Rockcliffe Formation interval. In this situation, the groundwater would flow from the intergranular pores in the bedrock blocks into the fractures, and then continue as fracture flow. This is referred to as double porosity (Streltsova-Adams, 1978).

The geochemistry of the Type II waters reflects the predominance of shale in the bedrock of the Pamelia to upper Rockcliffe Formation interval. The major ion chemistry of the waters, as well as the isotope analysis, also suggest a longer mean residence time and flow path for these waters. The absence of any tritium in the Type II samples confirms the absence of recent recharge infiltrating the aquifer in the IIa and IIb fault blocks.

6.2.3 Fracture Zones of the Contact of the Rockcliffe and Oxford Formations

This fracture zone is intersected by the deeper wells, P1 and M1 (M1-1/M1-B), in the IIb fault block. The permeability of this zone may be due to the disconformable contact between the two formations (Wilson, 1946), and the development of a weathered zone at the top of the Oxford Formation. The high hydraulic head measured within this interval is indicative of the confined, overpressured nature of these flow regimes. As noted previously, the high hydraulic heads recorded from this zone suggest there is significant loss of head within the open boreholes.

There is a discernable difference between the chemical composition of the groundwater from this zone, as represented by the samples from the M1-1/M1-B interval, and the groundwater from P1. Both sample sets are within the Type II category, however, groundwater from the M1-1/M1-B interval contains less sodium and more calcium than the samples from well P1. This variance, within the Type II waters, may be a result of lithology; there is less shale and more dolomite and sandstone within the groundwater flow path of the M1-1/M1-B interval. Based on the results of the tritium analysis, the mean residence time of the groundwater in the Rockcliffe-Oxford contact exceeds 35 years.

This zone may play a significant role in the deep groundwater flow regime of the westernmost fault block in the study area. This is based on the stratigraphy of the westernmost block and the apparent continuous nature of the fracture zones within stratigraphically similar fault blocks.

Chapter 7

CONCLUSIONS

Geological, geophysical and groundwater data were compiled and analysed in order to describe the undisturbed groundwater flow regime beneath the Carleton University campus, Ottawa, Ontario.

The results indicate that the hydrogeology of the study area is complex and heterogeneous, which is characteristic of fractured aquifer systems. The zones of enhanced hydraulic connection, identified by the Carleton University Groundwater Project pump tests, can be explained by groundwater flow through open, interconnected fracture networks associated with individual faults within the Gloucester Fault Zone.

Based on the stratigraphic information derived from lithology logs and multiparameter geophysical logging, the study area can be divided into at least six fault blocks. Total vertical displacement across the campus is approximately 200 m and has occurred primarily on the faults between the central and eastern blocks. Movement along the main northwest trending fault has been transposed to a cross fault located in the central part of the site. In general the fault blocks on the east side of the campus have been downdropped relative to the central and western blocks.

Geophysical logging identified the stratigraphic position of distinct water-bearing fractures or fracture zones intersected by the wells. The occurrence and flow of groundwater within the deep bedrock aquifers of the site appear to be controlled by three dominant flow systems defined by these fracture zones. The positions of these zones appear to be stratigraphically consistent from well to well. Consequently, the three dominant flow systems have been identified by the formation(s) in which they are located, namely: fracture zones of the Hull Formation; the porous and fractured zones in Pamelia and St. Martin Formations and the top of the Rockcliffe Formation; and the fractured, potentially weathered contact of the Rockcliffe and Oxford Formations.

Hydraulic head monitoring confirmed the existence of at least two of these flow regimes and revealed the confined, overpressured nature of the groundwater within them. The very low hydraulic gradients, particularly in the eastern fault blocks, is indicative of the high permeability of the fracture zones.

The effects of structural control on the groundwater flow are also evident in the geochemistry of the groundwater supply. Based on the chemical composition and isotope values of the well samples there are two distinct types of groundwater in the study area. One has no dominant cation and an approximately equal concentration of bicarbonate and chloride ions. The second type is dominated by sodium and chloride ions, with minor concentrations of calcium, magnesium, sulphate and bicarbonate ions. Differences in chemical composition can be directly related to differences in the rock types containing the various fracture networks. Apparent differences in the mean residence times and recharge conditions, as determined from the isotope analysis, supports the assumption that each groundwater type is associated with different flow systems.

The identification and characterisation of these separate flow regimes has increased the understanding of a rather complex and heterogeneous groundwater system at the Carleton University site. This knowledge should assist in the current operation and potential expansion of the Carleton University Groundwater Project.

REFERENCES

Al-Hashimi, W.S. 1976. Significance of strontium distribution in some carbonate rocks in the carboniferous of Northumberland, England. J. Sedimentary Petrology, 46(2):369-376.

Back, W. and Hanshaw, B.B. 1970. Comparison of chemical hydrogeology of the carbonate peninsulas of Florida and Yucatan. J. Hydrology, 8(3):43-51.

Beck, A.E. 1977. Climatically perturbed temperature gradients and their effect on regional and continental heat-flow means. Tectonophysics, 41:17-39.

Beck, A.E. 1976. The use of thermal resistivity logs in stratigraphic correlation. Geophysics, 41(2):300-309.

Boldizsar, T. 1958. The distribution of temperature in flowing wells. Amer. J. Science, 256:294-298.

Bristow, Q. 1979. Airborne and vehicle mounted geophysical data acquisition system controlled by NOVA minicomputers; in Proceedings of the 6th Annual Data Generals User Group Meeting, Dec. 4-7, New Orleans, pp. 615-634.

Bristow, Q. and Conaway, J.G. 1984. Temperature gradient measurements in boreholes using low noise high resolution digital techniques in Current Research, Part B, Geol. Surv. Canada Paper 84-1B, pp. 101-108.

Brandon, L.V. 1960. Preliminary report on hydrogeology, Ottawa-Hull area, Ontario and Quebec. Geol. Surv. Canada Paper 60-23, 17 p.

Charron, J.E. 1978. Hydrochemical study of groundwater flow in the interstream area between the Ottawa and St. Lawrence Rivers. Inland Water Directorate, Water Resources Branch, Environment Canada. Scientific Series No. 76, 28 p.

Cherry, J.A., Gilham, R.W., Anderson, E.G., and Johnson, P.E. 1983. Migration of contaminants in groundwater at a landfill: a case study. 2. Groundwater monitoring devices. J. Hydrology, 63:31-49.

Clark, I.D. 1984. Groundwater resources in the Sultanate of Oman: Origin, circulation times, recharge processes and palaeo-climatology; Isotopic and geochemical approaches. Unpublished Ph.D. thesis, University of Paris, Centre D'Orsey. Paris, France. 264 p.

Conaway, J. 1987. Temperature logging as an aid to understanding groundwater flow in boreholes: in Proceedings of the 2nd International Symposium on Borehole Geophysics for Minerals, Geotechnical and Groundwater Applications, October 6-8, Golden, Colorado, pp.51-59.

deKemp, E.A., Michel, F.A. and Donaldson, J.A. 1989. Report on the geology of the south wall, excavation for the World Exchange Plaza. Unpublished report prepared for McRostie, Genest, St. Louis and Associates Ltd., Ottawa, Ontario, 19 p.

deVries, J.J. and Greske A. 1988. Barometric tides in partly-saturated confined aquifers in Botswana. J. Hydrology, 104:17-32.

Drever, J.I. 1982. The Geochemistry of Natural Waters. Prentice-Hall Inc. Englewood Cliffs, New Jersey, 388 p.

Drury, M.J., Jessop, A.M. and Lewis, T.J. 1984. The detection of groundwater flow by precise temperature measurements in boreholes. Geothermics, 13(3):163-174.

Dyck, J.H., Keys, W.S. and Meneley, W.A. 1972. Application of geophysical logging to groundwater studies in southern Saskatchewan. Can. J. Earth Sciences, 9(1):78-94.

Environment Canada. 1988. Annual Meteorological Summary: Ottawa International Airport. Atmospheric Environment Service, 25 p.

Epp, M.S. 1989. Seismic refraction profiling of subsurface structures within the Carleton University campus, Ottawa, Ontario. Unpublished B.Sc.Hon. Thesis. Carleton University, Ottawa, Ontario, 80 p.

Freeze, R.A. and Cherry, J.A. 1979. Groundwater. Prentice-Hall Inc., Englewood Cliffs, New Jersey, 604 p.

Fritz, P., Drimmie, R.J., Frape, S.K. and O'Shea, K. 1987. The isotopic composition of precipitation and groundwater in Canada, in Isotope Techniques in Water Resources Development, Proc. IAEA Symposium, Vienna. pp. 539-550.

Geo-Analysis Inc. 1986. Technical report: Hydrogeology, Greens Creek Watershed Study. Unpublished report prepared for the National Capital Commission, Ottawa, Ontario. 16 p.

Goudge, M.F. 1938. Limestones in Canada; their occurrence and characteristics, Part IV, Ontario. Can. Dept. of Mines and Resources, No. 781, 362 p.

Hem, J.D. 1985. Study and interpretation of the chemical characteristics of natural water. U.S. Geol. Surv. Water-Supply Paper 2254, 263 p.

Holland, H.D., Kirsipu, T.V., Huebner, J.S. and Oxburgh, U.M. 1964. On some aspects of the chemical evolution of cave waters. J. Geology, 72(1):36-67.

Jackson, R.E., Patterson, R.J., Graham, B.W., Bahr, J., Belanger, D., Lockwood, J., and Priddle, M. 1985. Contaminant hydrogeology of toxic organic chemicals at a disposal site, Gloucester, Ontario. 1. Chemical concepts and site assessment. NHRI Paper No. 23, IWD Scientific Series No.141, 114 p.

Jessop, A.M. and Judge, A.S. 1971. Five measurements of heat flow in southern Canada. Can. J. Earth Sciences, 8:711-716.

Kay, G.M. 1942. Ottawa-Bonnechere graben and the Lake Ontario homocline. Bull. Geol. Soc. Amer., 53:585-646.

Keys, W.S. and Brown, R.F. 1978. The use of temperature logs to trace the movement of injected water. Ground Water, 16:32-48.

Keys, W.S. and MacCary, L.M. 1971. Application of borehole geophysics to water-resources investigations. Chapter E1, Techniques of Water-Resources Investigations of the U.S. Geol. Survey, 126 p.

Kinsman, D.J.J. 1969. Interpretation of Sr^{2+} concentrations in carbonate minerals and rocks. J. Sed. Pet., 39(2):486-508.

Kumarapeli, P.S. and Saull, V.A. 1966. The St. Lawrence Valley System; A North American equivalent of the East African rift valley system. Can. J. Earth Sciences, 3(5):639-658.

Langmuir, D. 1971. The geochemistry of some carbonate ground waters in central Pennsylvania. Geochim. et Cosmochim. Acta, 35:1023-1045.

Lattman, L.H. and Parizek, R.R. 1964. Relationship between fracture traces and the occurrence of ground water in carbonate rocks. J. Hydrology, 2:73-91

Lewis, T.J. 1975. A geothermal survey at Lake Dufault, Quebec. Unpublished Ph.D. thesis, University of Western Ontario. London, Ontario. pp. 110-120.

Lewis, D.C. and Burgy, R.H. 1964. Hydraulic characteristics of fractured and jointed rock. Ground Water, 2(3):4-9.

Lumbers, S.B. 1982. Summary of metallogeny, Renfrew County area. Ont. Geol. Surv. Rpt. 212, 58 p.

McFall, G. and Davidson, A. 1979. Generalized lithology of Lebreton Borehole LB-1, Ottawa, Ontario. Unpublished section and notes.

Michel, F.A. 1985. Report on the geology and hydrogeolgy of the Carleton University campus. Unpublished report prepared for Physical Plant, Carleton University, Ottawa, Ontario. 43 p.

Michel, F.A., Kubasiewicz, M., Jackson, R.E. and Patterson, R.J. 1984. Groundwater flow velocity derived from tritium measurements of the Gloucester landfill site, Gloucester, Ontario. Water Poll. Res. J. Canada, 19(2):13-22.

Novakowski, K. 1988. Introduction to field methods for parameter estimation in fractured rock. Unpublished paper prepared for course in Field Methods in Hydrogeology, U. of Waterloo, Waterloo, Ontario. 50 p.

Raven, K. 1986. Hydraulic characterization of a small ground-water flow system in fractured monzonitic gneiss. National Hydrology Research Institute, Ottawa, Ontario, NHRI Paper No. 30, 45 p.

Rojstaczer, S. 1987. The local effects of groundwater pumpage within a fault-influenced groundwater basin, Ash meadows, Wye County, Nevada. J. Hydrology, 91:319-337.

Runnels, D.D. 1969. Diagenesis, chemical sediments, and the mixing of natural waters. J. Sed. Pet., 39:1188-1201.

Sammel, E.A. 1968. Convective flow and its effect on temperature logging in small-diameter wells. Geophysics, 33(6): 1004-1012.

Schlumberger, 1972. Log interpretation, Vol. I: Principles. Schlumberger Ltd., New York, New York. 112 p.

Scott, J.S. 1967. St. Lawrence Lowlands hydrogeological region in Groundwater in Canada. Geological Survey of Canada, Economic Geology Report No. 24, pp. 98-119.

Simpson, D.G. 1978. A structural analysis of the Hogs Back Area, Ottawa, Ontario, Canada. Unpublished B.Sc. Thesis, Carleton University, Ottawa, Ontario. 79 p.

Skougstad, M.V. and Horr, C.A. 1963. Occurrence and distribution of strontium in natural water. U.S. Geol Surv. Water Supply Paper 1496-D, 93 p.

Streltsova-Adams, T.D. 1978. Well hydraulics in heterogeneous aquifer formations. Adv. Hydro. Sci., 11:357-423.

Sorey, M.L. 1971. Measurement of vertical groundwater velocity from temperature profiles in wells. Water Resources Research, 7(4):963-970.

Steele-Petrovich, H.M. 1989. A preliminary report on the lithostratigraphy of lower Middle Ordovician sedimentary rocks, lower Ottawa Valley, Ontario; in Current Research, Part B, Geol. Surv. Canada, Paper 89-1B, pp. 121-125.

____. 1986. Lithostratigraphy and a summary of the paleoenvironments of the lower Middle Ordovician sedimentary rocks, upper Ottawa Valley, Ontario; in Current Research, Part B, Geol. Surv. Canada, Paper 86-1B, pp. 493-506.

Thrailkill, J. 1985. Flow in a limestone aquifer as determined from water tracing and water levels in wells. J. Hydrology, 78:123-136.

Urbancic, T.I. and Mwenifumbo, C.J. 1986. Multiparameter logging techniques applied to gold exploration; in Borehole Geophysics for Mining and Geotechnical Applications, ed.. P.G. Killeen, Geol. Surv. Canada Paper 85-27, pp.13-28.

Vollrath, J.D. 1962. Geology of the Hogs Back Area from the White Bridge to Hogs Back. Unpublished B.Sc. Thesis, Carleton University, Ottawa, Ontario. 68 p.

WESA (Water and Earth Science Associates Ltd.), 1988. Energy from Groundwater Phase I Development, Carleton University, Colonel By Campus Unpublished Hydrogeologists draft report prepared for Physical Plant, Carleton University. Ottawa, Ontario. 90 p.

____. 1985. Drilling and aquifer testing of a test well for thermal evaluation, Carleton University, Phase 2A, Colonel By Campus. Unpublished report prepared for Physical Plant, Carleton University, Ottawa, Ontario. 45 p.

Wigley, T.M.L. and Plummer, L.N. 1976. Mixing of carbonate waters. Geochim. et Cosmochim. Acta, 40:989-995.

Williams, D. and Telford, P.G. 1987. Structure and Ordovician stratigraphy of the Ottawa area, southern Ontario. Geol. Soc. of Amer. Centennial Field Guide, Northeastern Section, 5:349-352.

____. 1986. Paleozoic geology of the Ottawa area. Geological Association of Canada, Mineralogical Association of Canada, Canadian Geophysical Union, Joint Annual Meeting, Ottawa '86, Field Trip 8: Guidebook, 25 p.

Wilson, A.E. 1956. A guide to the geology of the Ottawa District. Can. Field-Naturalist, Vol. 70, 68 p.

____. 1946. Geology of the Ottawa-St. Lawrence Lowland, Ontario and Quebec. Geol. Surv. Canada Memoir 241, 65 p.

____. 1923. Notes on the Pamelia Member of the Black River Formation of the Ottawa Valley. Amer. J. Science, 24:135-146.

Appendix 1

WELL INVENTORY

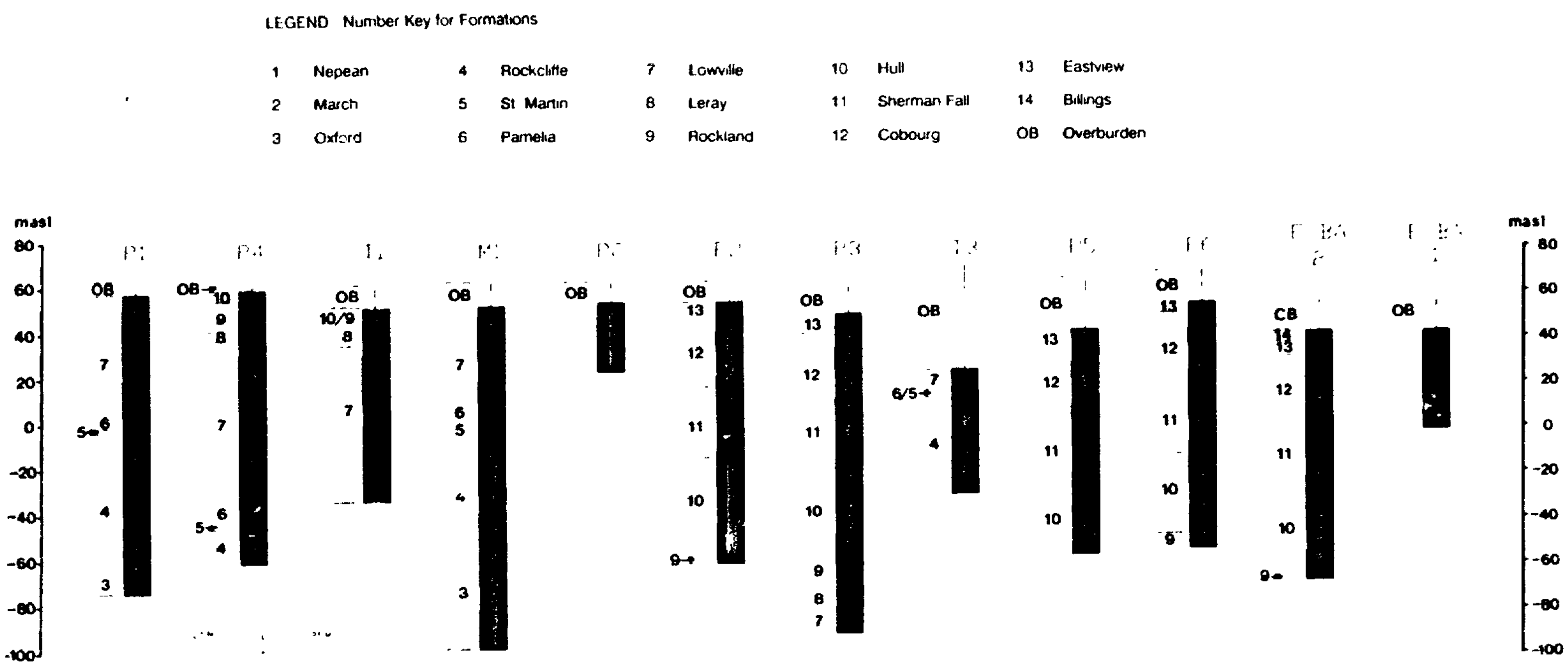

Schematic cross section of wells (elevations masl); top of dark cylinder is top of bedrock surface; and lines on cylinders are formational contacts.

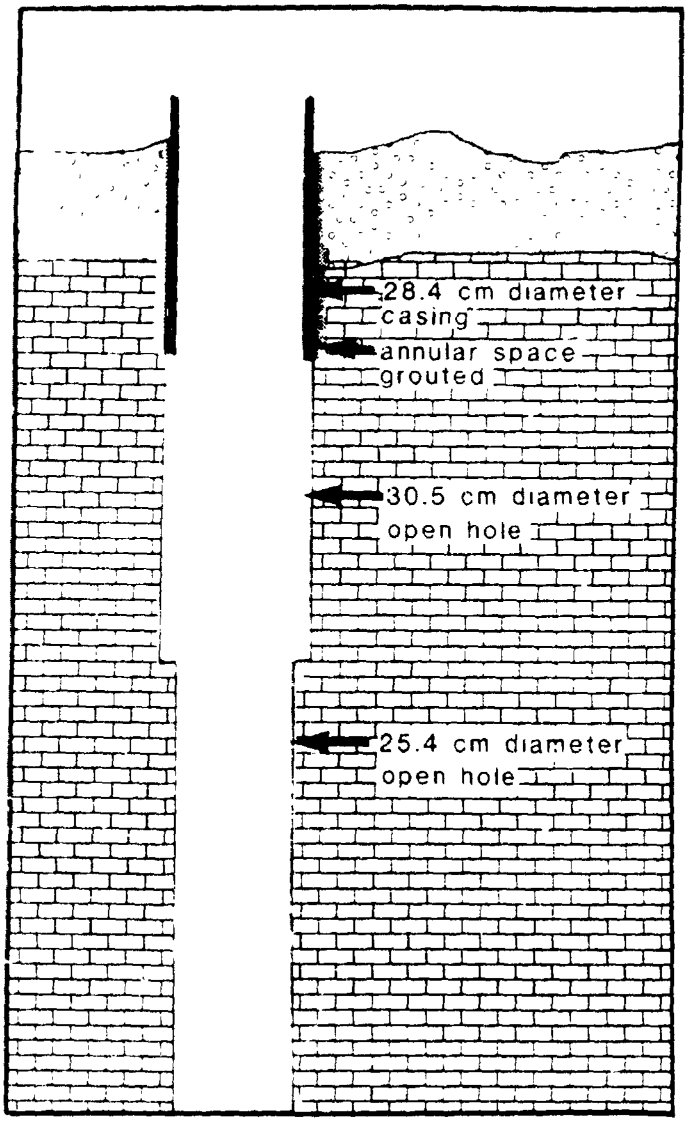

Production well construction.

Appendix 2

LITHOLOGY LOGS

Billings and Eastview Formations

The uppermost formation underlying the unconsolidated material in the eastern part of the study area is the Billings Formation, a black shale. The Billings Formation is transitionally underlain by the thin Eastview Formation, a dark grey, fine-grained limestone interbedded with dark shale. The Billings-Eastview contact is arbitrarily placed at the upper limit of limestone interbeds greater than 2 cm thick or at the top of the uppermost limestone bed (Williams and Tedford, 1986; Wilson, 1946). The Eastview thins out and disappears toward the east and is entirely absent west of the Gloucester fault (Wilson, 1946).

Ottawa Supergroup: Cobourg, Sherman Fall, Hull and Rockland Formations

The Eastview is underlain by the Ottawa Supergroup, a sequence of limestones and shales with small amounts of sandstone at the base. The upper part of the Ottawa Supergroup, referred to as the Trenton Group, consists of the Cobourg, Sherman Fall, Hull and Rockland Formations. The Cobourg Formation, which directly underlies the Eastview, is light to dark grey, sublithographic to coarsely crystalline limestone with abundant calcareous shaly partings. The Eastview-Cobourg contact is marked by a change upward from the grey limestone to the very dark, finer-grained limestone and interbedded shale.

The Sherman Fall Formation is about 30 m thick, conformably underlies the Cobourg and consists of medium to dark grey lithographic limestone and shaly limestone interbedded with calcarenite.

The Hull Formation conformably underlies the Sherman Fall and consists of approximately 37 m of interbedded shaly fossiliferous limestone and calcarenite. The Hull-Sherman Fall contact is marked by a 12 m interval of massive calcarenite of distinct purity located in the top of the Hull Formation.

The Rockland Formation conformably underlies the Hull and consists of approximately 13 m of medium to dark grey, sublithographic limestone with abundant shaly partings, especially in the upper part of the formation.

Black River Group:Leray, Lowville and Pamelia Formations

The Black River Group, consisting of the Leray, Lowville and Pamelia Formations, conformably underlies the Rockland Formation. The Leray Formation is approximately 9 m thick and consists of massive calcarenite with beds of calcilutite and a shaly calcilutite at the base. The Leray is conformably underlain by the Lowville Formation, a predominantly sublithographic, argillacious limestone with some shale, fossiliferous and calcarenite intervals. The Lowville becomes intermittently more dolomitic towards the base. The 67 m thick Lowville is conformably underlain by the 9 m thick Pamelia Formation which consists of a silty to sandy dolostone, with shaly partings and thin interbeds of quartz sandstone.

St. Martin Formation

The St. Martin and Rockcliffe Formations disconformably underlie the Pamelia. The St. Martin is considered by some to be a carbonate facies of the uppermost Rockcliffe. It consists of about 3 m of limestones and dolostones overlying, and grading into, some 51 m of first dolostones and shales and eventually shaly fine grained greenish-grey sandstone. The St. Martin Formation has not been identified north and west of the Hog's Back, and may or may not underlie the study area (Vollrath, 1962).

Rockcliffe Formation

The Rockcliffe is disconformably underlain by the Oxford Formation, a brown to greenish-grey dolostone up to 65 m thick. The March Formation, a dolomitic sandstone up to 6 m thick, and locally conformable, underlies the Oxford Formation and grades into the underlying Nepean Formation. The Nepean, a Cambro-Ordovician cream-coloured quartz arenite, can be up to 80 m thick. A major unconformity separates the Nepean from the underlying Precambrian basement rock of the Grenville province. The Precambrian basement was encountered at 370 m (LeBreton Well (LB-1), Geological Survey of Canada) 2 km north of the study area. This depth, however, will vary with location due to vertical displacement along faults.

Legend

Rock Types

Limestones


Argillaceous, dark to medium grey, sometimes brownish grey (calcilutite) limestone


Medium to dark grey, often recrystallised limestone

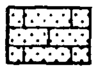
Light to medium grey, medium to coarse-grained (calcarenite) limestone


Medium to dark brown grey, silty (calcilutite) limestone with dark concretions and wavy laminae

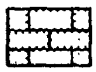
Medium to dark grey sublithographic (calcilutite) limestone

Shales

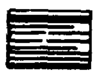
Dark grey to black, noncalcareous to slightly calcareous shale

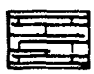
Dark grey, slightly calcareous to calcareous shale

Siltstones

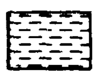
Light green to greenish grey to grey brown siltstone, sometimes fissile and calcareous

Sandstones

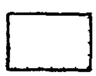
Medium to light grey green to greenish grey brown, fine-grained sandstone, sometimes calcareous

Dolostones


Dark to medium grey, fine-grained limey dolostone, sometimes argillaceous with calcite

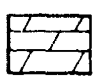
Medium grey brown dolostone and limey dolostone veins

Symbols

X coarse white calcite crystals

fossiliferous

(P) pyrite

(Fe) iron staining

(Ch) chert

≡ slickensides

P I

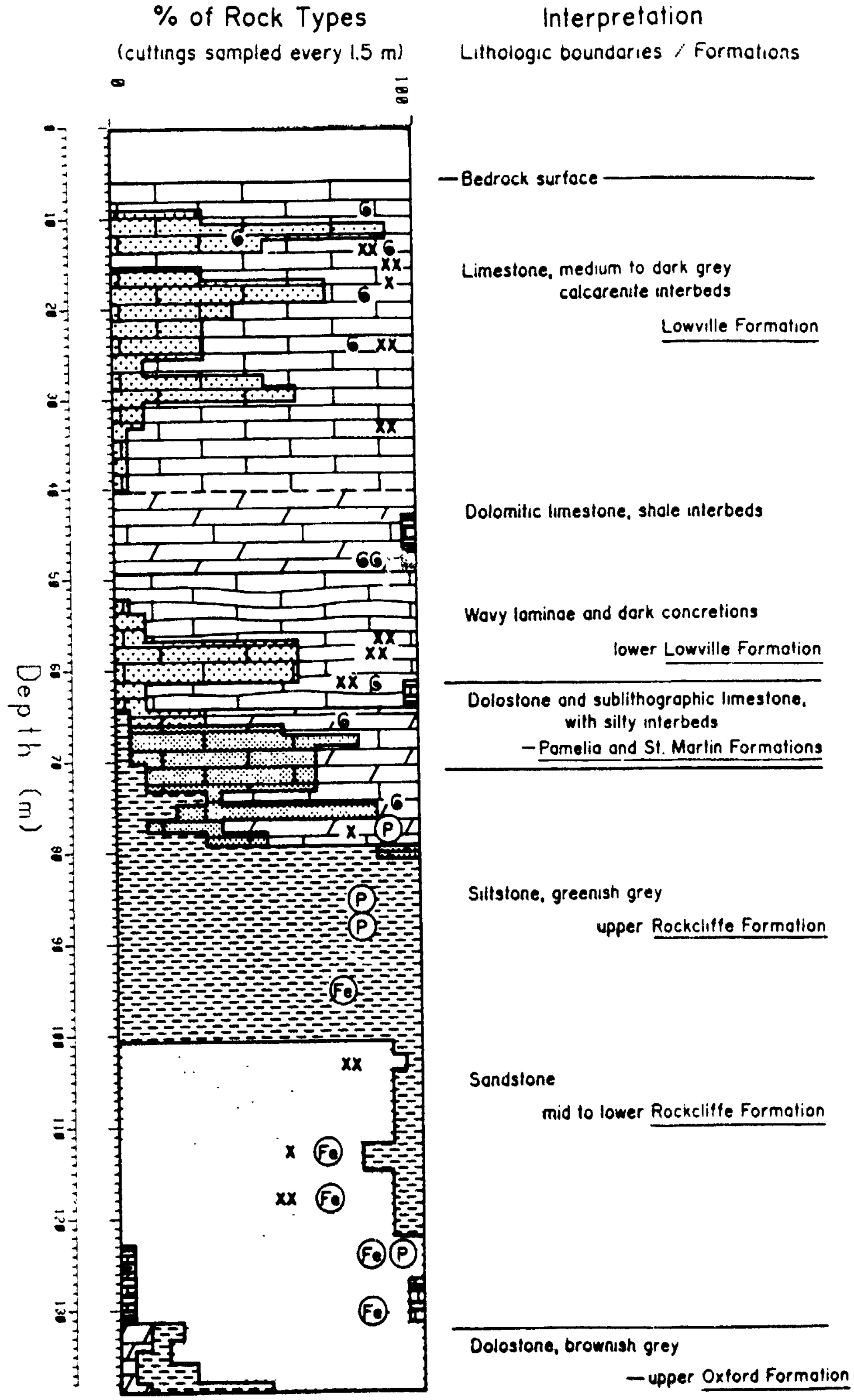
% of Rock Types
(cuttings sampled every 1.5 m)
Interpretation
Lithologic boundaries / Formations
Depth (m)
Bedrock surface
Limestone, medium to dark grey
calcarenite interbeds
Lowville Formation
Dolomitic limestone, shale interbeds
Wavy laminae and dark concretions
lower Lowville Formation
Dolostone and sublithographic limestone,
with silty interbeds
—Pamelia and St. Martin Formations
Siltstone, greenish grey
upper Rockcliffe Formation
Sandstone
mid to lower Rockcliffe Formation
Dolostone, brownish grey
—upper Oxford Formation

P 2

% of Rock Types
(cuttings sampled every 1.5 m)

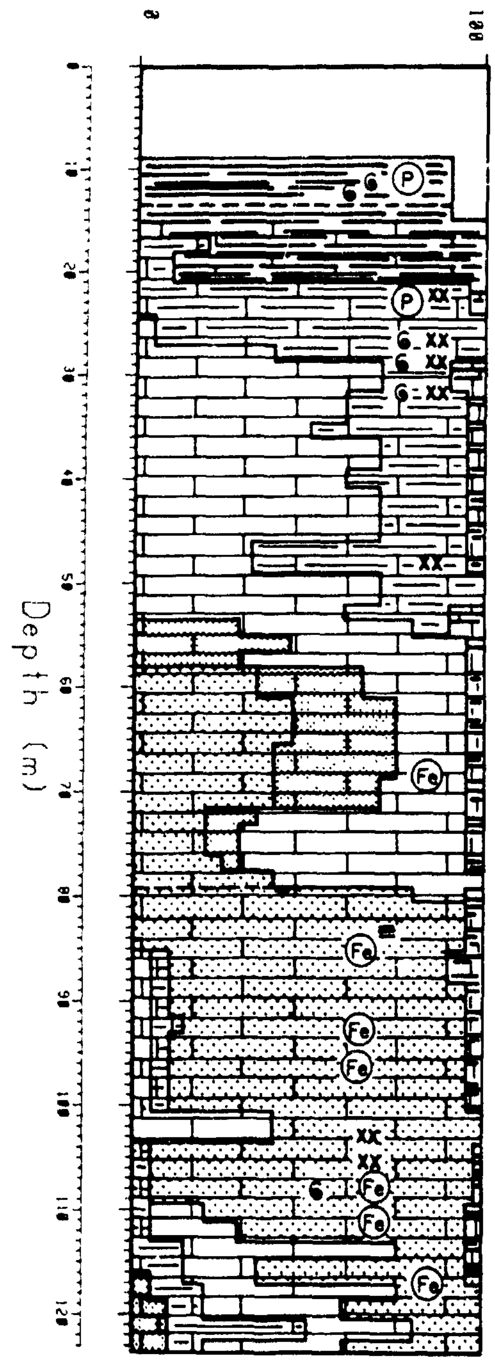

Interpretation
Lithologic boundaries / Formations

—Bedrock surface

Limestone and shale, dark grey
— Eastview Formation

Limestone, crystalline, interbedded with argillaceous limestone and shale
— Cobourg Formation

Limestone, crystalline with calcarenite, sublithographic limestone and shale interbeds
—Sherman Fall Formation

Limestone, calcarenite
—Hull Formation

Interbedded calcilutite and shale

Limestone, sublithographic and argillaceous
—Rockland Formation

P 3

% of Rock Types
(cuttings sampled every 1.5 m)

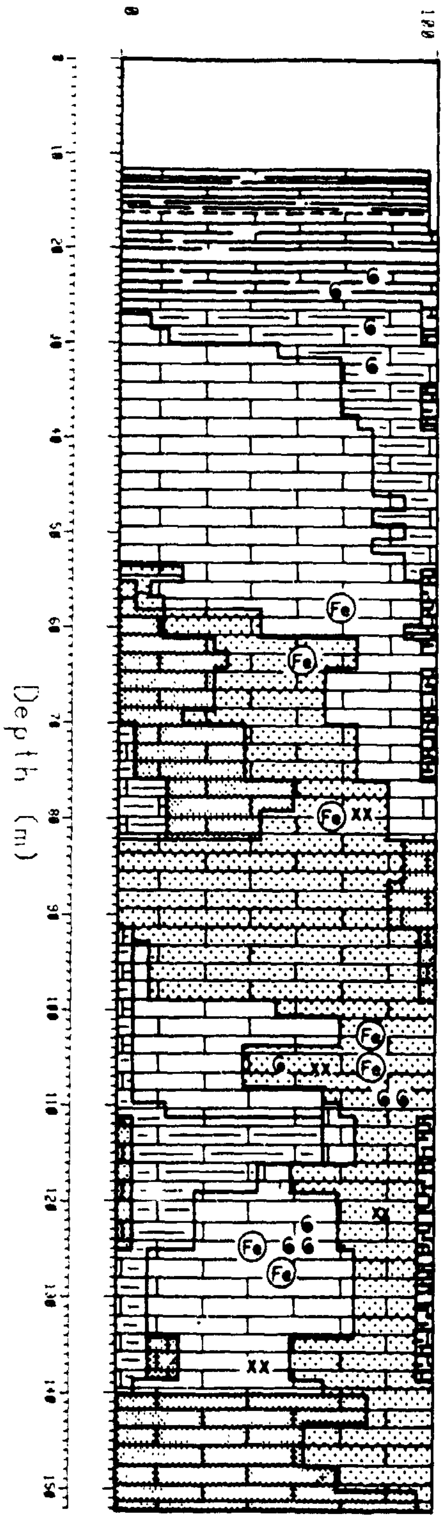

Interpretation
Lithologic boundaries / Formations

—Bedrock surface

Limestone and shale, dark grey
– Eastview Formation

Limestone, crystalline interbedded with argillaceous limestone and shale
– Cobourg Formation

Limestone, crystalline with calcarenite sublithographic limestone and shale interbeds
– Sherman Fall Formation

Limestone, calcarenite
– Hull Formation

interbedded argillaceous limestone

Limestone, sublithographic and argillaceous with shale interbeds
– Rockland Formation

Limestone, calcarenite
– Leroy Formation

Limestone, sublithographic with calcarenite interbeds
– Lowville Formation

P.4

% of Rock Types

(cuttings sampled every 1.5 m)

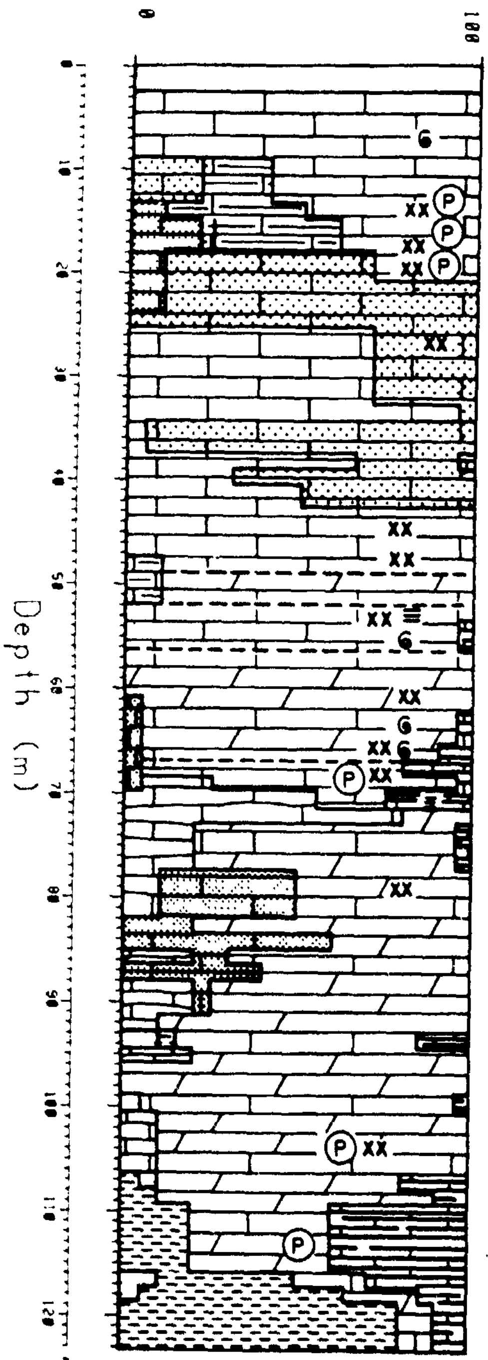

Interpretation

Lithologic boundaries / Formations

—Bedrock surface

Limestone, medium grained

—Hull Formation

Limestone, sublithographic and argillaceous

—Rockland Formation

Limestone, calcarenite

—Leray Formaton

Limestone, with shale and calcarenite interbeds

—Lowville Formation

Dolostone / limestone

—mid to lower Lowville Formation

Wavy laminae and dark concretions

—lower Lowville Formation

Sublithographic limestone interbeds

Dolostone, sandstone and shale interbeds interbeds

—Pamelia / St. Martin Formations

Siltstone greenish grey

— upper Rockcliffe Formation

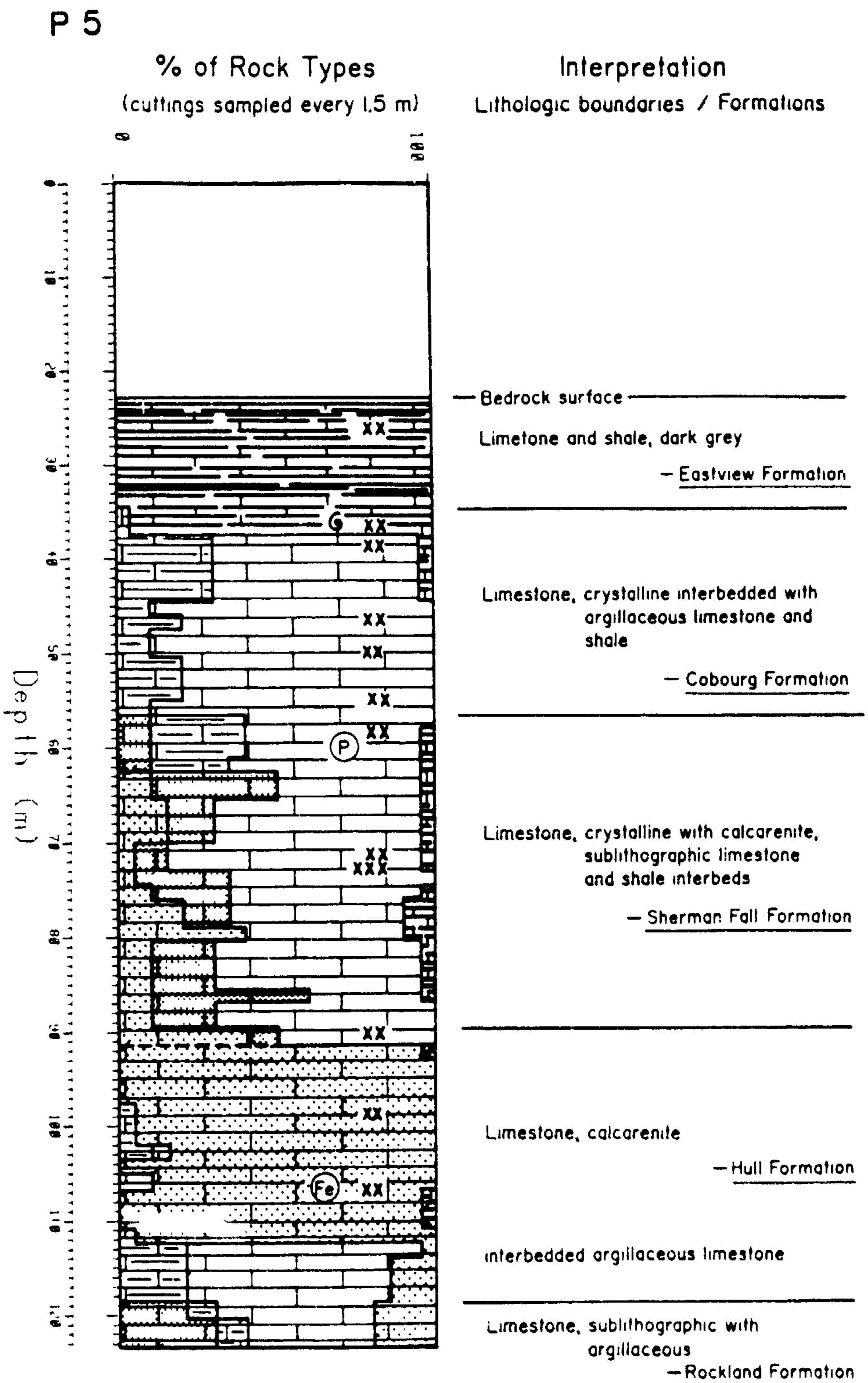
P 5
% of Rock Types
(cuttings sampled every 1.5 m)
0
100
Interpretation
Lithologic boundaries / Formations
Depth (m)
0
10
20
30
40
50
60
70
80
90
100
110
120
Bedrock surface
Limetone and shale, dark grey
– Eastview Formation
Limestone, crystalline interbedded with argillaceous limestone and shale
– Cobourg Formation
Limestone, crystalline with calcarenite, sublithographic limestone and shale interbeds
– Sherman Fall Formation
Limestone, calcarenite
– Hull Formation
interbedded argillaceous limestone
Limestone, sublithographic with argillaceous
– Rockland Formation

P 6

% of Rock Types
(cuttings sampled every 1.5 m)

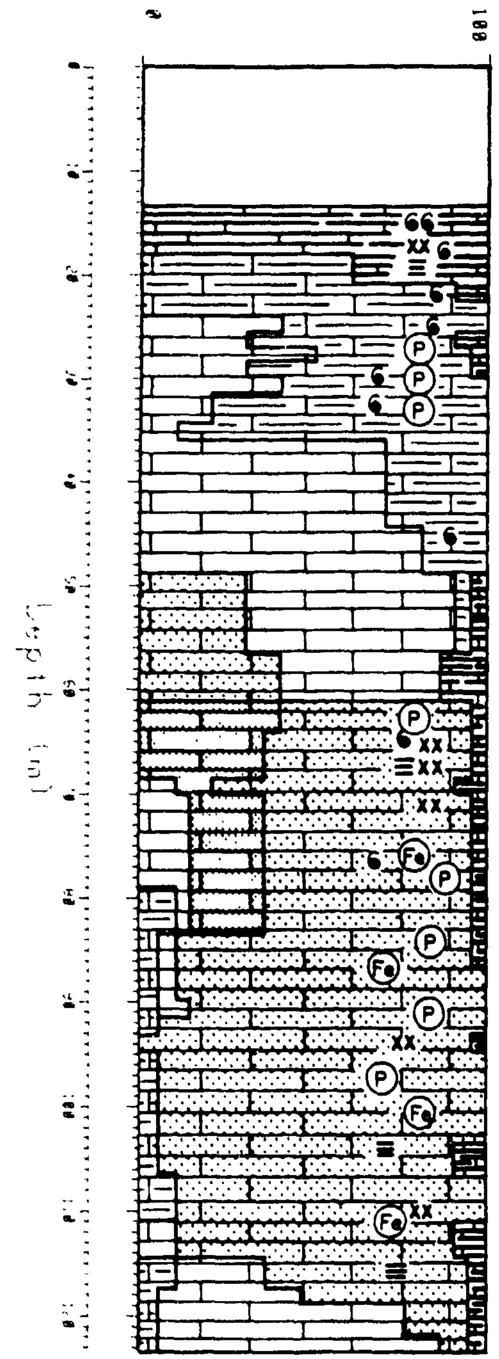

Interpretation
Lithologic boundaries / Formations

— Bedrock surface
Limestone and shale, dark grey
— Eastview Formation

Limestone, crystalline with calcarenite, sublithographic limestone and shale interbeds
— Cobourg Formation

Limestone, crystalline, interbedded with argillaceous limestone and shale
— Sherman Fall Formation

Limestone, calcarenite
— Hull Formation

interbedded argillaceous limestone

Limestone, sublithographic and argillaceous with shale interbeds
— Rockland Formation

ELBA 2

% of Rock Types | Interpretation
(cuttings sampled every 1.5 m) | Lithologic boundaries / Formations

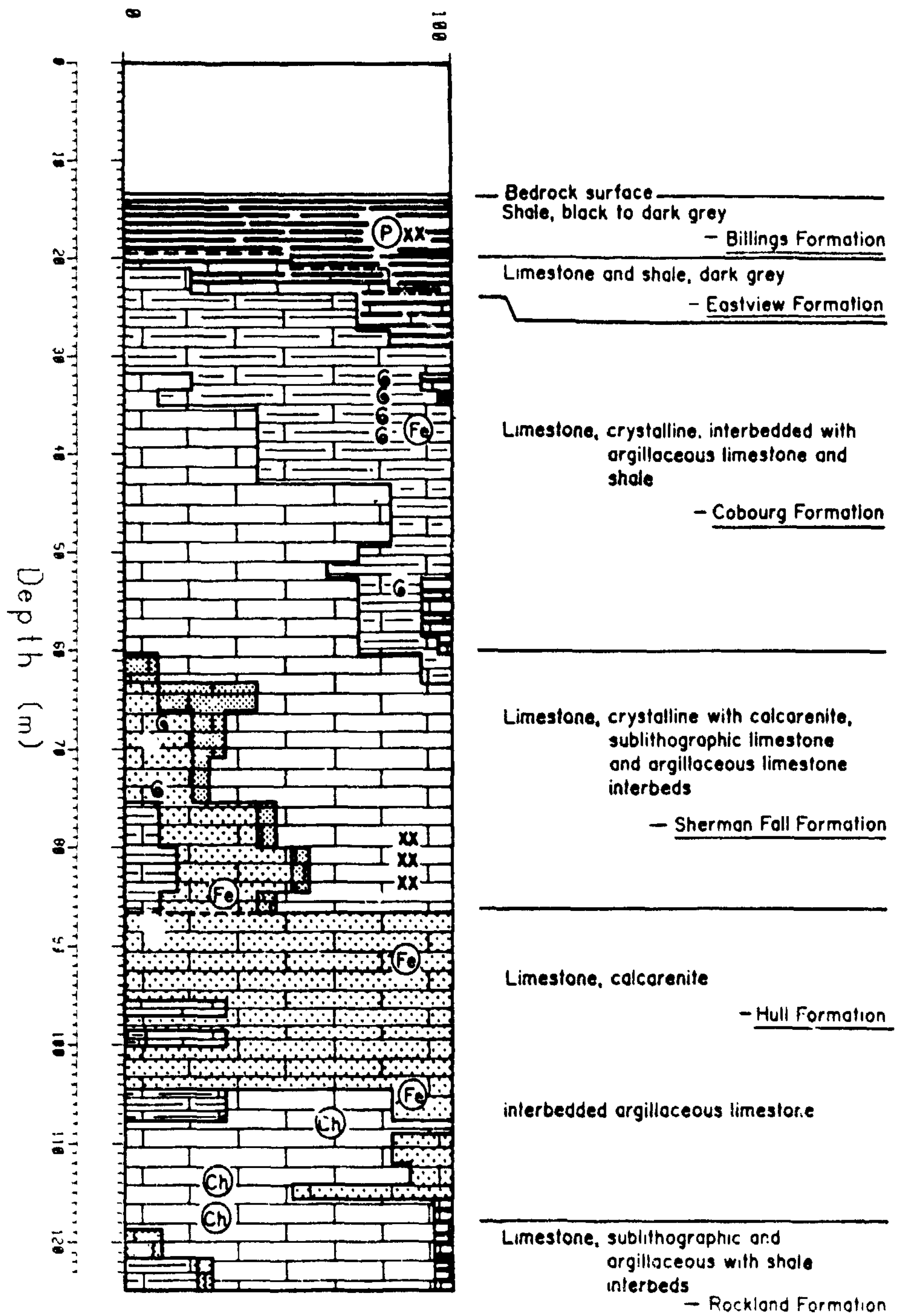

T I

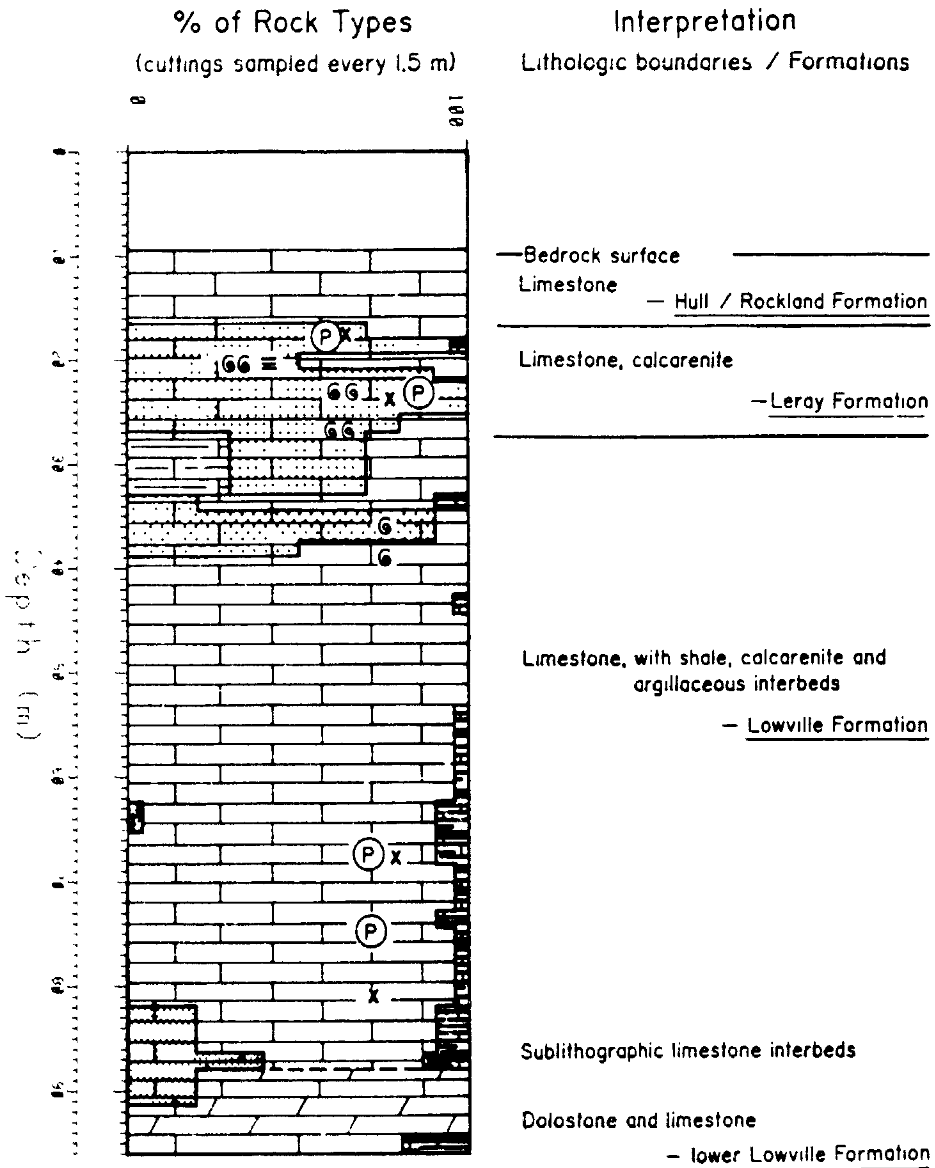
% of Rock Types
(cuttings sampled every 1.5 m)
Interpretation
Lithologic boundaries / Formations
Depth (m)
—Bedrock surface
Limestone
— Hull / Rockland Formation
Limestone, calcarenite
—Leray Formation
Limestone, with shale, calcarenite and argillaceous interbeds
— Lowville Formation
Sublithographic limestone interbeds
Dolostone and limestone
— lower Lowville Formation

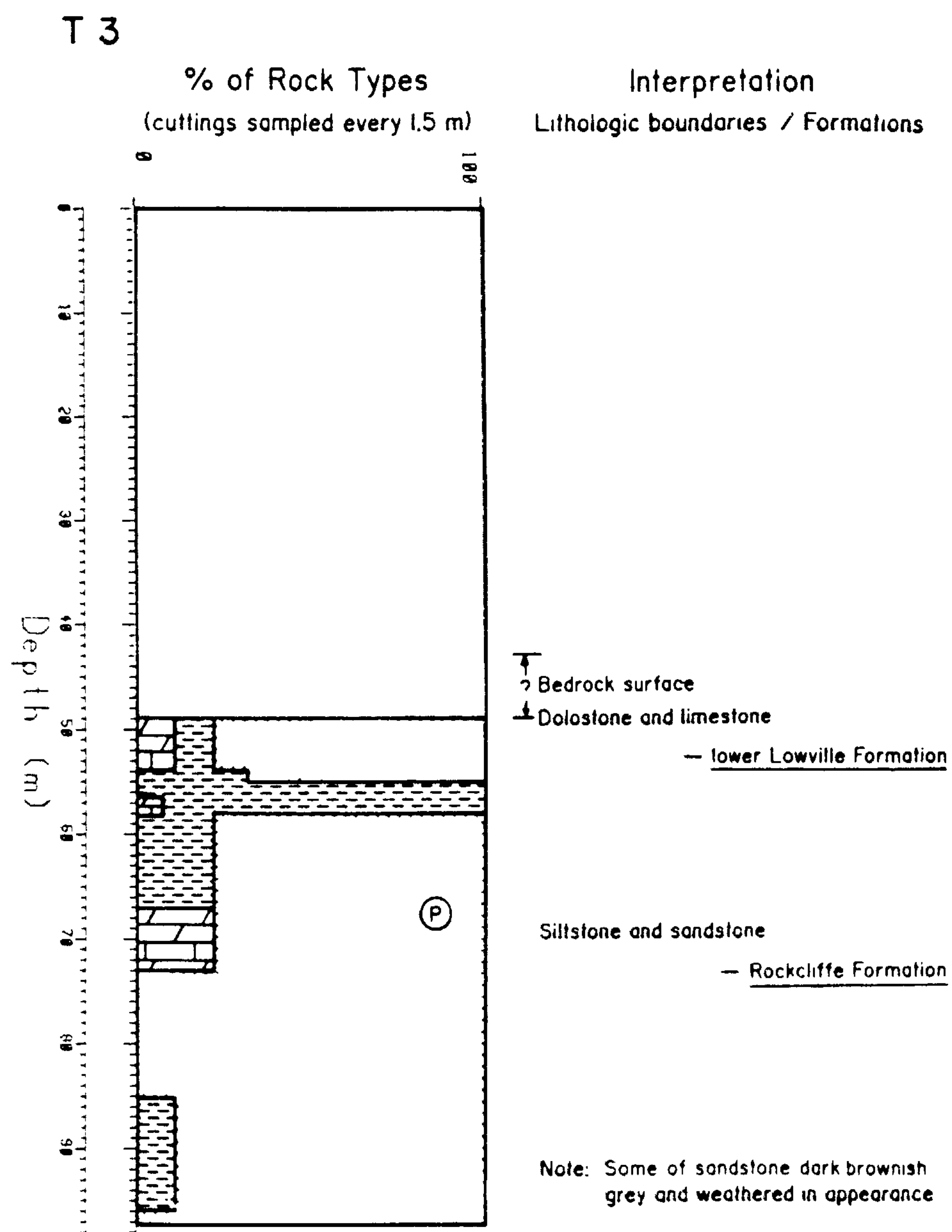
T 3
% of Rock Types
(cuttings sampled every 1.5 m)
Interpretation
Lithologic boundaries / Formations
Depth (m)
? Bedrock surface
Dolostone and limestone
— lower Lowville Formation
Siltstone and sandstone
— Rockcliffe Formation
Note: Some of sandstone dark brownish grey and weathered in appearance

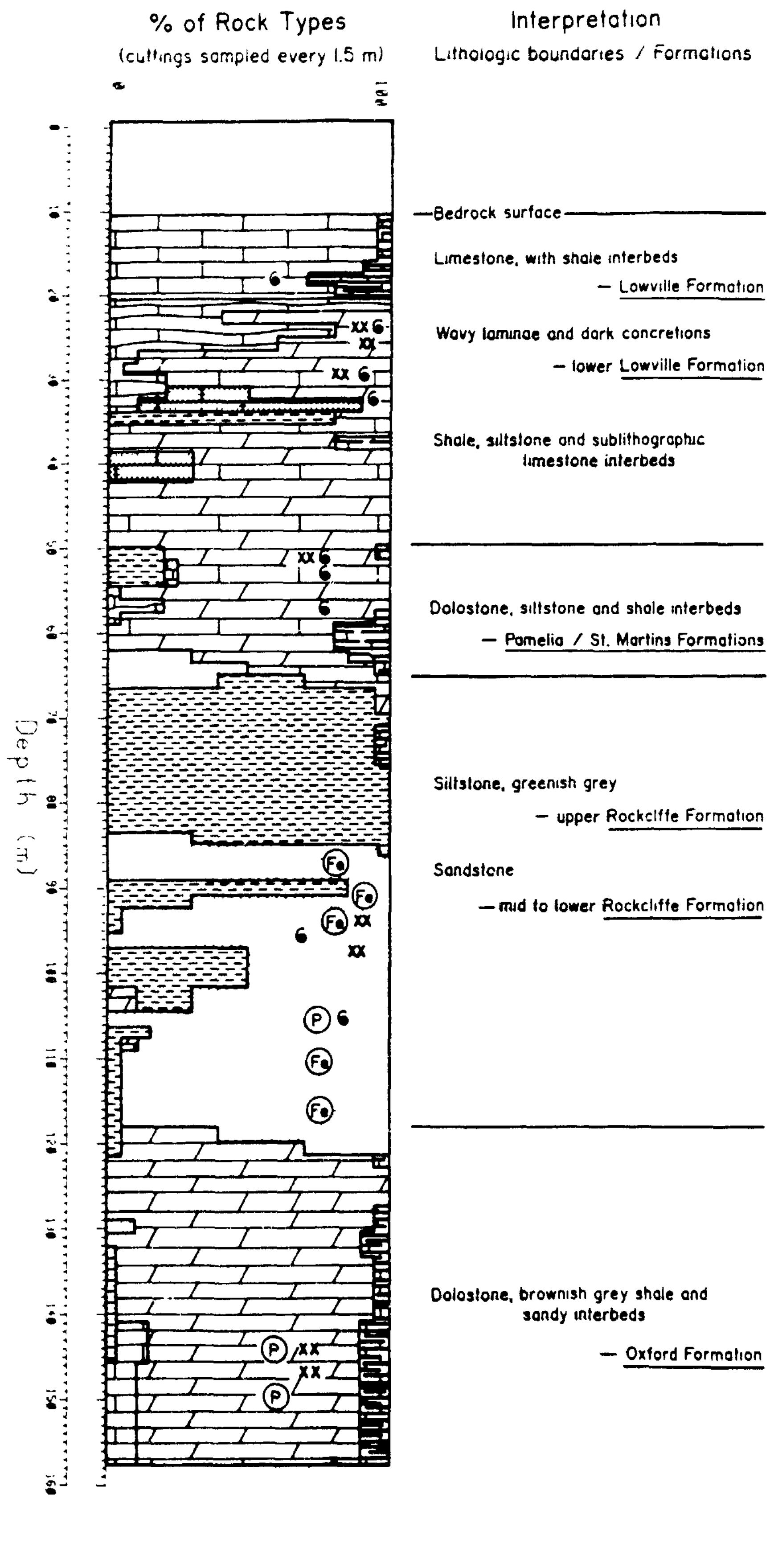
% of Rock Types
(cuttings sampled every 1.5 m)
Interpretation
Lithologic boundaries / Formations
Depth (m)
—Bedrock surface
Limestone, with shale interbeds
— Lowville Formation
Wavy laminae and dark concretions
— lower Lowville Formation
Shale, siltstone and sublithographic limestone interbeds
Dolostone, siltstone and shale interbeds
— Pamelia / St. Martins Formations
Siltstone, greenish grey
— upper Rockcliffe Formation
Sandstone
— mid to lower Rockcliffe Formation
Dolostone, brownish grey shale and sandy interbeds
— Oxford Formation

Appendix 3

GEOPHYSICAL LOGS

Introduction

The following is an account of the placement of each formational contact and the correlations made between lithologic and geophysical logs shown in this Appendix. The Billings-Eastview contact, found in well Elba 2, was defined by the transition from non- to slightly calcareous shale to calcareous shale interbedded with limestone. The boundary was placed just at the base of a sharp decrease in the gamma ray count and the first occurrence of calcareous shale.

The Eastview-Cobourg contact, encountered in wells Elba 2, P2, P3, P5 and P6, was placed at the bottom of the last major shale-rich unit within the transition zone of interbedded dark grey shale and limestone. The Cobourg-Sherman Fall contact was placed just above a shale unit overlying a coarse-grained limestone unit. The Sherman Fall-Hull contact proved to be a marker bed for wells Elba 2, P2, P3, P5 and P6 since the sharp contrast between the 12 metre interval of pure calcarenite on top of the Hull and the relatively shale-rich beds of the overlying Sherman Fall was clearly evident in the natural gamma and resistivity logs. The Hull-Rockland contact was placed at the top of a dark grey sublithographic limestone, present in the geology logs, and in the middle of a transition zone of gradually increasing shale content which was identified from the natural gamma ray increase.

The Rockland-Leray contact, intersected in wells P3 and P4, was marked by a sharp decrease in the gamma ray count, an increase in apparent resistivity and the occurrence of calcarenite in the geology log. The Leray-Lowville contact, also intersected by wells P3 and P4 was marked by an increase in the shale content/gamma ray count. The lower limit of the Leray calcarenite is more clearly defined in the P4 gamma ray log than in the P3 log which may be due to borehole effects (Schlumberger, 1972) that may be more prevalent at the bottom of well P3.

The Lowville-Pamelia contact, intercepted by wells P4 and P1, was placed at the first intense gamma log spike, corresponding to the first shale-rich unit and the first occurrence of chips from silty and sandy beds. The St. Martin was identified by a noticeable 2 to 3 m interlude of low gamma ray count immediately overlying an extensive shale-rich section of the upper Rockcliffe. The 12 m interval of green-grey to brown shale at the top of the Rockcliffe Formation proved to be another marker bed, in the P1 and P4 wells, both in the geological and geophysical logs. The Rockcliffe-Oxford contact, only intersected by well P1, was positioned where a sharp decrease in gamma ray count and an increase in the apparent resistivity coincide with a limey dolomite unit in the geological log.

Legend

Rock Types

Limestones

- Argillaceous, dark to medium grey sometimes brownish grey (calcilutite) limestone
- Medium to dark grey, often recrystallized limestone
- Light to medium grey, medium to coarse-grained (calcarenite) limestone
- Medium to dark brown grey, silty (calcilutite) limestone with dark concretions and wavy laminae
- Medium to dark grey sublithographic (calcilutite) limestone

Shales

- Dark grey to black, noncalcareous to slightly calcareous shale
- Dark grey, slightly calcareous to calcareous shale

Siltstones

- Light green to greenish grey to grey brown siltstone, sometimes fissile and calcareous

Sandstones

- Medium to light grey green to greenish grey brown, fine-grained sandstone, sometimes calcareous

Dolostones

- Dark to medium grey, fine-grained limey dolostone, sometimes argillaceous with calcite
- Medium grey brown dolostone and limey dolostone veins

Symbols

X coarse white calcite crystals

fossiliferous

(P) pyrite

(Ch) chert

(Fe) iron staining

≡ slickensides

Geophysical Logs

Litho (%)	-	Lithology % of rock types in every 1 5 metre sample
TC (CPS)	-	Gamma ray log (counts per second)
Density	-	Gamma-gamma ray log
RHO (1)	-	Resistivity log - symmetrical lateral
RHO (2)	-	Resistivity log - normal array
IP	-	Instantaneous potential
Temp	-	Temperature (°C)
Temp Grad	-	Temperature gradient (°C/km of depth)
Litho	-	Lithology - generalised from litho (%) log

Symbols

- - - - - bottom of casing

⇦ groundwater entering the borehole

⇨ groundwater exiting the borehole

Note Borehole diameter change from 30 5 to 25 4 cm in all wells at 81 metres depth

HOLE F-1

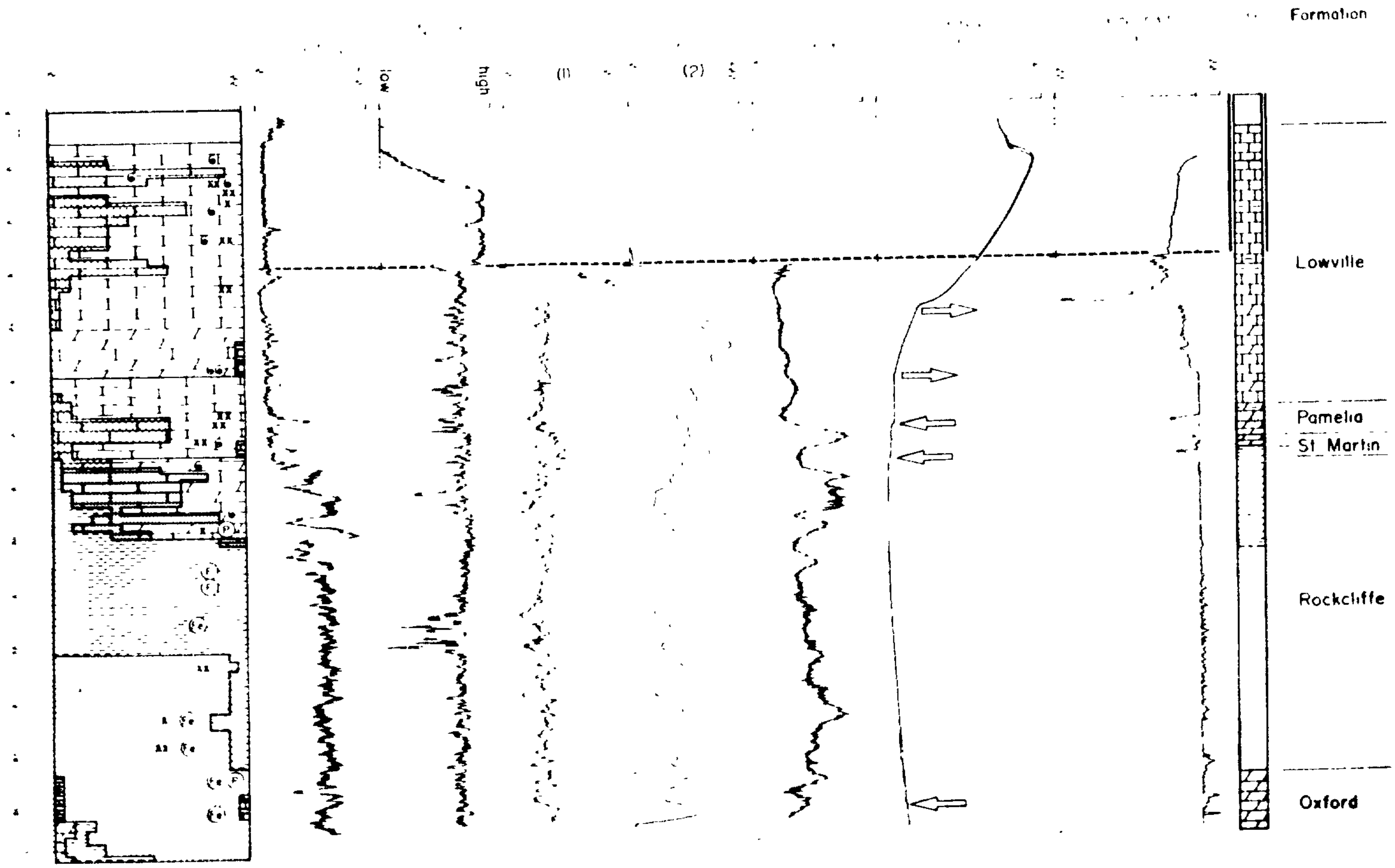

Formation
Lowville
Pamelia
St. Martin
Rockcliffe
Oxford
low
high
(1)
(2)

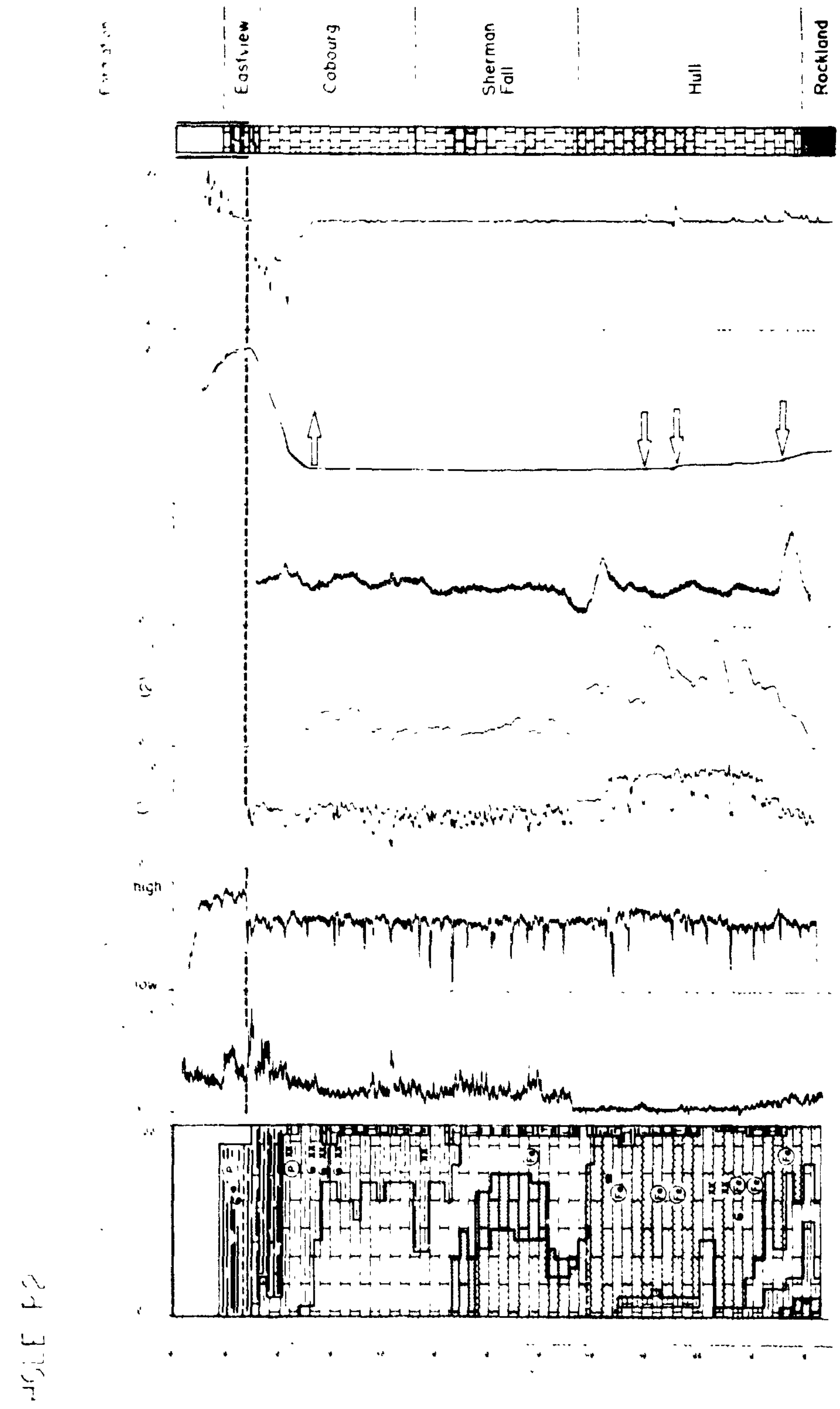

Eastview
Cobourg
Sherman Fall
Hull
Rockland
high
low

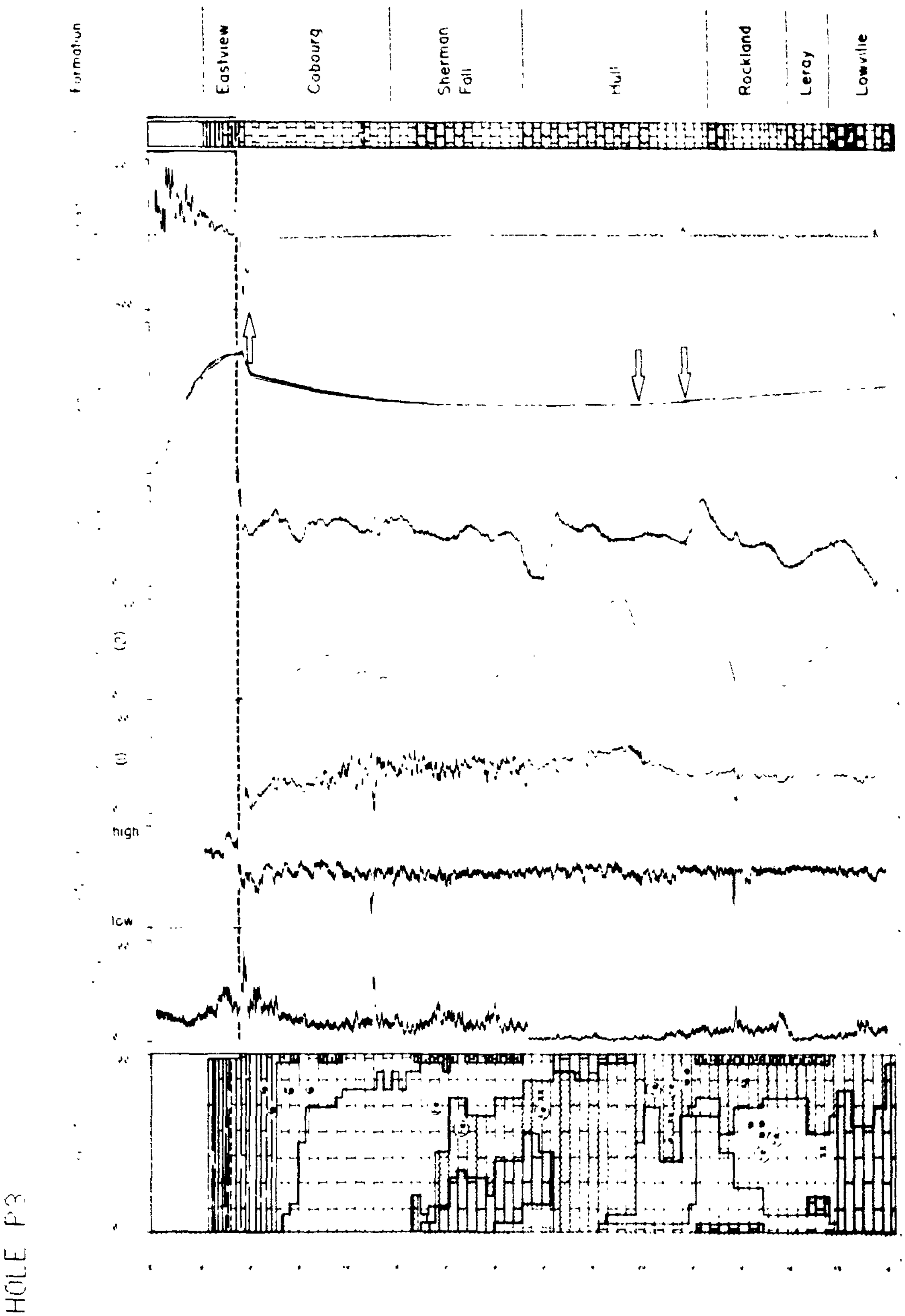

Formation
Eastview
Cobourg
Sherman Fall
Hull
Rockland
Leray
Lowville
high
low
HOLE P3

Chemistry Data: May, 1989

Field Parameters (Continued)

Well	Sample	Date	Temp (C)	Eh (V)	pH field	pH lab	EC (uS/cm) field	Alk.(mg/l) field	Alk.(mg/l) lab	Sulphide (mg/l) field	Sulphide (mg/l) lab	log(PCO2) calc. (bar)
P6	-35m	10/5/89	11	-0.04	7.3	7.4	1330	405	304	0.67	-	-1.83
	-55m	10/5/89	12	-0.23	7.4	7.5	1010	325	314	0.42	-	-2.02
	-80m	10/5/89	11	-0.23	7.4	7.6	970	330	288	0.40	-	-2.02
	-110m	10/5/89	11	-0.25	7.5	8.1	1010	346	304	0.25	-	-2.03
P6	-35m(2)	19/5/89	13	-0.28	7.5	7.6	1630	-	366	0.90	-	-2.01
	-55m(2)	19/5/89	13	-0.27	7.6	7.9	1340	-	323	0.30	-	-2.16
	-80m(2)	19/5/89	12	-0.29	7.5	7.7	1070	-	316	0.40	0.17	-2.10
	-110m(2)	19/5/89	12	-0.29	7.4	7.8	1410	-	323	0.45	-	-1.96
Elba 2	-30m	18/5/89	12	-0.44	8.0	7.8	940	265	230	>2.25	-	-2.68
	-55m	18/5/89	12	-0.41	8.3	7.8	930	250	250	>2.25	-	-3.04
	-85m	18/5/89	11	-0.42	8.1	8.1	1020	259	242	>2.25	4.51	-2.83
	-108m	18/5/89	11	-0.41	7.9	8.0	1000	265	230	>2.25	-	-2.60
M1	-61m	01/6/89	12	0.06	8.2	8.2	2760	-	200	<.25	-	-3.03
	-82.3m	01/6/89	12	-0.07	7.9	8.1	3000	-	284	<.25	-	-2.59
	-122m	01/6/89	12	-0.09	7.9	7.9	3260	-	180	<.25	<.1	-2.77

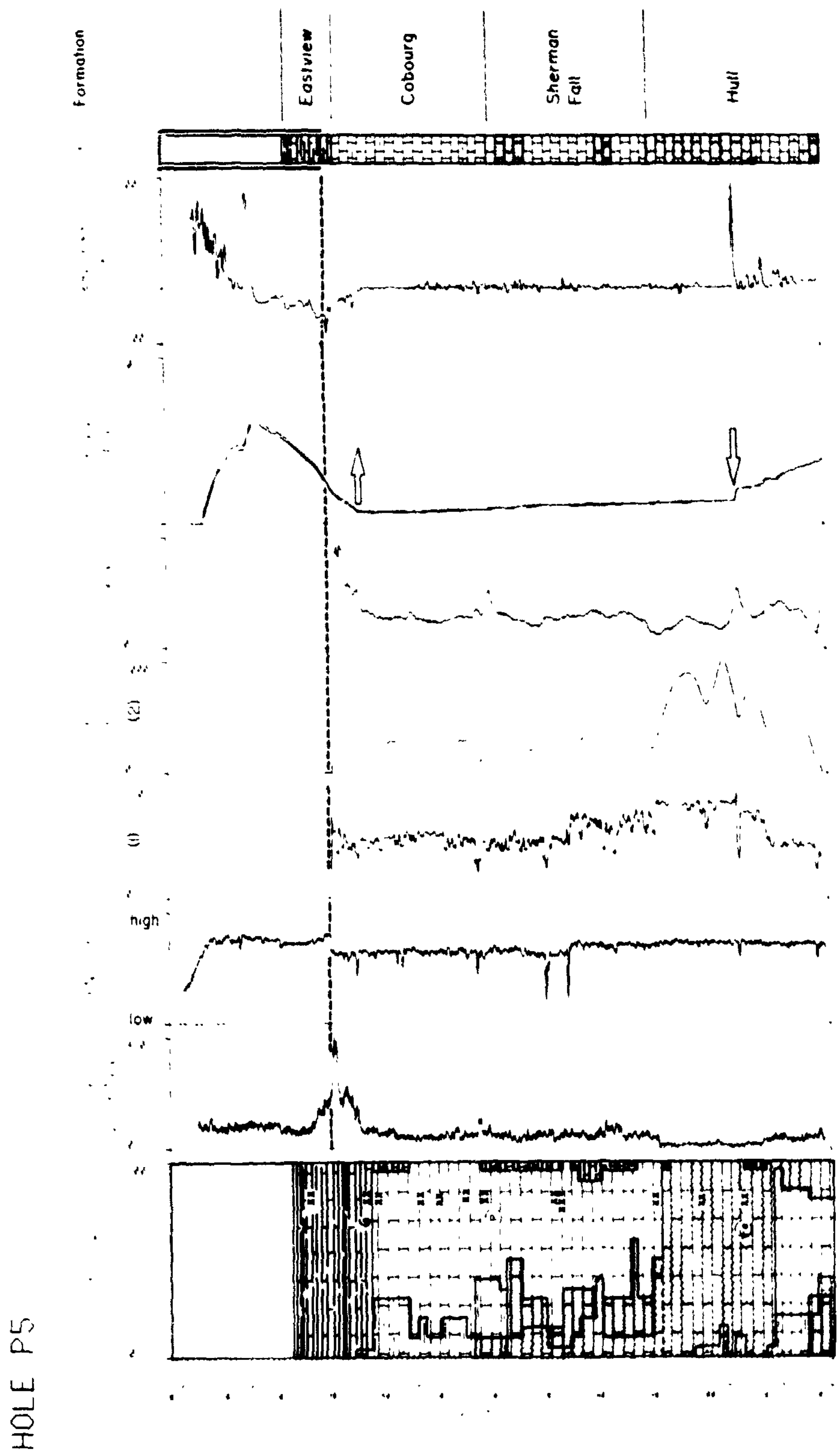
Formation
Eastview
Cobourg
Sherman Fall
Hull
high
low
HOLE P5

HOLE F6

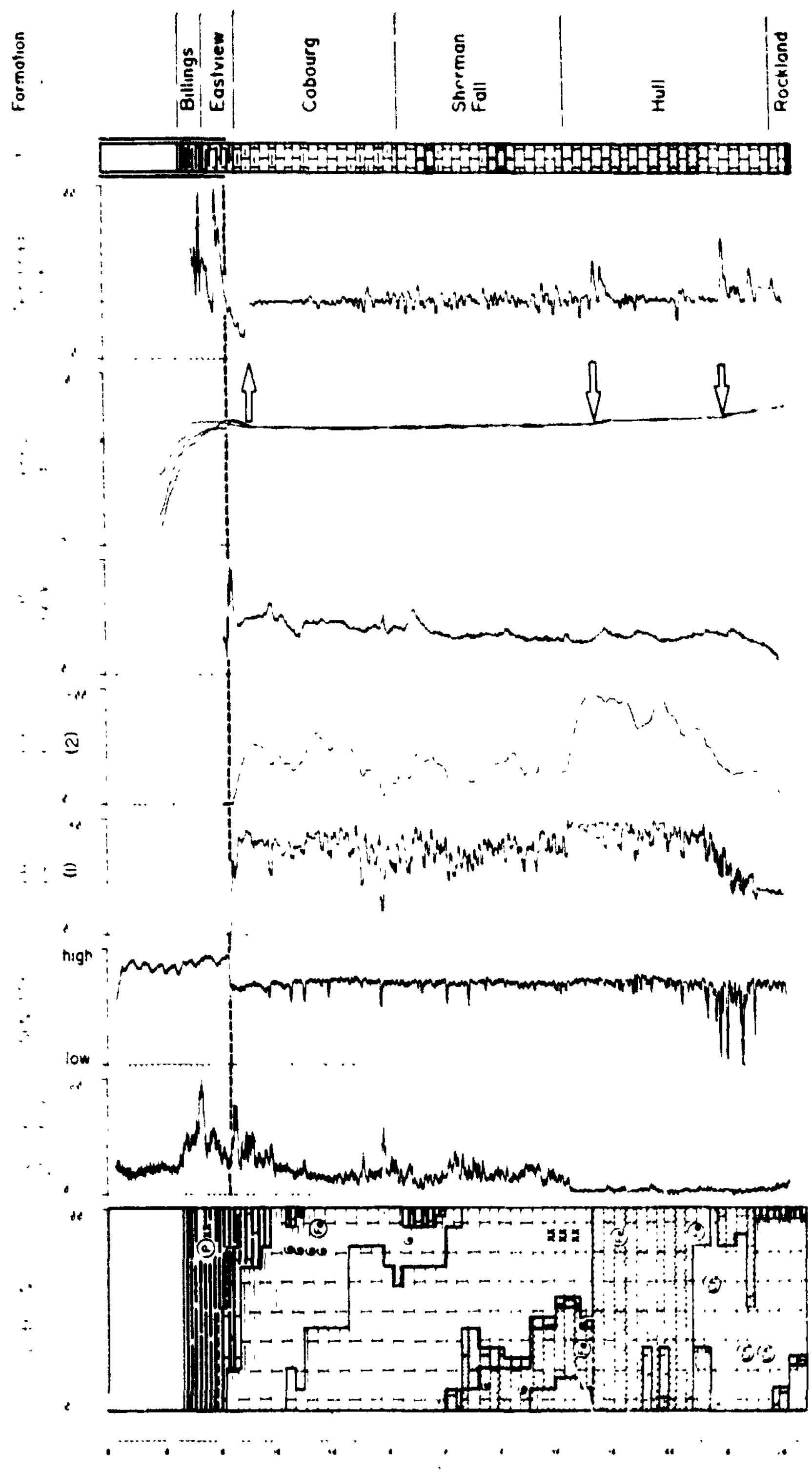
Formation
Billings
Eastview
Cobourg
Sherman Fall
Hull
Rockland
(2)
(1)
high
low

HOLE ELBA2

Appendix 4

TEMPERATURE AND TEMPERATURE GRADIENT LOGS

Legend

⇨	exit
←	entry
↑	direction of groundwater flow within borehole
①	local surface and infrastructure temperature effects
① *	local surface and infrastructure temperature effects augmented by groundwater flow outside of casing
②	isothermal (or near isothermal) conditions due to relatively rapid flow
③	temperature gradient reversal (Lewis, 1973; Drury *et al*., 1984)
④	temperature changes possibly related to changes in lithology
⑤	water circulation and eddies in borehole

HOLE P1

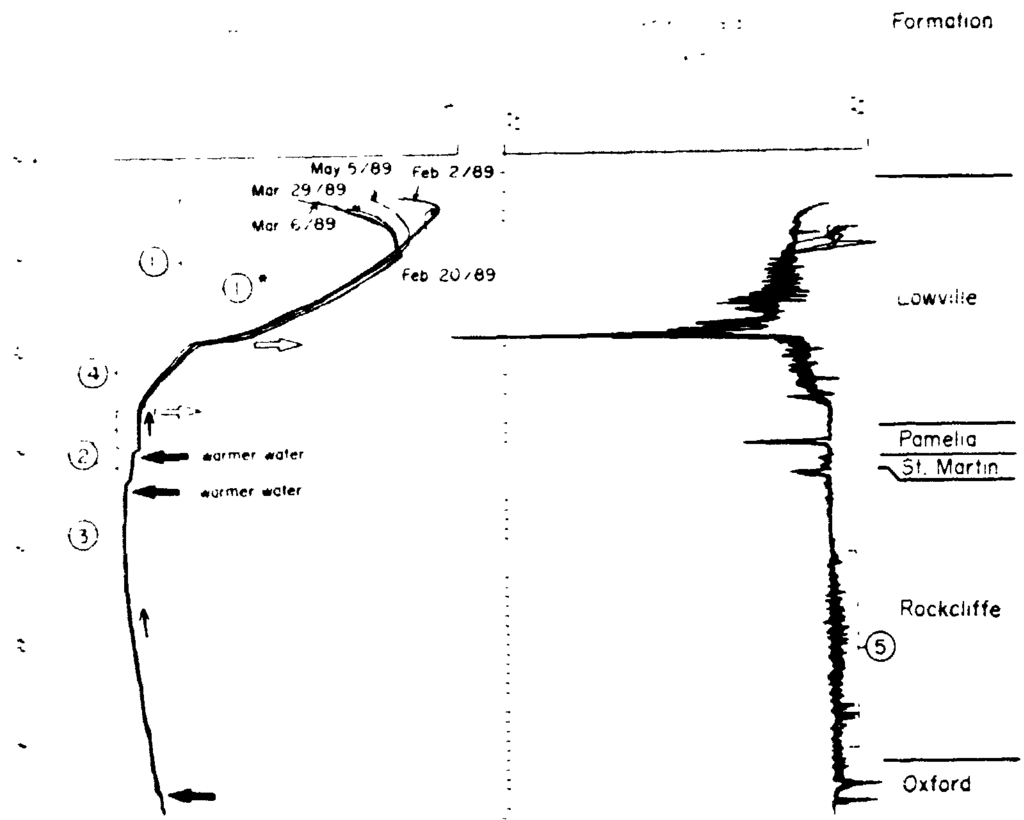
Formation
May 5/89
Feb 2/89
Mar 29/89
Mar 6/89
Feb 20/89
warmer water
warmer water
Lowville
Pamelia
St. Martin
Rockcliffe
Oxford

HOLE P2

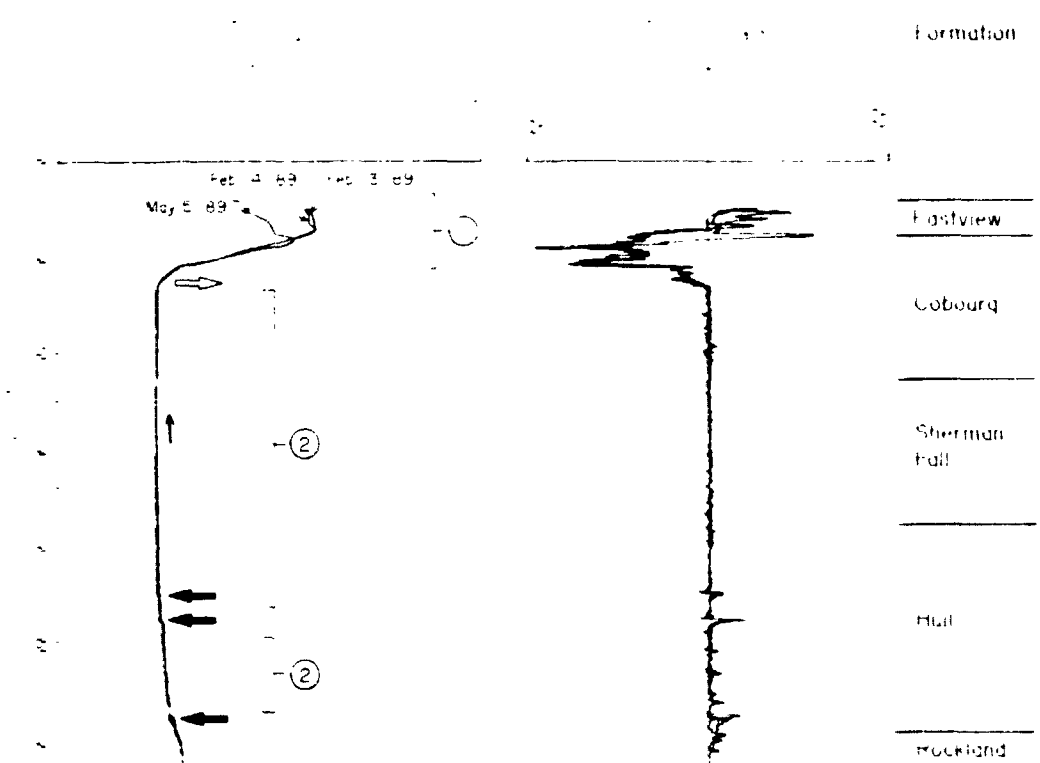
Formation
Feb 4 89
Feb 3 89
May 5 89
Eastview
Cobourg
Sherman Fall
Hull
Rockland

HOLE P3

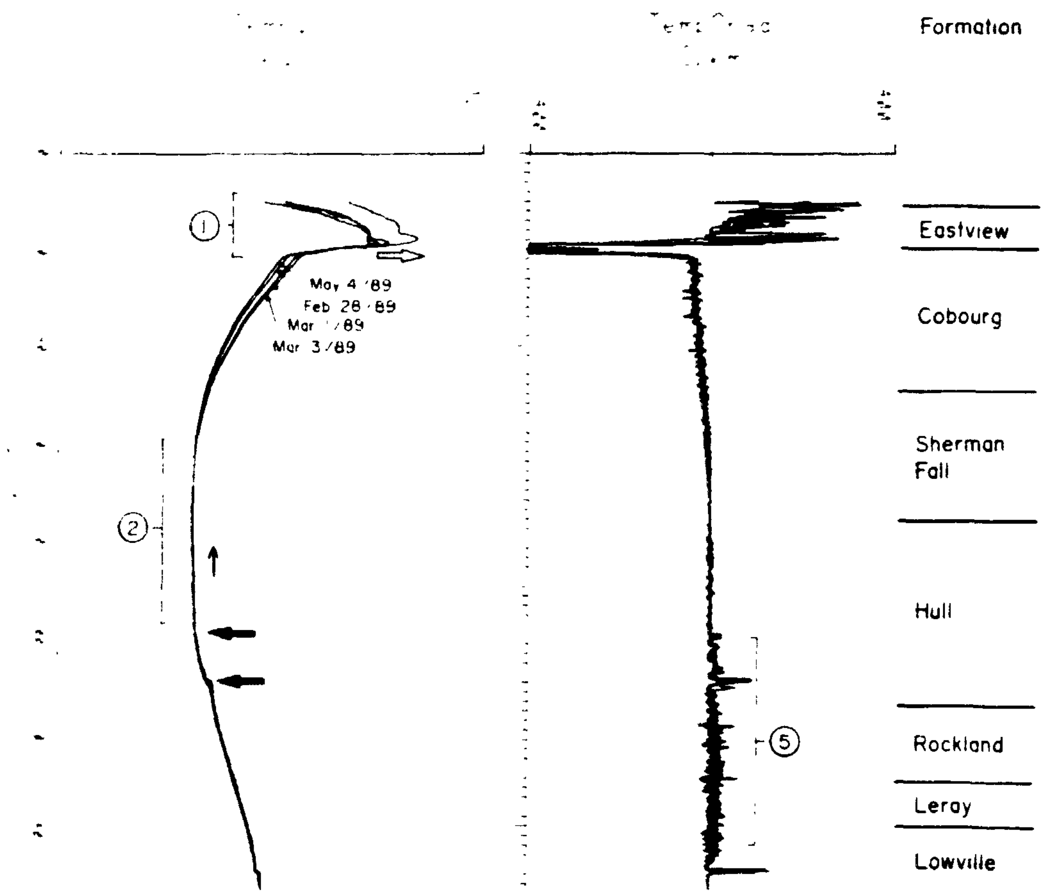
Formation
May 4 '89
Feb 28 '89
Mar 3 '89
Eastview
Cobourg
Sherman
Fall
Hull
Rockland
Leray
Lowville

HOLE P4

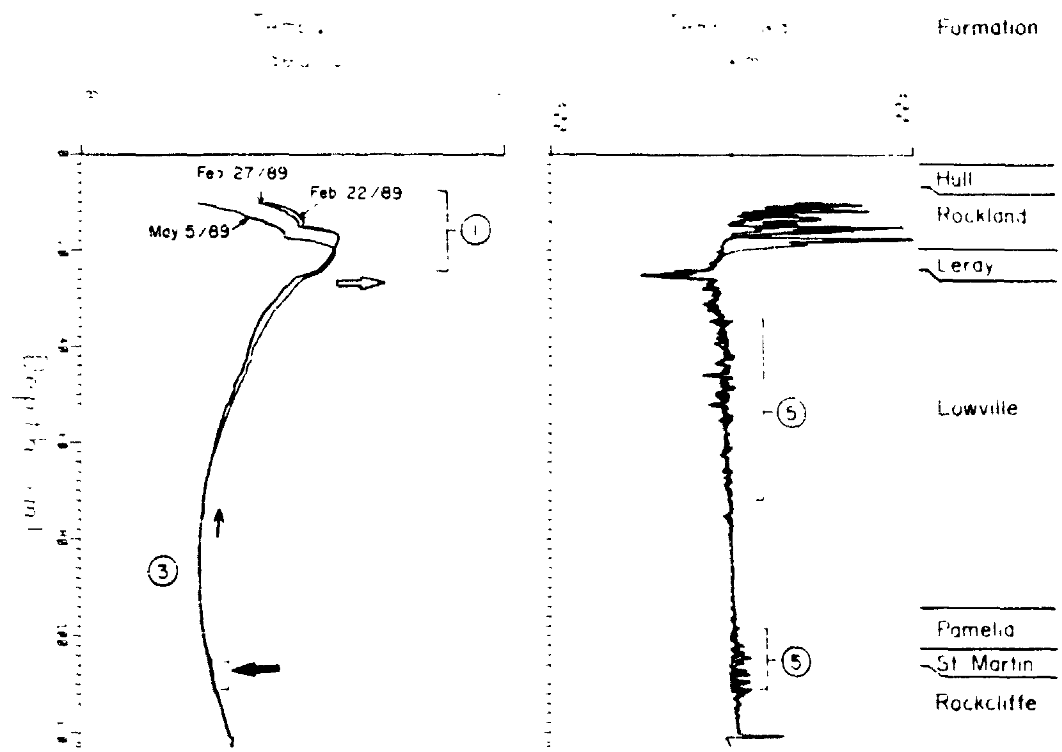

Formation
Feb 27/89
Feb 22/89
May 5/89
1
3
5
5
Hull
Rockland
Leray
Lowville
Pamelia
St Martin
Rockcliffe

HOLE P5

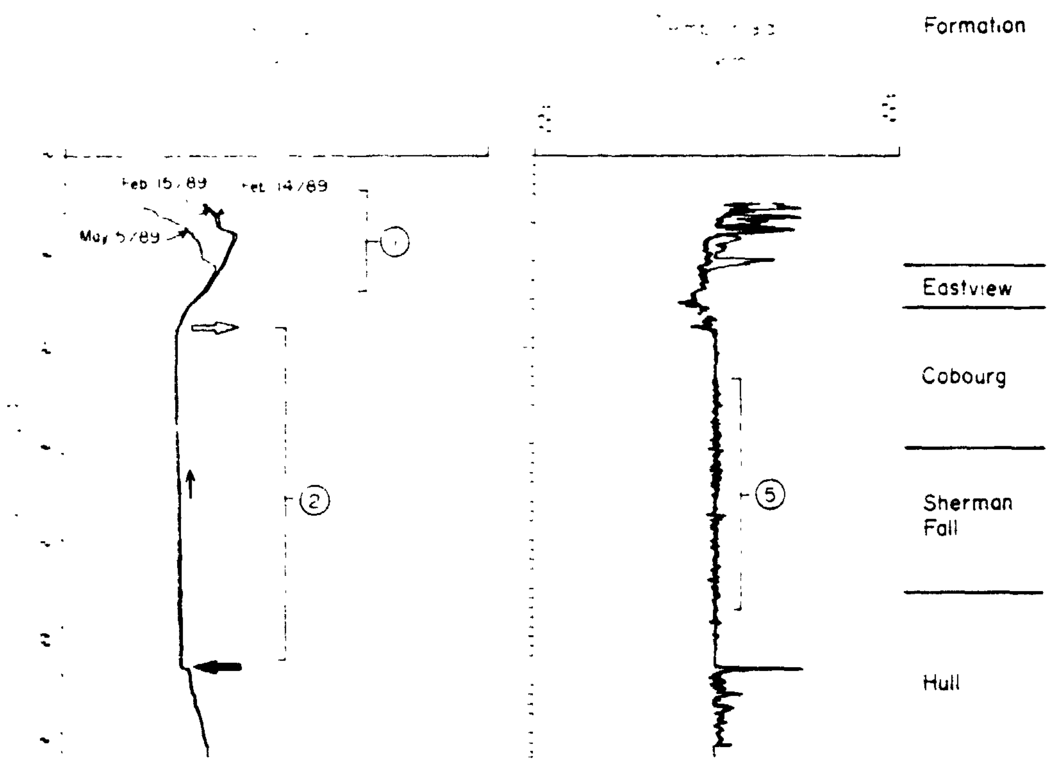
Formation
Feb 15/89
Feb 14/89
May 5/89
1
2
5
Eastview
Cobourg
Sherman
Fall
Hull

HOLE P6

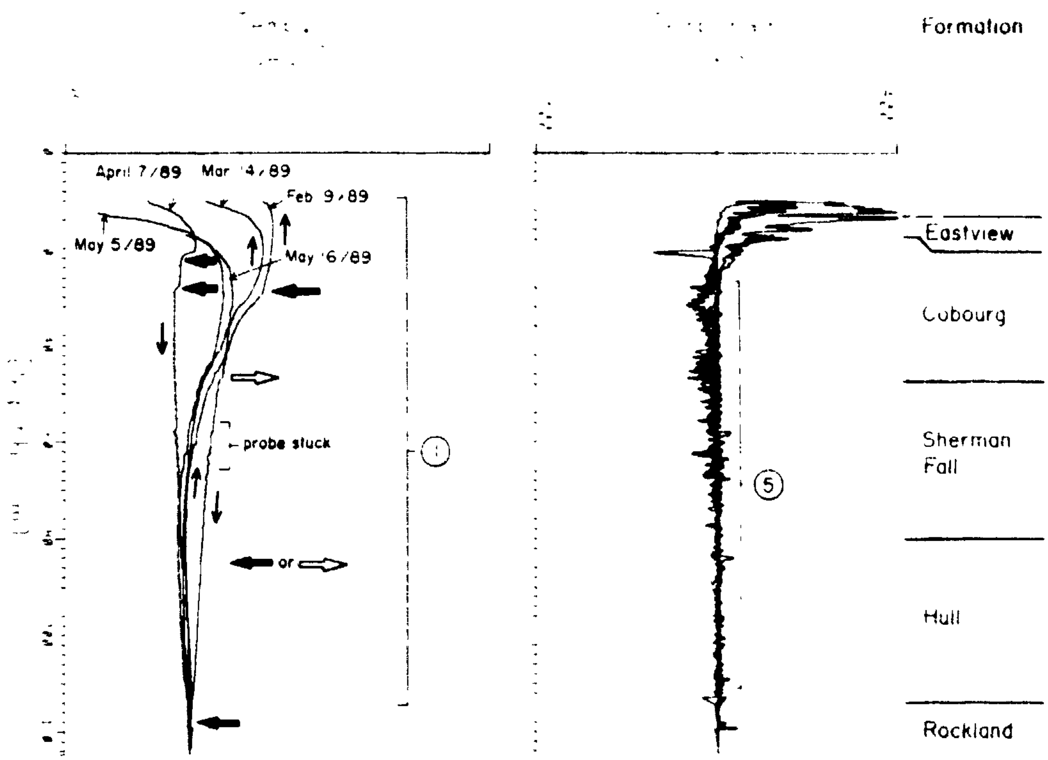
Formation
April 7/89
Mar 14/89
Feb 9/89
May 5/89
May 16/89
probe stuck
or
5
Eastview
Cobourg
Sherman
Fall
Hull
Rockland

HOLE ELBA2

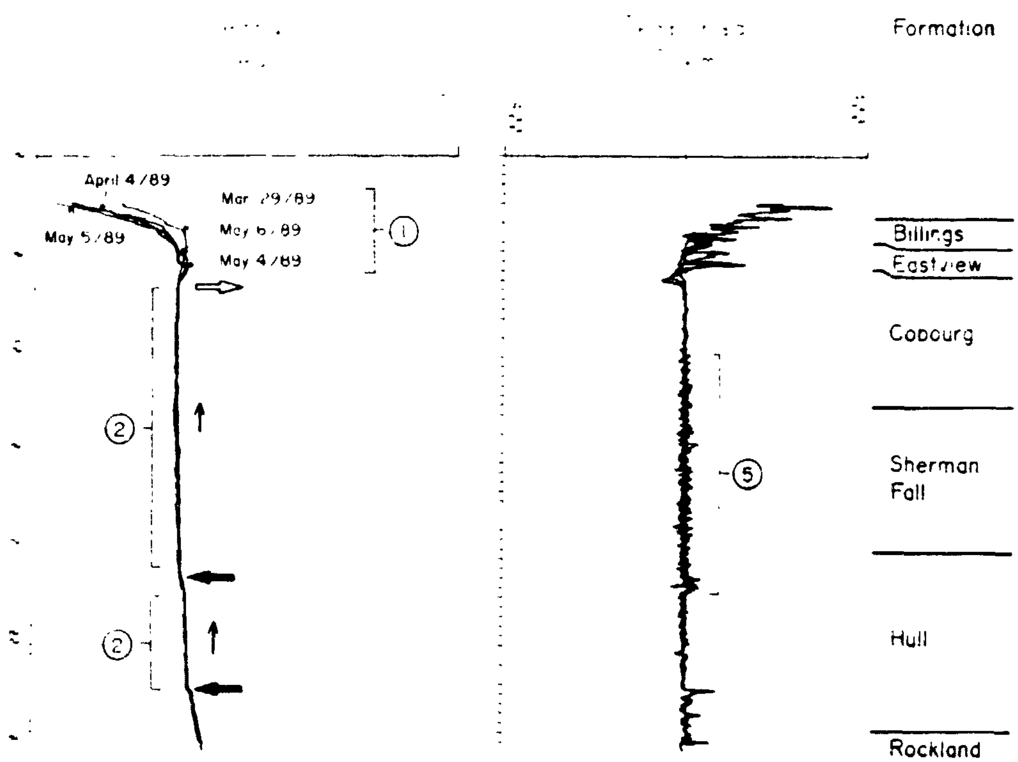

Formation
April 4/89
Mar 29/89
May 5/89
May 6/89
May 4/89
①
②
②
⑤
Billings
Eastview
Cobourg
Sherman Fall
Hull
Rockland

Appendix 5

FIELD AND LABORATORY CHEMICAL DATA

Chemistry Data: May, 1989

Field Parameters

Well	Sample	Date	Temp (C)	Eh(Pt) (V)	pH field	pH lab	EC (uS/cm) field	Alk.(mg/l) field	Alk.(mg/l) lab	Sulphide (mg/l) field	Sulphide (mg/l) lab	log(PCO2) calc. (bar)
P1	-34m	17/5/89	14	-0.26	8.5	8.3	1760	159	117	0.25	-	-3.35
	-55m	17/5/89	12	-0.29	8.3	8.0	2480	170	142	0.35	-	-3.25
	-64m	17/5/89	13	-0.29	8.2	7.9	2180	178	172	0.35	-	-3.08
	-100m	17/5/89	12	-0.32	8.1	7.8	2850	170	148	0.50	-	-3.02
	-130m	17/5/89	12	-0.43	8.0	7.8	3030	188	167	0.60	0.27	-2.81
P2	-20m	18/5/89	13	-0.32	7.9	7.9	960	256	244	>2.25	-	-2.58
	-55m	18/5/89	13	-0.39	7.8	8.0	990	258	246	2.70	-	-2.48
	-87m	18/5/89	12	-0.39	7.8	8.0	980	259	234	2.70	2.36	-2.55
	-93m	18/5/89	12	-0.39	7.8	7.9	1000	256	244	3.20	-	-2.50
	-120m	18/5/89	12	-0.45	8.3	7.9	1180	303	254	20.00	19.60	-2.95
P3	-25m	19/5/89	13	-0.43	7.9	7.8	930	265	232	8.00	-	-2.61
	-55m	19/5/89	13	-0.41	7.9	7.8	980	259	262	9.25	-	-2.61
	-109m	19/5/89	13	-0.44	8.0	7.8	1250	303	241	>11.25	8.74	-2.65
	-150m	19/5/89	12	-0.43	7.8	7.8	1010	288	250	>11.25	-	-2.51
P4	-25m	17/5/89	14	-0.32	8.6	8.3	1020	173	186	0.50	-	-3.54
	-55m	17/5/89	13	-0.35	8.6	8.2	1230	190	170	0.95	-	-3.43
	-110m	17/5/89	12	-0.38	8.0	8.2	1380	199	193	1.50	1.30	-2.78
P5	-34m	16/5/89	12	-0.34	7.9	7.7	1030	257	234	>2.25	2.82	-2.64
	-55m	16/5/89	12	-0.39	7.8	7.5	1090	351	231	>2.25	-	-2.48
	-105m	16/5/89	12	-0.40	7.8	7.6	1150	255	236	>2.25	-	-2.55
	-120m	16/5/89	11	-0.39	7.9	7.6	1230	252	236	>2.25	4.88	-2.67

Chemistry Data: May, 1989

Field Parameters (Continued)

Well	Sample	Date	Temp (C)	Eh (V)	pH field	pH lab	EC (uS/cm) field	Alk.(mg/l) field	Alk.(mg/l) lab	Sulphide (mg/l) field	Sulphide (mg/l) lab	log(PCO2) calc. (bar)
P6	-35m	10/5/89	11	-0.04	7.3	7.4	1330	405	304	0.67	-	-1.83
	-55m	10/5/89	12	-0.23	7.4	7.5	1010	325	314	0.42	-	-2.02
	-80m	10/5/89	11	-0.23	7.4	7.6	970	330	288	0.40	-	-2.02
	-110m	10/5/89	11	-0.25	7.5	8.1	1010	346	304	0.25	-	-2.03
P6	-35m(2)	19/5/89	13	-0.28	7.5	7.6	1630	-	366	0.90	-	-2.01
	-55m(2)	19/5/89	13	-0.24	7.6	7.9	1340	-	323	0.30	-	-2.16
	-80m(2)	19/5/89	12	-0.29	7.5	7.7	1070	-	316	0.40	0.17	-2.10
	-110m(2)	19/5/89	12	-0.29	7.4	7.8	1410	-	323	0.45	-	-1.96
Elba 2	-30m	18/5/89	12	-0.44	8.0	7.8	940	265	230	>2.25	-	-2.68
	-55m	18/5/89	12	-0.41	8.3	7.8	930	250	250	>2.25	-	-3.04
	-85m	18/5/89	11	-0.42	8.1	8.1	1020	259	242	>2.25	4.51	-2.83
	-108m	18/5/89	11	-0.41	7.9	8.0	1000	265	230	>2.25	-	-2.60
M1	-61m	01/6/89	12	0.06	8.2	8.2	2760	-	200	<.25	-	-3.03
	-82.3m	01/6/89	12	-0.07	7.9	8.1	3000	-	284	<.25	-	-2.59
	-122m	01/6/89	12	-0.09	7.9	7.9	3260	-	180	<.25	<.1	-2.77

Chemistry Data: May, 1989

Chemical Analyses

Well	Sample	Ca ppm	Mg ppm	Na ppm	K ppm	CO3 ppm	HCO3 ppm	SO4 ppm	Cl ppm	N-NO3 ppm	N-NH3 ppm	Sr ppm	Fe (Total) ppm	Mn ppm	Total Hardness (CaCO3)	TDS (mg/l)	Ion Balance (%)
P1	-34m	32	23	250	7.1	<1	143	117	263	0.2	0.4	19	0.03	<0.01	175	820	9.5
	-55m	39	26	395	7.0	<1	173	260	418	<0.1	0.4	25	0.05	<0.01	204	1272	5.0
	-64m	48	31	500	7.3	<1	210	292	532	0.1	0.4	27	0.05	<0.01	248	1456	7.0
	-100m	46	29	483	7.4	<1	180	268	507	0.1	0.4	29	0.28	<0.01	234	1380	8.2
	-130m	61	34	498	7.5	<1	204	296	596	<0.1	0.4	29	0.10	<0.01	292	1740	4.4
P2	-20m	73	44	64	6.0	<1	298	63	124	<0.1	0.4	23	0.02	0.02	389	500	9.2
	-55m	87	44	62	6.0	<1	300	68	127	0.3	0.4	24	<0.01	0.02	425	620	10.9
	-87m	97	44	62	[illegible]	<1	285	66	127	<0.1	0.4	23	0.21	0.02	449	560	13.2
	-93m	79	43	63	6.0	<1	298	69	128	<0.1	0.4	23	0.14	0.07	400	536	8.7
	-120m	51	33	167	7.0	<1	310	81	160	<0.1	0.4	18	0.12	0.02	284	664	8.4
P3	-25m	52	34	84	6.0	<1	283	63	141	0.6	0.5	19	0.40	<0.01	292	544	0.2
	-55m	52	34	82	6.0	<1	320	60	143	0.3	0.5	20	0.21	<0.01	293	540	0.4
	-109m	47	32	120	6.0	<1	294	68	164	1.0	0.5	18	<0.01	<0.01	270	568	-1.1
	-150m	87	32	119	6.0	<1	305	56	160	0.7	0.5	20	0.10	<0.01	372	552	10.6
P4	-25m	34	30	164	6.6	<1	227	95	202	0.5	0.3	16	0.03	0.12	209	676	6.2
	-55m	32	30	166	7.0	<1	207	87	175	<0.1	0.3	17	0.23	0.09	205	612	9.6
	-110m	37	29	207	7.0	<1	233	104	199	0.3	0.3	18	0.36	0.07	212	696	11.6
P5	-34m	63	46	86	6.8	<1	285	52	150	<0.1	0.3	26	0.42	0.04	347	160	9.5
	-55m	70	49	86	7.2	<1	282	58	174	<0.1	0.2	27	0.06	0.01	374	648	8.1
	-105m	69	49	87	6.5	<1	288	60	165	<0.1	0.3	27	0.03	0.01	373	588	9.2
	-120m	63	46	131	7.0	<1	288	69	229	<0.1	0.3	29	0.03	0.01	349	732	5.9

Chemistry Data: May, 1989

Chemical Analyses (Continued)

Well	Sample	Ca	Mg	Na	K	CO3	HCO3	SO4	Cl	N-NO3	N-NH3	Sr	Fe (Total)	Mn	Total Hardness	TDS	Ion Balance
		ppm	ppm	ppm	ppm	ppm	ppm	ppm	ppm	ppm	ppm	ppm	ppm	ppm	(CaCO3)	(mg/l)	(%)
P6	-35m	119	34	131	4.9	<1	371	64	203	<0.1	0.1	8	10.22	0.39	437	812	4.8
	-55m	102	27	113	5.0	<1	383	47	191	<C.1	0.3	8	3.53	0.34	368	672	4.1
	-80m	102	27	114	5.1	<1	351	48	176	<0.1	0.2	9	3.92	0.30	364	664	5.8
	-110m	102	27	111	4.9	<1	371	48	184	<0.1	0.1	8	3.18	0.32	367	668	3.0
P6	-35m(2)	160	24	176	2.0	<1	447	75	265	0.3	<0.10	4	4.23	0.75	504	924	9.0
	-55m(2)	139	25	111	4.0	<1	394	60	185	<0.1	<0.10	7	2.51	0.39	458	536	9.6
	-80m(2)	140	26	132	3.0	<1	386	68	212	0.1	<0.10	7	1.82	0.28	465	772	9.6
	-110m(2)	135	26	113	4.0	<1	394	61	182	<0.1	<0.10	6	3.04	0.51	451	740	9.8
Elba 2	-30m	57	40	98	7.0	<1	281	59	131	<0.1	0.4	20	0.40	0.06	330	556	9.2
	-55m	57	40	92	7.0	<1	305	60	127	0.3	0.4	19	0.60	0.10	329	548	9.8
	-85m	55	39	94	7.0	<1	295	63	130	<0.1	0.4	21	0.02	0.01	322	536	7.8
	-108m	50	38	105	7.0	<1	281	59	129	0.3	0.4	21	0.20	0.03	305	524	8.5
M1	-61m	45	29	334	6.0	<1	244	100	498	0.1	<0.10	21	<0.01	<0.01	235	1528	1.0
	-82.3m	46	42	398	8.0	<1	346	101	553	<0.1	<0.10	29	<0.01	<0.01	288	1728	3.5
	-122m	64	47	351	9.0	<1	216	101	588	<0.1	<0.10	33	<0.01	<0.01	352	1852	3.8

[Ca]/[Mg] Ratios

Well	Depth	[Ca] /[Mg]	([Ca]+[Sr]) /[Mg]
P1	-34m	0.84	1.07
	-55m	0.91	1.18
	-64m	0.94	1.18
	-100m	0.96	1.24
	-130m	1.09	1.32
P2	-20m	1.01	1.15
	-55m	1.20	1.35
	-87m	1.34	1.48
	-93m	1.11	1.26
	-120m	0.94	1.09
P3	-25m	0.93	1.08
	-55m	0.93	1.09
	-109m	0.89	1.05
	-150m	1.65	1.82
P4	-25m	0.69	0.84
	-55m	0.65	0.80
	-110m	0.77	0.95
P5	-34m	0.83	0.98
	-55m	0.87	1.03
	-105m	0.87	1.02
	-120m	0.83	1.01

Well	Depth	[Ca] /[Mg]	([Ca]+[Sr]) /[Mg]
P6	-35m	2.13	2.19
	-55m	2.26	2.34
	-80m	2.33	2.41
	-110m	2.28	2.36
P6	-35m(2)	4.04	4.09
	-55m(2)	3.37	3.45
	-80m(2)	3.27	3.34
	-110m(2)	3.15	3.21
Elba 2	-30m	0.86	1.00
	-55m	0.86	1.00
	-85m	0.86	1.00
	-108m	0.80	0.95
M1	-61m	0.94	1.14
	-82.3m	0.66	0.86
	-122m	0.83	1.02

Saturation Indices for Mineral Phases from WATEQ 2

Well	Depth	$CaCO_3$ Calcite	$CaCO_3$ Aragonite	$CaMg(CO_3)_2$ Dolomite	$MgCO_3$ Magnesite	$SrCO_3$ Strontianite	$FeCO_3$ Siderite	FeOOH Goethite	FeS Mackinawite	$CaSO_4$ Gypsum
P1	34m	0.4	0.1	0.8	0.1	2.9	-0.9	4.3	1.3	-1.9
	55m	0.3	0.0	0.5	-0.1	2.9	-0.8	3.6	1.5	-1.6
	64m	0.2	-0.1	0.4	-0.1	2.8	-1.0	3.1	1.4	-1.5
	100m	0.1	-0.2	0.1	-0.3	2.7	-0.3	3.1	2.2	-1.5
	130m	0.1	-0.2	0.1	-0.3	2.6	-0.9	0.2	1.6	-1.4
P2	20m	0.4	0.1	0.6	0.0	2.7	-1.4	1.4	1.6	-1.8
	55m	0.3	0.0	0.5	-0.2	2.6				-1.7
	87m	0.5	0.1	0.7	-0.1	2.6	-0.4	1.0	2.6	-1.7
	93m	0.3	0.0	0.4	-0.2	2.6	-0.6	0.8	2.4	-1.8
	120m	0.6	0.3	1.1	0.2	3.0	-0.2	1.0	3.7	-1.9
P3	25m	0.3	0.0	0.5	-0.1	2.6	0.0	0.8	3.4	-1.9
	55m	0.2	-0.1	0.4	-0.1	2.6	-0.4	0.9	3.2	-2.0
	109m	0.4	0.1	0.7		2.7				-2.0
	150m	0.4	0.1	0.6	-0.2	2.6	-0.7	0.0	2.8	-1.8
P4	25m	0.6	0.3	1.3	0.4	3.1	-0.6	1.9	1.9	-2.0
	55m	0.6	0.3	1.2	0.3	3.1	0.2	4.1	3.0	-2.0
	110m	0.0	-0.3	0.1	-0.3	2.5	-0.2	1.8	2.7	-1.9
P5	34m	0.4	0.0	0.7	0.0	2.8	0.0	2.5	3.0	-2.0
	55m	0.2	-0.1	0.4	-0.1	2.6	-1.0	0.2	2.0	-1.9
	105m	0.3	0.0	0.5	-0.1	2.7	-1.5	0.0	1.8	-1.9
	120m	0.3	0.0	0.6	0.0	2.8	-1.2	0.5	2.1	-1.9
P6	35m	0.2	-0.1	0.0	-0.5	1.8	0.8	7.3	2.9	-1.7
	55m	0.2	-0.1	-0.1	-0.6	1.8	0.5	3.9	2.5	-1.8
	80m	0.2	-0.1	-0.1	-0.6	1.9	0.6	3.9	2.5	-1.8
	110m	0.2	-0.1	0.0	-0.6	1.9	0.5	3.5	2.3	-1.8

Saturation Indices for Mineral Phases from WATEQ 2 (Continued)

Well	Depth	$CaCO_3$ Calcite	$CaCO_3$ Aragonite	$CaMg(CO_3)_2$ Dolomite	$MgCO_3$ Magnesite	$SrCO_3$ Strontianite	$FeCO_3$ Siderite	FeOOH Goethite	FeS Mackinawite	$CaSO_4$ Gypsum
		Mineral / Phase								
P6(2)	35m	0.4	0.1	0.1	-0.6	1.6	0.6	3.1	2.9	-1.5
	55m	0.4	0.1	0.2	-0.5	1.9	0.5	3.1	2.4	-1.5
	80m	0.3	0.0	0.0	-0.6	1.8	0.2	2.7	2.3	-1.6
	110m	0.2	-0.1	-0.2	-0.7	1.6	0.4	2.6	2.4	-1.6
Elbe 2	30m	0.4	0.1	0.7	0.0	2.7	0.0	0.9	3.2	-1.9
	55m	0.7	0.4	1.3	0.3	3.0	0.5	2.5	3.7	-1.9
	80m	0.5	0.2	0.9	0.1	2.9	-1.2	0.3	2.1	-1.9
	110m	0.3	-0.1	0.5	-0.1	2.7	-0.3	0.9	2.9	-2.0
M1	61m	0.3	0.0	0.6	-0.1	2.8	-	-	-	-1.9
	82.3m	0.2	-0.1	0.4	0.0	2.8	-	-	-	-1.9
	122m	0.1	-0.2	0.2	-0.2	2.6	-	-	-	-1.8

Note: The Langmuir (1971) classification system for stauration is used: a sample is designated as being saturated if its saturation index, expressed in logarithmic form, is in the range -0.1 to +0.1.

Appendix 6

TRILINEAR DIAGRAMS OF THE MAJOR ION COMPOSITION OF INDIVIDUAL WELL SAMPLES

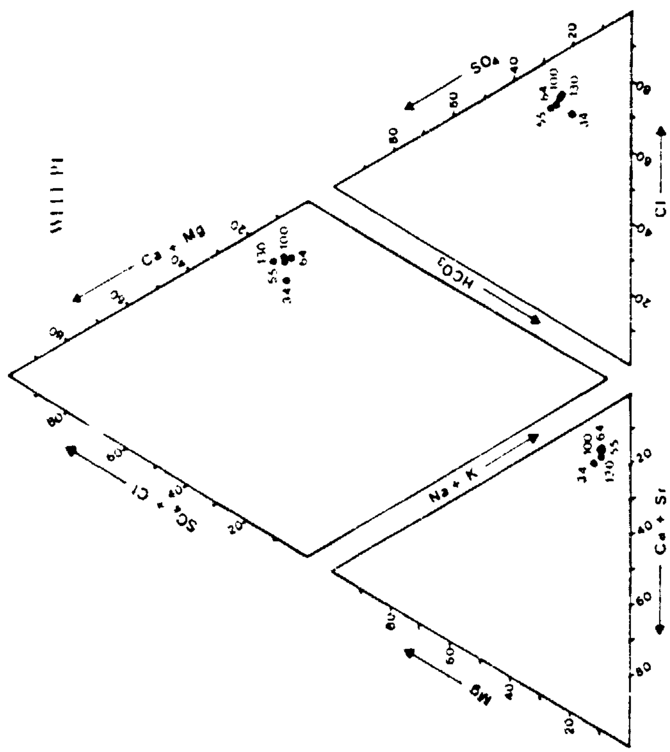

SO4
Cl
HCO3
Ca + Mg
SO4 + Cl
Na + K
Ca + Sr
Mg

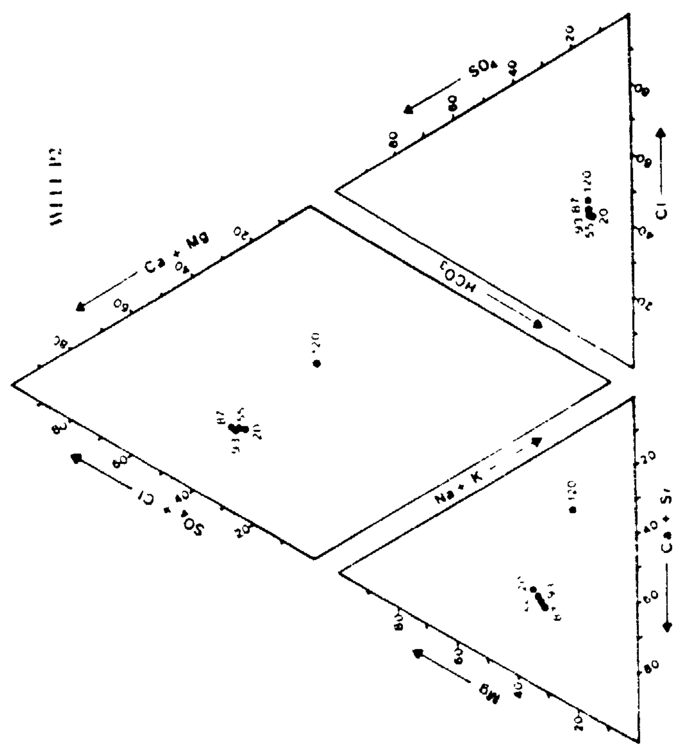
WELL P2
Ca + Mg
SO4 + Cl
SO4
Cl
HCO3
Na + K
Mg
Ca + Sr

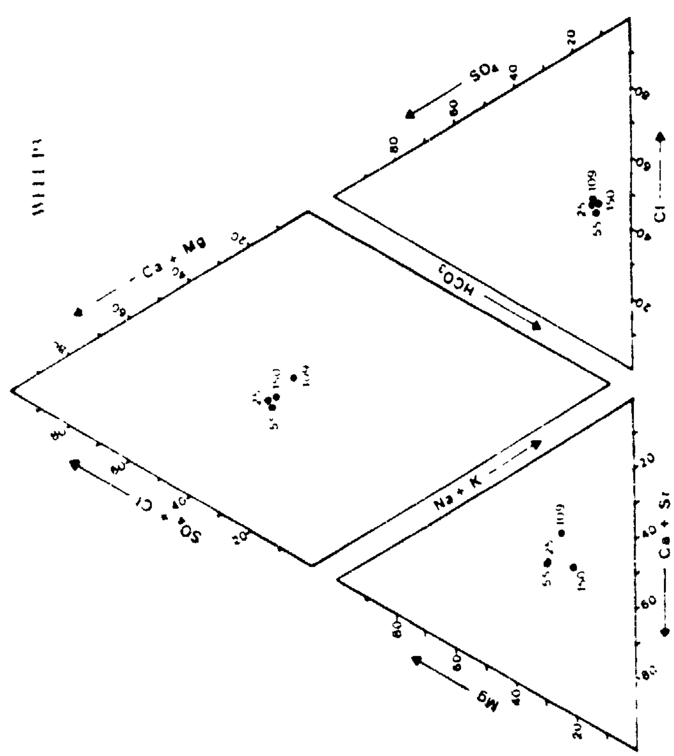

SO4
Cl
HCO3
Ca + Mg
SO4 + Cl
Na + K
Mg
Ca + Sr

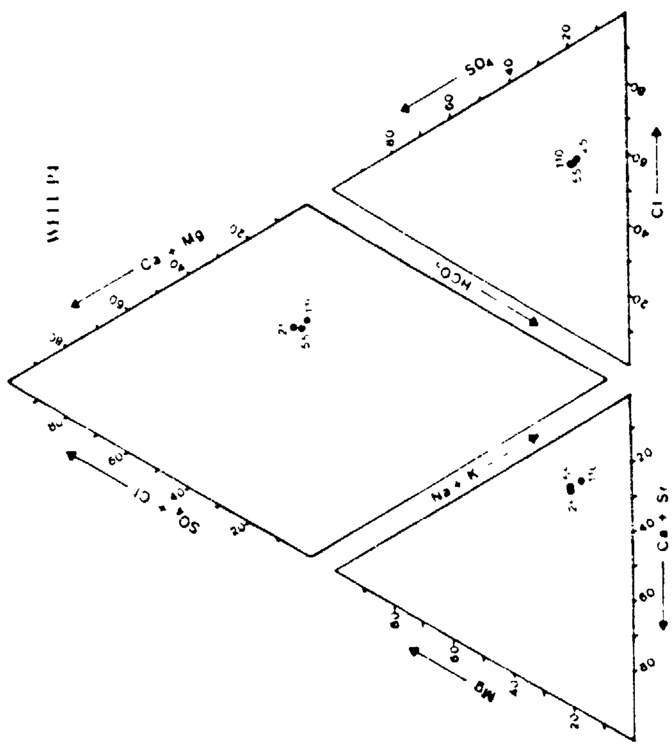

SO_4
Cl
HCO_3
Ca + Mg
SO_4 + Cl
Na + K
Ca + Sr
Mg

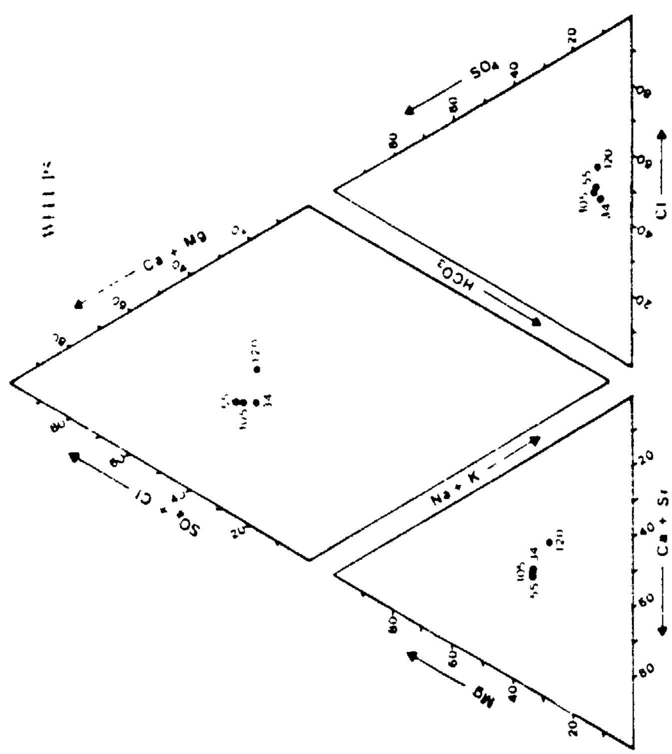
Ca + Mg
SO4 + Cl
Na + K
HCO3
SO4
Cl
Mg
Ca + Sr

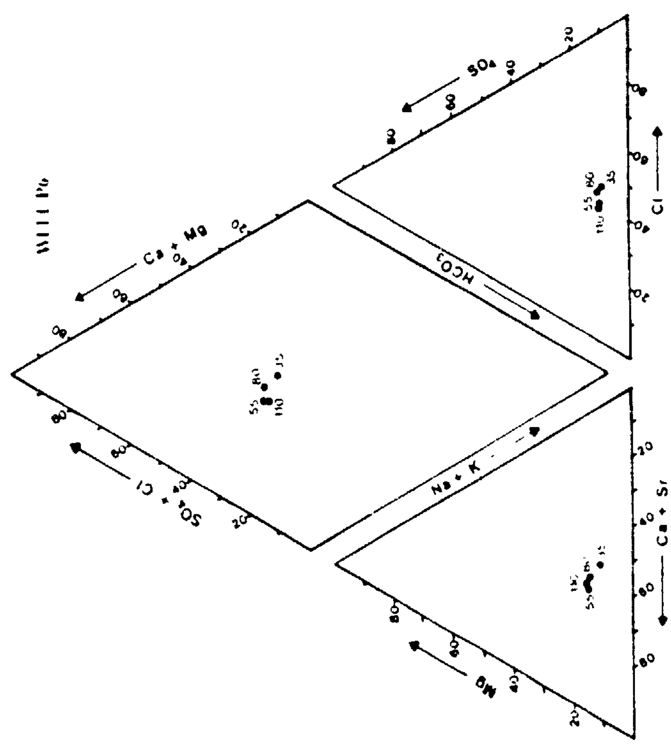
Ca + Mg
SO4 + Cl
HCO3
Na + K
SO4
Cl
Ca + Sr
Mg

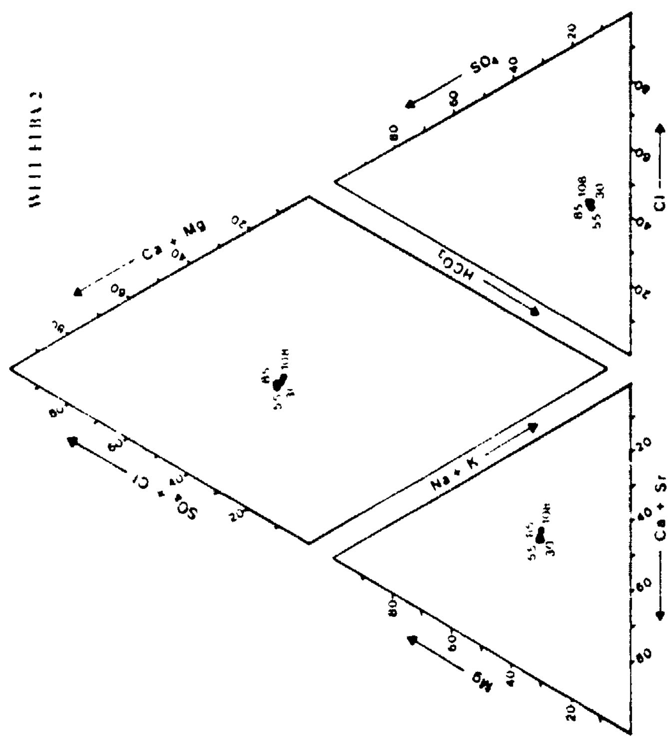

FIGURE 2

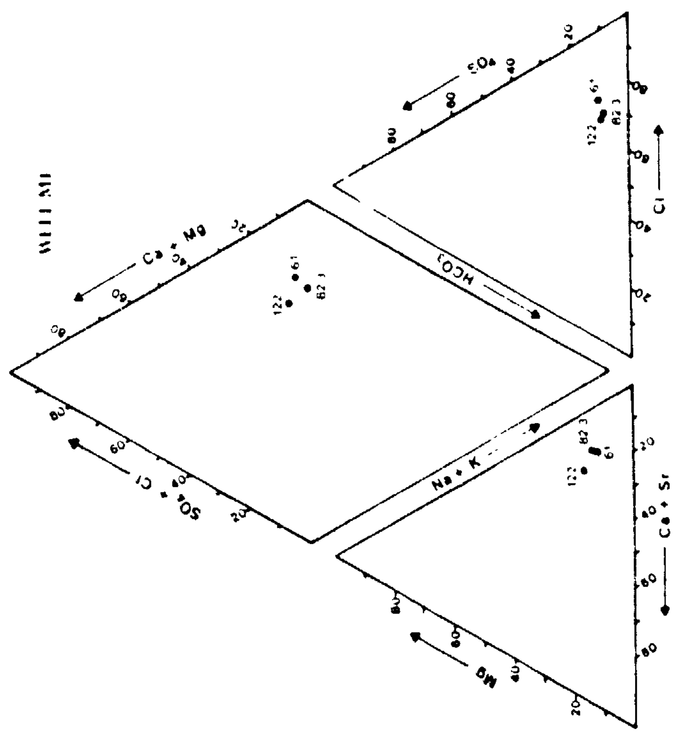
Ca + Mg
SO4 + Cl
Na + K
HCO3
SO4
Cl
Mg
Ca + Sr

Appendix 7

ISOTOPE DATA

Isotope Analysis for Well Water Samples

Well	Depth	^{18}Oxygen $^{0}/oo$ SMOW[1]	Deuterium $^{0}/oo$ SMOW[2]	Deuterium $^{0}/oo$ SMOW[2] duplicate	Tritium T.U.[3]	Tritium T.U.[3] duplicate
P1	34m	-12.3	-89	-88	<6	-
	55m	-12.4	-88	-	6	-
	64m	-12.4	-92	-	<6	-
	100m	-12.4	-87	-	<6	<6
	130m	-12.3	-88	-91	<6	-
P2	20m	-11.6	-85	-	41	-
	55m	-11.6	-82	-89	34	-
	87m	-11.4	-87	-	39	-
	93m	-11.4	-85	-	40	-
	120m	-11.7	-84	-	27	-
P5	34m	-11.4	-83	-	35	-
	120m	-11.8	-87	-	32	-
P6	35m	-9.7	-68	-	23	-
	55m	-9.8	-75	-	20	-
	80m	-9.9	-77	-	24	-
	110m	-9.5	-74	-73	31	-
P6(2)	35m	-9.4	-72	-	15	-
	55m	-9.6	-73	-	25	-
	80m	-9.6	-73	-	20	-
	110m	-9.7	-71	-72	29	33
M1	61m	-12.4	-88	-	<6	-
	82.3m	-12.1	-86	-	<6	-
	122m	-12.5	-86	-87	<6	-

[1] Values are +/- 0.2
[2] Values are +/- 2
[3] Values are +/- 8

Static Water Levels: September, 1988
(metres above sea level)

Well	Date 12	13	14	15	16	21	22
P1	60.09	60.09	60.08	60.04	60.05	60.26	-
P2	60.98	60.98	60.96	60.91	60.92	60.98	-
RC	60.97	60.97	60.95	60.90	60.92	60.97	-
P3	>60.51	>60.51	>60.51	>60.51	>60.51	>60.51	>60.51
P4	60.07	60.07	60.07	60.03	60.04	60.17	-
T1/M3	60.41	60.40	60.38	60.36	60.38	-	-
P5	60.98	60.98	60.97	60.91	60.93	60.98	-
P6	-	-	-	-	-	-	60.96
Elba 1	60.82	60.82	60.80	60.75	60.77	60.82	-
Elba 2	60.98	60.98	60.96	60.91	60.92	60.97	-
T3/M4	-	61.66	61.66	61.62	61.65	61.72	-
Tory	59.82	59.82	-	-	59.80	59.87	59.84
M1-PVC	>63.56	>63.56	>63.56	>63.56	>63.56	>63.56	>63.56
M1-B	>63.56	>63.56	>63.56	>63.56	64.26	64.38	64.36
M1-1	>63.56	>63.56	>63.56	>63.56	63.95	64.06	64.02
M1-2	60.23	60.27	60.29	60.29	60.29	60.39	60.39
M1-3	61.61	61.62	61.62	61.58	61.82	61.75	61.72
M1-4	60.54	60.53	60.52	60.49	60.50	60.63	60.61
M1-5	60.25	60.28	60.27	60.25	60.27	60.35	60.34
M1-6	59.65	59.64	59.63	59.61	59.62	59.64	59.63

Isotope Analysis for Well Water Samples during Pump Tests

Well	^{18}Oxygen $^{o}/oo$ SMOW[1]	^{18}Oxygen $^{o}/oo$ SMOW[1] duplicate	Deuterium $^{o}/oo$ SMOW[2]	Deuterium $^{o}/oo$ SMOW[2] duplicate	A ^{14}C pmC[2]	δ ^{13}C $^{o}/oo$ PDB[3]	δ $^{13}C_{calcite}$ $^{o}/oo$ PDB[3] Depth	δ $^{13}C_{calcite}$ $^{o}/oo$ PDB[3] Rock	δ $^{13}C_{calcite}$ $^{o}/oo$ PDB[3] Depth	δ $^{13}C_{calcite}$ $^{o}/oo$ PDB[3] Crystals
P1	-12.1		-80	-88						
P2	-12.0	-11.8	-87		48	-11.7	30m	-0.3	21/27m	4.1
					(P2 to P4)		70m	0.7		
							91m	1.9	88/110m	1.1
							120m	1.8		
P3	-11.7		-86							
P4	-12.1		-88							
P5	-11.9		-88							
Elba 2	-11.5		-83							
T1	-12.3		-89							
T3	-12.0		-87							
T4	-11.8		-86							

1 Values are +/- 0.2
2 Values are +/- 2
3 Values are +/- 0.1

Isotope Analysis for Surface Water Samples

	^{18}Oxygen $^{0}/oo$ SMOW[1]	^{18}Oxygen $^{0}/oo$ SMOW[1] duplicate	Deuterium $^{0}/oo$ SMOW[2]	Deuterium $^{0}/oo$ SMOW[2] duplicate	Tritium T.U.[3]	Tritium T.U.[3] duplicate
Rideau Canal (Aug/89)	-6.6	-6.7 -5.9	-54		27	34
Rideau Canal (Oct/89)	-5.9					

1 Values are +/- 0.2
2 Values are +/- 2
3 Values are +/- 8

Appendix 8

HYDRAULIC HEAD DATA

Static Water Levels: Monthly Records, Sept/88 to Aug/89
(metres above sea level)

Well	Date 15-Sep	03-Oct	15-Oct	01 Nov	17-Nov	24-Nov	01-Dec	08-Dec	20-Dec	19-Jan	01-Feb	06-Mar	31-Mar	03-Apr	20-Apr	29-Apr
P1	60.04	-	60.16	60.38	60.52	60.48	60.37	60.30	60.30	60.20	60.17	60.13	-	60.59	60.44	60.39
P2	60.91	60.95	60.98	61.23	61.40	61.33	61.13	61.05	61.04	60.93	60.91	60.84	61.59	61.51	61.32	61.33
RC	60.90	60.94	60.97	61.22	61.39	61.33	61.13	61.04	61.03	60.91	60.93	60.82	-	61.49	61.32	61.32
P3	>60.51	>60.51	>60.51	>60.51	>60.51	>60.51	>60.51	>60.51	>60.51	>60.51	>60.51	60.80	-	-	61.29	61.29
P4	60.03	-	60.09	60.31	60.45	60.41	60.30	60.23	60.23	60.12	60.10	60.07	60.59	60.54	60.37	60.33
T1/M3	60.36	-	-		60.46	60.39	60.28	60.22	60.22	60.11	60.09	60.05	-	60.53	60.36	60.32
P5	60.91	60.94	60.98	61.23	61.39	61.34	61.15	61.06	61.05	60.94	60.93	60.85	61.60	61.51	61.34	61.33
P6	-	-	61.00	61.25	61.42	61.36	61.16	61.08	61.06	60.95	60.93	60.86	61.63	61.54	61.35	61.35
Elba 1	60.75	60.78	60.82	61.07	61.24	61.18	61.00	60.92	60.91	60.81	60.79	60.72	61.46	61.37	61.20	61.19
Elba 2	60.91	60.94	60.97	61.22	61.39	61.33	61.13	61.05	-	-	-	-	>61.56	-	61.34	61.34
T3/M4	61.62	61.70	61.79	62.02	62.17	62.15	62.01	61.95	62.00	61.91	61.86	61.82	62.12	62.10	62.05	62.04
Tory	-	59.75	-	-	-	-	60.01	59.90	-	-	59.80	59.77	-	60.25	60.05	59.99
M1-PVC	>63.56	-	-	-	>63.56	>63.56	>64.09	>64.64	64.50	>63.56	64.69	>63.56	-	>63.56	>63.56	>63.56
M1-B	>63.56	-	-	-	64.69	64.67	64.84	65.07	64.78	64.73	64.70	64.66	-	65.04	65.13	65.26
M1-1	>63.56	-	-	-	64.37	64.34	64.39	-	64.46	64.41	64.40	64.41	-	64.83	64.97	65.05
M1-2	60.29	-	-	-	60.66	60.63	60.61	60.57	60.47	60.41	60.27	60.24	-	60.58	61.38	63.52
M1-3	61.58	-	-	-	62.06	62.04	61.98	62.00	62.01	62.07	62.11	62.15	-	62.54	62.47	62.52
M1-4	60.49	-	-	-	60.92	60.88	60.76	60.71	-	-	60.57	60.59	-	61.00	60.82	60.77
M1-5	60.25	-	-	-	60.75	60.53	60.45	-	-	-	60.22	60.18	-	60.62	60.47	60.43
M1-6	59.61	-	-	-	59.75	-	-	-	-	-	59.57	59.55	-	59.86	59.76	59.74

Static Water Levels: Monthly Records, Sept/88 to Aug/89
(metres above sea level) (Continued)

Well	Date 19-May	25-May	02-Jun	07-Jul	25-Jul	01-Aug
P1	60.61	60.49	60.43	60.35	60.29	-
P2	61.64	61.47	61.40	61.31	-	-
RC	-	61.46	61.39	61.30	61.26	61.32
P3	-	-	61.36	61.25	61.21	61.26
P4	60.56	60.44	60.38	60.29	60.24	-
T1/M3	-	60.44	60.37	60.28	60.23	60.26
P5	-	61.48	61.40	61.31	61.27	-
P6	61.66	61.49	61.42	61.34	61.29	61.35
Elba 1	-	61.33	61.26	61.18	61.13	61.19
Elba 2	-	61.48	61.40	61.32	61.28	61.34
T3/M4	-	62.27	62.27	62.33	62.32	-
Tory	-	60.09	60.03	59.92	59.87	-
M1-PVC	>63.56	>63.56	>63.56	>63.56	>63.56	>63.56
M1-B	65.58	65.59	65.65	65.60	65.54	65.64
M1-1	65.40	65.42	65.48	65.44	65.39	65.53
M1-2	61.34	63.51	63.57	-	61.83	63.25
M1-3	62.68	62.63	62.57	-	62.37	62.39
M1-4	60.98	60.87	60.83	-	60.70	60.71
M1-5	60.66	60.59	60.28	-	60.37	60.35
M1-6	59.93	59.86	59.83	-	59.44	59.44

Static Water Levels: September, 1988
(metres above sea level)

Well	Date 12	13	14	15	16	21	22
P1	60.09	60.09	60.08	60.04	60.05	60.26	-
P2	60.98	60.98	60.96	60.91	60.92	60.98	-
RC	60.97	60.97	60.95	60.90	60.92	60.97	-
P3	>60.51	>60.51	>60.51	>60.51	>60.51	>60.51	>60.51
P4	60.07	60.07	60.07	60.03	60.04	60.17	-
T1/M3	60.41	60.40	60.38	60.36	60.38	-	-
P5	60.98	60.98	60.97	60.91	60.93	60.98	-
P6	-	-	-	-	-	-	60.96
Elba 1	60.82	60.82	60.80	60.75	60.77	60.82	-
Elba 2	60.98	60.98	60.96	60.91	60.92	60.97	-
T3/M4	-	61.66	61.66	61.62	61.65	61.72	-
Tory	59.82	59.82	-	-	59.80	59.87	59.84
M1-PVC	>63.56	>63.56	>63.56	>63.56	>63.56	>63.56	>63.56
M1-B	>63.56	>63.56	>63.56	>63.56	64.26	64.38	64.36
M1-1	>63.56	>63.56	>63.56	>63.56	63.95	64.06	64.02
M1-2	60.23	60.27	60.29	60.29	60.29	60.39	60.39
M1-3	61.61	61.62	61.62	61.58	61.82	61.75	61.72
M1-4	60.54	60.53	60.52	60.49	60.50	60.63	60.61
M1-5	60.25	60.28	60.27	60.25	60.27	60.35	60.34
M1-5	59.65	59.64	59.63	59.61	59.62	59.64	59.63

Static Water Levels: October, 1988
(metres above sea level)

Well	Date 3	4	6	11	12	13	14	15	17	18	20	21	22	24	25	26
P1	-	-	-	-	60.15	60.15	60.18	60.16	60.15	60.13	60.11	60.12	60.16	60.36	60.45	60.43
P2	60.95	60.97	60.97	61.00	60.97	60.97	61.01	60.98	60.95	60.91	60.84	60.86	60.91	61.25	61.40	61.36
RC	60.94	60.96	60.9[illegible]	60.98	60.96	60.97	61.00	60.97	60.94	60.91	60.84	60.86	60.90	61.23	61.38	61.33
P3	>60.51	>60.51	>60.51	>60.51	>60.51	>60.51	>60.51	>60.51	>60.51	>60.51	>60.51	>60.51	>60.51	>60.51	>60.51	>60.51
P4	-	-	-	-	60.07	60.07	60.10	60.09	60.07	60.05	60.03	60.04	60.08	60.29	60.38	60.35
T1/M3	-	-	-	-	-	-	-	-	-	-	-	60.03	60.08	60.24	60.37	60.36
P5	60.94	60.97	60.96	60.99	60.97	60.97	61.01	60.98	60.95	60.92	60.85	60.87	60.92	61.24	61.40	61.35
P6	-	-	-	-	61.00	61.00	61.04	61.00	60.97	60.94	60.87	60.89	60.94	61.27	61.42	61.37
Elba 1	60.78	60.80	60.80	60.83	60.81	60.81	60.85	60.82	60.79	60.76	60.70	60.72	60.76	61.08	61.22	61.18
Elba 2	60.94	60.96	60.96	60.98	60.96	60.96	61.00	60.96	60.94	60.91	60.84	60.86	60.90	61.24	61.39	61.34
T3/M4	61.70	61.76	61.71	61.77	61.75	61.76	61.81	61.79	61.79	61.78	61.77	61.80	61.85	61.94	61.99	61.99
Tory	59.75	-	-	59.78	59.77	59.76	59.80	-	-	-	-	59.75	-	-	-	-
M1-PVC	-	-	-	-	-	-	-	-	-	-	-	-	-	-	-	-
M1-B	-	-	-	-	-	-	-	-	-	-	-	-	-	-	-	-
M1-1	-	-	-	-	-	-	-	-	-	-	-	-	-	-	-	-
M1-2	-	-	-	-	-	-	-	-	-	-	-	-	-	-	-	-
M1-3	-	-	-	-	-	-	-	-	-	-	-	-	-	-	-	-
M1-4	-	-	-	-	-	-	-	-	-	-	-	-	-	-	-	-
M1-5	-	-	-	-	-	-	-	-	-	-	-	-	-	-	-	-
M1-6	-	-	-	-	-	-	-	-	-	-	-	-	-	-	-	-

Static Water Levels: October, 1988
(metres above sea level) (Continued)

Well	Date 27	28	29	31
P1	60.39	60.40	60.38	60.39
P2	61.30	61.31	61.25	61.24
KC	61.28	61.29	61.24	61.22
P3	>60.51	>60.51	>60.51	>60.51
P4	60.32	60.34	60.30	60.32
T1/M3	60.32	60.35	60.32	60.33
P5	61.30	61.31	61.25	61.24
P6	61.32	61.33	61.28	61.26
Elba 1	61.07	61.14	61.09	61.08
Elba 2	61.29	61.30	61.24	61.23
T3/M4	61.97	62.01	61.97	62.01
Tory	-	60.02	-	-
M1-PVC	-	-	-	-
M1-B	-	-	-	-
M1-1	-	-	-	-
M1-2	-	-	-	-
M1-3	-	-	-	-
M1-4	-	-	-	-
M1-5	-	-	-	-
M1-6	-	-	-	-

Static Water Levels: November, 1988
(metres above sea level)

Well	Date 1	2	3	4	5	7	8	9	10	12	15	16	17	18	19	20	21
P1	60.38	60.41	60.41	60.44	60.46	60.63	60.62	60.60	60.64	-	60.52	60.55	60.52	60.46	-	-	60.46
P2	61.23	61.29	61.28	61.32	61.34	61.59	61.58	61.54	61.58	-	-	-	61.40	-	-	-	-
RC	61.22	61.27	61.27	61.31	61.33	61.57	61.56	61.53	61.56	-	-	-	61.39	-	-	-	-
P3	>60.51	>60.51	>60.51	>60.51	>60.51	>60.51	>60.51	>60.51	>60.51	-	-	-	>60.51	-	-	-	-
P4	60.31	60.34	60.34	60.37	60.39	60.56	60.56	60.54	60.58	-	-	-	60.45	-	-	-	-
T1/M3	60.32	60.34	60.35	60.38	50.39	60.57	60.55	60.53	60.57	-	-	-	60.46	-	-	-	-
P5	61.23	61.29	61.28	61.32	61.34	61.58	61.57	61.54	61.57	-	-	-	61.39	-	-	-	-
P6	61.25	61.31	61.30	61.34	61.36	61.61	61.60	61.56	61.60	-	-	-	61.42	-	-	-	-
Elba 1	61.07	61.12	61.17	61.16	61.18	61.41	61.41	61.38	61.41	-	-	-	61.24	-	-	-	-
Elba 2	61.22	61.28	61.27	61.31	61.33	-	-	61.26	-	-	-	-	61.39	-	-	-	-
T3/M4	62.02	62.06	62.02	62.06	62.09	62.14	62.16	62.14	62.26	-	62.14	62.21	62.17	62.10	-	-	62.12
Tory	-	-	-	60.07	-	-	-	-	-	-	-	-	-	-	-	-	-
M1-PVC	-	-	-	-	-	-	-	-	-	>63.57	>63.57	>63.57	>63.57	>63.57	>63.57	>63.57	>63.57
M1-B	-	-	-	-	-	-	-	-	-	64.69	64.65	64.70	64.69	64.64	64.64	64.70	64.68
M1-1	-	-	-	-	-	-	-	-	-	64.29	64.32	64.37	64.37	64.31	64.33	64.39	64.37
M1-2	-	-	-	-	-	-	-	-	-	60.67	60.67	60.68	60.66	60.65	60.64	60.66	60.63
M1-3	-	-	-	-	-	-	-	-	-	62.05	62.04	62.09	62.06	62.00	62.02	62.06	62.02
M1-4	-	-	-	-	-	-	-	-	-	60.96	60.93	60.97	60.92	60.86	60.88	60.92	60.86
M1-5	-	-	-	-	-	-	-	-	-	60.63	61.13	60.59	60.75	60.66	60.60	-	-
M1-6	-	-	-	-	-	-	-	-	-	59.78	59.76	59.79	59.75	-	59.67	-	-

Static Water Levels: November, 1988
(metres above sea level) (Continued)

Well	22	23	24	25	26
P1	60.46	60.48	60.48	60.48	60.43
P2	-	-	61.33	-	-
RC	-	-	61.33	-	-
P3	-	-	>60.51	-	-
P4	-	-	60.41	-	-
T1/M3	-	-	60.39	-	-
P5	-	-	61.34	-	-
P6	-	-	61.36	-	-
Elba 1	-	-	61.18	-	-
Elba 2	-	-	61.33	-	-
T3/M4	62.12	62.15	62.15	62.16	62.07
Tory	-	-	-	-	-
M1-PVC	>63.57	>63.57	>63.57	>63.57	>63.57
M1-B	64.65	64.68	64.67	64.70	64.72
M1-1	64.32	64.34	64.34	64.35	64.47
M1-2	60.61	60.62	60.63	60.63	60.78
M1-3	61.91	62.04	62.04	62.05	62.12
M1-4	60.87	60.89	60.88	60.89	60.82
M1-5	60.54	60.53	60.53	60.52	60.52
M1-6	59.71	-	-	-	-

Diurnal Fluctuations
Measurement of Hydraulic Head, July 25 to July 28, 1989
(metres above sea level)

Well	July25 1700h	July26 800h	July26 1430h	July26 1730h	July27 0830h	July27 1730h	July28 0830h	July28 1700h
P1	60.291	60.266	60.291	60.291	60.271	60.331	-	-
P6	61.294	61.254	61.294	61.299	61.264	61.329	61.299	61.349
Elba 2	61.280	61.240	61.280	61.285	61.255	61.310	61.280	61.335
M1-B	65.535	65.535	65.575	-	65.575	-	65.575	65.635
M1-1	65.385	65.375	65.445	-	65.495	-	65.555	65.525
M1-2	61.825	62.135	63.415	-	63.435	-	63.295	63.245
M1-3	62.365	62.345	62.365	-	62.335	-	62.345	62.385
M1-4	60.695	60.665	60.685	-	60.665	-	60.675	60.705
M1-5	60.365	60.365	60.345	-	60.355	-	60.345	60.345
M1-6	59.435	59.435	59.435	-	59.435	-	59.435	59.435
Pressure (mbar)	100.5	100.6	100.4	100.1	99.9	99.4	99.6	99.8
Temperature (C)	33.2	25.4	32.5	33.2	27.0	19.6	17.7	22.3
Precipitation (mm)	0.0	0.0	0.0	0.0	0.0	36.6	0.0	0.0

END

20.02.91

FIN